Title	Two-Particle Correlations in the Statistical Model for High-Energy Heavy- Ion Reactions
Author(s)	Nakai, Tetsuo
Citation	大阪大学, 1982, 博士論文
Version Type	VoR
URL	https://hdl.handle.net/11094/1545
rights	
Note	

Two-Particle Correlations in the Statistical Model for High-Energy Heavy-Ion Reactions

Tetsuo Nakai

Two-Particle Correlations in the Statistical Model for High-Energy Heavy-Ion Reactions

Tetsuo Nakai

Department of Applied Mathematics, Faculty of Engineering Science
Osaka University, Toyonaka 560

Abstract:

Inclusive spectra and the two-particle correlation functions of nucleons and pions in high-energy heavy-ion reactions are investigated based on the statistical model. Our formulation is fully relativistic and is applicable to the reaction including multi-pion production. The dynamical correlation results from the strong interactions among nucleons and pions in the thermal system. Using the S-matrix formulation of the grand partition function, we derive expressions for inclusive cross sections and the correlation functions in terms of the phase shifts of hadron-hadron scatterings.

We calculate these functions for selected heavy-ion reactions with high-multiplicities using a large amount of experimental data on the phase shifts. Some results for the reactions Fe+Cu and Ar+KCl at 400 MeV/A are shown and discussed. Furthermore the calculated proton-proton correlation is compared with experimental data on the reaction Ar+KCl at 1.8 GeV/A. We find that the reasonable value of parameter ρ_c (the density of the thermal system) should satisfy the condition, $\rho_c \gtrsim 0.5\rho_0$, ρ_0 being the density of the normal nuclear matter. Also, it appears that the contribution of the ρ meson resonance to the pion-pion correlation is very small because of its larger mass than the threshold of $\pi\pi$ scattering. Our analyses for the pion-nucleon interaction reveal that the finite width of the Δ resonance plays an important role for the pion spectra.

Contents:

§1. Introduction

The primary motivation for studying high-energy heavy-ion collisions has been to achieve high nuclear densities and high temperatures during the collision, and to obtain an information on the nature of nuclear matter beyond the point of normal nuclear density and temperature. Various new phenomena, such as shock waves[1.1], pion condensation[1.2], nuclear density isomers[1.3], the transition from nuclear- to quark- matter[1.4] and hidden color (QCD) effect[1.5], etc, have been predicted to occur under such extreme conditions. A large amount of experimental data concerning the relativistic heavy-ion reactions with beam energies from a few hundred MeV to a few GeV per nucleon have been accumulated.[1.6] These have come mostly from the Bevalac at the Lawrence Berkeley Laboratory.

However, until now those expected unusual phenomena are not confirmed yet experimentally. Various reasons for this situation are considered: (i) The incident beam energy is not enough to induce these phenomena. (ii) As these various processes occur simultaneously, the observed data are largely smoothed as if there is no such abnormal feature. (iii) Production cross sections of the new phenomena are so small that they are buried in the ordinary processes. (iv) The physical quantities observed so far are not suitable for detecting such phenomena.

Therefore it is important to calculate accurately the background value for these phenomena with theoretical models in order to find out the extraordinary feature.

A great variety of theoretical models have been used to calculate the background processes. They are the statistical model[1.7] with a simplified participant-spectator geometry[1.8] (the nuclear fireball model), the nuclear fluid-dynamical model[1.9] and the microscopic cascade model[1.10], etc[1.11]. All these models have been successful in describing at least the gross feature of inclusive distributions[1.12]. Various quantities to provide a test of these models have been suggested such as the particle correlation[1.13], the energy dependence of the pion multiplicity[1.14], the ratio of deuteron to proton[1.15], the collective hydrodynamical side-way flow[1.16], the strange particle production[1.17] and the antiproton production[1.18]. In particular, under the present experimental situation, obvious differences among the existing dynamical models will appear in the particle correlations, which may be sensitive to the existence of the exotic phenomena. Thus a detailed investigation of the correlation functions is essential to select out a reasonable theoretical model and to reveal the new physics.

Among the various models the statistical model is considered to be an appealing one for the following reasons:

(i) It is simple, and (ii) the recent data mostly sorted into central collisions are well described by the statistical model in the gross feature[1.19]. Note that the data averaged over the impact parameter should not be compared directly with the statistical model based on the assumption of the thermal equilibrium, because such data contain a considerable contribution of the peripheral collision. In the latter collision, the number of participating particles is not enough to reach an equilibrium.

The purpose of this paper is to investigate in detail the system produced by the central high-energy heavy-ion collision basing on the statistical model. We take account of various interactions among hadrons involved in it in terms of the scattering phase shifts. Our formulation is fully relativistic and is applicable to a system with super high temperature. Using the method of statistical mechanics formulated by Dashen, Ma and Bernstein[1.20] for the relativistically interacting system, we derive expressions for the one-particle distribution and the two-particle correlation function. These functions involve, in addition to well known terms of ideal-gas, some new remarkable terms due to the interactions. These are written by using the phase shifts of the nucleon-nucleon, the nucleon-pion and the pion-pion scattering. Then we calculate the inclusive cross section and the correlation of protons and pions for selected heavy-ion reactions with high-multiplicities. A large amount of experimental data on the phase shifts is utilized in our calculation.

The proton-proton correlation function has been studied by Koonin[1.21]. However, his treatment is nonrelativistic and formulated by using a nuclear potential between protons. So the method is not applicable to the system including pions. Above the energy about 1.0 GeV/A the contribution of the pion production can not be negligible.

In Kapusta's simple fireball model[1.22], the system contains the Δ resonance with zero width. His treatment is insufficient because, according to our analyses, the finite width of the resonance plays an important role for the pion spectra.

The contents of this work are as follows: In §2 we give a brief review of the S-matrix formulation of the grand partition function for the system composed of one species of particle which was presented in Ref. 1.20. The two-particle correlation function is expressed in terms of the scattering phase shifts in §3. Section 4 is devoted to the summary of an interferometric correlation effect of the identical particles in our framework. We derive in §5 the expression of the two-proton correlation and inclusive distribution functions integrated over the impact parameter for the reaction of equal-mass nuclei. Then we apply them to heavy-ion reactions Fe+Cu and Ar+KCl at 400 MeV/A. Contributions due to the pion production are neglected at this energy.

In §6 we treat the system composed of pions and nucleons, and generalize the formulas for the inclusive cross section and the two-particle correlation function in §5 so as to include the pion production. Using these formulas, we calculate in §7 the proton-proton correlation functions at higher energies and compare them with preliminary experiments in the reaction Ar+KCl at 1.8 GeV/A[1.23]. We find that the reasonable value of the parameter ρ_c (density of the thermal system) should satisfy the condition, $\rho_c \gtrsim 0.5\rho_0$, with ρ_0 being the normal density of the nuclear matter. The pion-pion correlation functions are also calculated for various combinations of colliding nuclei. It appears that the contribution of the ρ meson resonance to the dynamical correlation function is very small because of its larger mass than the threshold of the pion-pion scattering. The remainder of §7 is devoted to calculations for the inclusive distributions of protons and pions and we compare them with the data for the reaction Ar+KCl at 0.8 GeV/A[1.24]. Our result fits better to the data of pion spectra than the simple fireball model does.

Finally, section 8 contains a summary of our results and some concluding remarks. Appendix A gives some convenient formulas for the derivation of Eq. (2.13) in §2. In Appendix B we describe a brief review of the simple nuclear fireball model formulated by Kapusta[1.22] and generalize it so as to include the hadron-hadron interactions.

§2. S-matrix formulation of grand partition function

In this section S-matrix formulation[2.1] of the grand partition function is briefly reviewed. For the simplicity of discussion, we treat the system composed of one species of particles with Boltzmann statistics. The grand partition function is given by

$$\Xi = \mathrm{tr}\,\exp[-\beta(H - \mu N)] \quad , \tag{2.1}$$

where β^{-1} is the temperature, μ the chemical potential, and

$$H = H_0 + H_I \quad , \tag{2.2}$$

H_0 and H_I being the free and interacting Hamiltonian, respectively. To evaluate the trace, we use the complete set of H_0. The eigenstate of H_0 is labelled by the set $\{\kappa_N\} = \{\mathbf{k}_1, \mathbf{k}_2, .., \mathbf{k}_N\}$, and is denoted as

$$|\,\mathbf{k}_1, \mathbf{k}_2, .., \mathbf{k}_N\rangle = |\mathbf{k}_1\rangle|\mathbf{k}_2\rangle ...|\mathbf{k}_N\rangle$$

for N-particle state. Here $|\mathbf{k}\rangle$ is a single particle state of H_0 with momentum $\mathbf{k}$. Then the grand partition function is

$$\Xi = \sum_N \lambda^N \,\mathrm{tr}_N\, e^{-\beta H} \quad , \tag{2.3}$$

where

$$\mathrm{tr}_N\, e^{-\beta H} = \sum_{\{\kappa_N\}} \langle \mathbf{k}_1 \mathbf{k}_2 .. \mathbf{k}_N | e^{-\beta H} | \mathbf{k}_1 \mathbf{k}_2 .. \mathbf{k}_N \rangle \quad . \tag{2.4}$$

and λ is the fugacity

$$\lambda = \exp(\beta\mu) \quad . \tag{2.5}$$

The right-hand side of Eq. (2.4) may be interpreted as the amplitude of finding the state $|\mathbf{k}_1\mathbf{k}_2..\mathbf{k}_N\rangle$ at the imaginary time $-i\beta$ when the state $|\mathbf{k}_1\mathbf{k}_2..\mathbf{k}_N\rangle$ is given at time zero. Let us write Eq. (2.4) as the Feynman-Dyson diagrammatic expansion as shown in Fig. 1. In the figure the circular boxes mean the connected diagram with all order interactions. Let $C_\nu(\kappa_\nu)$ be the contribution of the connected diagram with ν particles with momenta $\mathbf{k}_1, \mathbf{k}_2, \ldots, \mathbf{k}_\nu$ as shown in Fig. 2, then

$$\mathrm{tr}_N\, e^{-\beta H} = \sum_{\{m_\nu\}} \prod_\nu \frac{1}{m_\nu !} \left(\sum_{\kappa_\nu} C_\nu\,(\kappa_\nu)\,\right)^{m_\nu} \quad , \tag{2.6}$$

where the positive integer m_ν is selected so as to satisfy

$$\sum_\nu \nu m_\nu = N \quad .$$

The division by $\Pi_\nu\, m_\nu!$ is to avoid counting the same amplitude more than once. This is in accord with the basic rule of statistical mechanics that each distinct configuration must be counted only once. Summing over N, we find

$$\Xi = \prod_{m_\nu=0}^{\infty} \frac{1}{m_\nu!} \left(\lambda^\nu \sum_{\kappa_\nu} C_\nu(\kappa_\nu) \right)^{m_\nu}$$

$$= \exp \left[\sum_{\nu=1}^{\infty} \lambda^\nu \, (\mathrm{tr}_\nu \, e^{-\beta H})_c \right] \quad . \tag{2.7}$$

Hereafter we use the suffix n instead of ν. The subscript c denotes that only the connected diagrams are kept. We write Eq. (2.7) as

$$\Xi = \Xi_0 \cdot \Xi_{int} \quad , \tag{2.8}$$

$$\Xi_0 = \exp(\lambda \, \mathrm{tr}_1 e^{-\beta H}) \quad , \tag{2.9}$$

$$\Xi_{int} = \exp \left[\sum_{n=2}^{\infty} \lambda^n \, (\mathrm{tr}_n e^{-\beta H})_c \right]$$

$$= \exp \left[V \sum_{n=2}^{\infty} \lambda^n \, a_n^{int} \right] \quad , \tag{2.10}$$

where

$$V a_n^{int} = (\mathrm{tr}_n \, e^{-\beta H})_c \quad ,$$

and V is the volume of the system. The partition function Ξ_0 is the ideal-gas part of Ξ.

Now we express Ξ_{int} in terms of the S-matrix. Let us first calculate the term from n=2. We have

$$(\mathrm{tr}_2 e^{-\beta H})_c = \mathrm{tr}_2 (e^{-\beta H} - e^{-\beta H_0})$$

$$= -\frac{1}{\pi}\int_0^\infty dE\, e^{-\beta E}\, \mathrm{Im}\, tr_2(G-G_0) \quad , \qquad (2.11)$$

where

$$G = \frac{1}{E - H} \quad , \qquad G_0 = \frac{1}{E - H_0} \quad . \qquad (2.12)$$

Using the identity[2.1] in the formal theory of scattering(see Appendix A)

$$tr(S^{-1} \overleftrightarrow{\frac{\partial}{\partial E}} S) = -4i\, \mathrm{Im}\, tr(G-G_0) \quad , \qquad (2.13)$$

Eq. (2.11) can be written as

$$(tr_2\, e^{-\beta H})_c = \frac{1}{4\pi i}\int_0^\infty dE\, e^{-\beta E}\, (tr_2\, S^{-1} \overleftrightarrow{\frac{\partial}{\partial E}} S)_c \quad . \qquad (2.14)$$

One can obtain the similar result as above for the terms $n \geqq 3$;

$$(tr_n\, e^{-\beta H})_c = \frac{1}{4\pi i}\int_0^\infty dE\, e^{-\beta E}\, (tr_n\, S^{-1} \overleftrightarrow{\frac{\partial}{\partial E}} S)_c \quad . \qquad (2.15)$$

Eq. (2.15) can be extended to quantum statistics[2.1]. Also the quantity Ξ_0 must be replaced by the one calculated with quantum statistics, and is given as follows[2.2]:

$$\Xi_0 = \exp\,[\, V \sum_{n=1}^{\infty} \lambda^n a_n^{(0)}\,] \quad , \qquad (2.16)$$

$$V a_n^{(0)} = \frac{(-\gamma)^{n-1}}{n}\, \frac{gV}{(2\pi)^3} \int d^3p\, e^{-n\beta\sqrt{p^2+m^2}} \quad , \qquad (2.17)$$

where g is the statistical weight of spin, and

$$\gamma = \begin{cases} +1 & \text{(the Fermi-Dirac statistics)} \\ -1 & \text{(the Bose-Einstein statistics)} \\ 0 & \text{(the Boltzmann statistics)} \end{cases} .$$

From Eqs. (2.10) and (2.16), the partition function can be expressed as

$$\Xi = \exp(V \sum_{n=1}^{\infty} \lambda^n a_n) \quad , \tag{2.18}$$

$$a_n = a_n^{(0)} + a_n^{int} \quad (n \geqq 2) \quad ,$$

$$a_1 = a_1^{(0)} \quad . \tag{2.19}$$

In the application to high-energy heavy-ion reactions, contributions of a_n^{int} $(n \geqq 3)$ to the grand partition function could be negligible. In the next section we express the two-particle correlation function due to interactions in terms of the scattering phase shifts by taking account of only a_2^{int}.

§3. Phase-shift representation for two-particle correlation function

By using the relation

$$S = 1 - 2\pi i \delta(E-H_0)T \qquad (3.1)$$

Eq. (2.14) can be divided into three terms:

$$(\mathrm{tr}_2\, e^{-\beta H})_c$$

$$= \int_0^\infty dE\, e^{-\beta E}\, \mathrm{tr}_2\{ -\frac{1}{2}\frac{\partial}{\partial E}[\delta(E-H_0)(T+T^+)]$$

$$-\pi i[\delta(E-H_0)T^+\delta(E-H_0)\frac{\partial T}{\partial E} - \delta(E-H_0)\frac{\partial T^+}{\partial E}\delta(E-H_0)T]$$

$$-\pi i[\delta(E-H_0)T^+\frac{\partial\delta(E-H_0)}{\partial E}T - \frac{\partial\delta(E-H_0)}{\partial E}T^+\delta(E-H_0)T]\}. \qquad (3.2)$$

The third term above gives no contribution, because it reads

$$-\pi i \sum_{ab} e^{-\beta E_b}\frac{\partial\delta(E_b-E_a)}{\partial E_b}[|\langle a|T|b\rangle|^2 - |\langle b|T|a\rangle|^2]. \qquad (3.3)$$

The second term in Eq. (3.2) which we denote as A_2 can be written as follows:

$$A_2 = -\pi i \sum_{ab} e^{-\beta E_a}\delta(E_a-E_b)[T^+_{ba}(E_b)\frac{\overleftrightarrow{\partial}}{\partial E_b}T_{ba}(E_b)] \qquad (3.4)$$

$$= -\pi i \frac{1}{2} \left[\frac{V}{(2\pi)^3}\right]^4 \sum_{\text{spin } a,b} \int d^3p_1 d^3p_2 d^3p_1' d^3p_2' \, e^{-\beta E_a}$$

$$\times \delta(E_a - E_b) \left[T^+_{ba}(E_b) \frac{\overleftrightarrow{\partial}}{\partial E_b} T_{ba}(E_b)\right] \quad , \qquad (3.5)$$

where

$$E_a = \sqrt{p_1^2+m^2} + \sqrt{p_2^2+m^2} \quad , \quad E_b = \sqrt{p_1'^2+m^2} + \sqrt{p_2'^2+m^2} \quad .$$

Division by 2! in Eq. (3.5) is done from the same reason as the division by $\prod_\nu m_\nu!$ in Eq. (2.6). Note that the replacement of summation by integration is done relativistically[3.1]. The contribution of inelastic reaction is neglected. Using the relations

$$T_{ba} = -\frac{(2\pi)^4 \delta^{(3)}(\mathbf{p}_1'+\mathbf{p}_2'-\mathbf{p}_1-\mathbf{p}_2)}{V^2} \frac{\sqrt{s}}{\sqrt{p_1^0 p_2^0 p_1'^0 p_2'^0}} f_{ba} \quad , \qquad (3.6)$$

and

$$\frac{(2\pi)^3}{V} \delta^{(3)}(0) \to 1 \quad , \qquad (3.7)$$

we obtain the expression for A_2 as

$$A_2 = \left[\frac{V}{(2\pi)^3}\right]^2 \sum_{\text{spin } a,b} \int \frac{d^3p_1 d^3p_2}{p_1^0 \, p_2^0} e^{-\beta(p_1^0+p_2^0)} \frac{(p_1^0+p_2^0)\sqrt{s}}{4}$$

$$\times \frac{1}{V} \left(\frac{-i}{4}\right) \int d\Omega_{p'} \left(f^*_{ba} \frac{\overleftrightarrow{\partial}}{\partial p'} f_{ba}\right)_{p'=p} \quad , \qquad (3.8)$$

where f_{ba} is the scattering amplitude of particles with momenta p_1 and p_2 to p_1' and p_2', p is the magnitude of momentum of particles in their c.m. system, and

$$s = (p_1+p_2)^2 \quad , \quad p_k^0 = \sqrt{p_k^2 + m^2} \quad (k=1,2) \quad . \tag{3.9}$$

The first term in Eq. (3.2) which we call as A_1 becomes

$$A_1 = [\frac{V}{(2\pi)^3}]^2 \sum_{\text{spin } a,b} \int \frac{d^3p_1 d^3p_2}{p_1^0\, p_2^0} e^{-\beta(p_1^0+p_2^0)}$$

$$\times \frac{\beta\pi}{V} \frac{\sqrt{s}}{2} (f_{aa} + f_{aa}^*)_{\theta=0} \quad , \tag{3.10}$$

θ being the c.m. scattering angle.

In the following we treat the case of spinless particles in order to simplify the formulation. We will consider the case of particles with spin later. By using the expansion

$$f(\theta) = \frac{1}{2ip} \sum_L (2L+1)(e^{2i\delta_L} - 1)P_L(\cos\theta) \quad , \tag{3.11}$$

we obtain the identity

$$\sum_L (2L+1)\frac{d\delta_L}{dp} = -\frac{ip^2}{4\pi} \int d\Omega_p (f^* \overleftrightarrow{\frac{\partial}{\partial p}} f) + \frac{1}{2}\frac{\partial}{\partial p}(pf^*+pf)_{\theta=0} \quad . \tag{3.12}$$

Then Eq. (3.2) becomes

$$(\mathrm{tr}_2\ e^{-\beta H})_c$$

$$= A_1 + A_2$$

$$= [\frac{V}{(2\pi)^3}]^2 \int \frac{d^3p_1 d^3p_2}{p_1^0\ \ p_2^0}\ e^{-\beta(p_1^0+p_2^0)}\ \frac{1}{V}\ \{\frac{(p_1^0+p_2^0)\sqrt{s}}{4}$$

$$\times[\frac{\pi}{p^2}\ \sum_L\ (2L+1)\ \frac{d\delta_L}{dp} - \frac{\pi}{2p^2}\frac{\partial}{\partial p}\ (pf+pf^*)_{\theta=0}]$$

$$+ \frac{\beta\pi}{2}\sqrt{s}\ (f + f^*)_{\theta=0}\ \} \quad . \qquad (3.13)$$

Thus we obtain the following result:

$$\lambda^2 V a_2^{int} = \lambda^2\ (\mathrm{tr}_2\ e^{-\beta H})_c$$

$$= \frac{1}{2}\int d^3p_1 d^3p_2\ C^{int}(\mathbf{p}_1,\mathbf{p}_2) \quad , \qquad (3.14)$$

where

$$C^{int}(\mathbf{p}_1,\mathbf{p}_2)$$

$$= [\frac{\lambda V}{(2\pi)^3}]^2\ e^{-\beta(p_1^0+p_2^0)}\{\ \frac{(p_1^0+p_2^0)\sqrt{s}}{4p_1^0\ p_2^0}\ \frac{1}{V}\ \frac{2\pi}{p^2}\ \sum_L(2L+1)\ \frac{d\delta_L}{dp}$$

$$+ \frac{\sqrt{s}}{2Vp_1^0p_2^0}\ [2\pi\beta(f+f^*)_{\theta=0} - \frac{(p_1^0+p_2^0)\pi}{2p^2}\ \frac{\partial}{\partial p}(pf+pf^*)_{\theta=0}]\} \ .(3.15)$$

The quantity C^{int} becomes the dynamical two-particle correlation function due to the interactions, which we shall discuss in §5. We define a quantity $R^{int}(\mathbf{p}_1,\mathbf{p}_2)$ as

$$R^{int}(\mathbf{p}_1,\mathbf{p}_2) = C^{int}(\mathbf{p}_1,\mathbf{p}_2)/(\frac{1}{\sigma_{in}}\frac{d\sigma}{d^3p_1})_0(\frac{1}{\sigma_{in}}\frac{d\sigma}{d^3p_2})_0 , \quad (3.16)$$

σ_{in} being the inelastic total cross section. For ideal Boltzmann gas the inclusive cross section is given as

$$(\frac{1}{\sigma_{in}}\frac{d\sigma}{d^3p})_0 = \frac{\lambda V}{(2\pi)^3} e^{-\beta p^0} . \quad (3.17)$$

Then $R^{int}(\mathbf{p}_1,\mathbf{p}_2)$ can be expressed in terms of phase shifts as

$$R^{int}(\mathbf{p}_1,\mathbf{p}_2) = \frac{(p_1^0+p_2^0)\sqrt{s}}{4p_1^0p_2^0}\frac{1}{V} 8\pi \sum_L (2L+1)R_L(p) , \quad (3.18)$$

where

$$R_L(p) = \frac{1}{p^2}\sin\delta_L [\frac{2\beta p}{p_1^0+p_2^0}\cos\delta_L + \frac{d\delta_L}{dp}\sin\delta_L] . \quad (3.19)$$

For the case of particles with spin, Eqs. (3.17), (3.18) and (3.19) are replaced as follows:

$$(\frac{1}{\sigma_{in}}\frac{d\sigma}{d^3p})_0 = \frac{gV\lambda}{(2\pi)^3} e^{-\beta p^0} , \quad (3.20)$$

$$R^{int}(\mathbf{p}_1,\mathbf{p}_2) = \frac{(p_1^0+p_2^0)\sqrt{s}}{4p_1^0p_2^0}\frac{1}{V}\frac{8\pi}{g^2}\sum_S\sum_J (2J+1)R_J^S(p) , \quad (3.21)$$

$$R_J^S(p) = \frac{1}{p^2} \sin\delta_J^S \left[\frac{2\beta p}{p_1^0+p_2^0} \cos\delta_J^S + \frac{d\delta_J^S}{dp} \sin\delta_J^S \right] , \qquad (3.22)$$

where J and S are total angular momentum and spin, respectively.

The correlation R^{int} has the following features: (i) The expression is simple and relativistic, and (ii) it is expressed in terms of phase shift of which we have a large amount of experimental data. In the energy region we deal with in §5, the first term in Eq. (3.19) is dominant. (iii) So if the interaction is attractive (repulsive), the correlation becomes positive (negative). (iv) Contribution of s wave is dominant in the small relative momentum region, because

$$R_L(p) \xrightarrow[p \to 0]{} \begin{cases} \text{finite} & (L=0) \\ 0 & (L\neq 0) \end{cases} . \qquad (3.23)$$

§4. Identical particle effect

In the quantum statistics there is an interferometric correlation effect of identical particles even for ideal gas known as the Hanbury Brown-Twiss effect in radio astrophysics.[4.1] In this section we derive the correlation function for various statistics.

The fluctuation of particle number for the system of identical free particles is given by the relation

$$\lambda^2 \frac{\partial^2}{\partial\lambda^2} \log \Xi_0$$

$$= V \sum_{n=2} n(n-1)\, a_n^{(0)}\, \lambda^n \tag{4.1}$$

$$= \int d^3p\, \frac{gV}{(2\pi)^3} (-\gamma)\lambda^2\, e^{-2\beta p^0}\, \frac{1}{(1+\gamma\lambda e^{-\beta p^0})^2} \tag{4.2}$$

$$= \int d^3p_1 d^3p_2\, \frac{gV}{(2\pi)^3} (-\gamma)\lambda^2\, e^{-\beta(p_1^0+p_2^0)}\, \delta^{(3)}(\mathbf{p}_1-\mathbf{p}_2)$$

$$\times \frac{1}{[1+\gamma\lambda e^{-\beta(p_1^0+p_2^0)/2}]^2}\ , \tag{4.3}$$

where g is the statistical weight of spin. The integrand of Eq. (4.3), which we denote as $C^{(0)}(\mathbf{p}_1,\mathbf{p}_2)$, can be interpreted as the correlation function of identical free particles as shown in §5:

$$C^{(0)}(\mathbf{p}_1,\mathbf{p}_2) = \left(\frac{1}{\sigma_{in}}\frac{d\sigma}{d^3p_1}\right)_0 \left(\frac{1}{\sigma_{in}}\frac{d\sigma}{d^3p_2}\right)_0 \frac{(2\pi)^3}{gV}\,\delta^{(3)}(\mathbf{p}_1-\mathbf{p}_2)$$

$$\times \frac{(-\gamma)}{[1+\gamma\lambda e^{-\beta(p_1^0+p_2^0)/2}]^2} \quad . \tag{4.4}$$

$C^{(0)}(\mathbf{p}_1,\mathbf{p}_2)$ has a definite sign independent of $\mathbf{p}_1$ and $\mathbf{p}_2$. As the condition $|\lambda e^{-\beta p^0}|<<1$ is fulfilled in our application to haevy-ion reactions in the following section, Eq. (4.4) can be written approximately as

$$C^{(0)}(\mathbf{p}_1,\mathbf{p}_2) = \left(\frac{1}{\sigma_{in}}\frac{d\sigma}{d^3p_1}\right)_0 \left(\frac{1}{\sigma_{in}}\frac{d\sigma}{d^3p_2}\right)_0 (-\gamma)\,\frac{(2\pi)^3}{gV}\,\delta^{(3)}(\mathbf{p}_1-\mathbf{p}_2) \ . \tag{4.5}$$

We define $R^{(0)}(\mathbf{p}_1,\mathbf{p}_2)$ as

$$R^{(0)}(\mathbf{p}_1,\mathbf{p}_2) = C^{(0)}(\mathbf{p}_1,\mathbf{p}_2) \Big/ \left(\frac{1}{\sigma_{in}}\frac{d\sigma}{d^3p_1}\right)_0 \left(\frac{1}{\sigma_{in}}\frac{d\sigma}{d^3p_2}\right)_0$$

$$= (-\gamma)\,\frac{(2\pi)^3}{gV}\,\delta^{(3)}(\mathbf{p}_1-\mathbf{p}_2) \quad . \tag{4.6}$$

We replace hereafter the delta function $\delta^{(3)}(\mathbf{p}_1-\mathbf{p}_2)$ with

$$\frac{1}{(\sqrt{2\pi}\sigma')^3}\, e^{-(\mathbf{p}_1-\mathbf{p}_2)^2/2\sigma'^2} \qquad ,$$

considering the finiteness of volume of the thermal system. From Eq. (3.7) the parameter σ' can be determined as

$$\sigma' = \frac{\sqrt{2\pi}}{V^{1/3}} \quad . \tag{4.7}$$

Then we obtain

$$C^{(0)}(\mathbf{p}_1,\mathbf{p}_2)$$

$$= \left(\frac{1}{\sigma_{in}}\frac{d\sigma}{d^3p_1}\right)_0 \left(\frac{1}{\sigma_{in}}\frac{d\sigma}{d^3p_2}\right)_0 \frac{(-\gamma)}{g}\, e^{-(\mathbf{p}_1-\mathbf{p}_2)^2/2\sigma'^2} \quad , \tag{4.8}$$

and

$$R^{(0)}(\mathbf{p}_1,\mathbf{p}_2) = \frac{(-\gamma)}{g}\, e^{-(\mathbf{p}_1-\mathbf{p}_2)^2/2\sigma'^2} \quad . \tag{4.9}$$

§5. Two-particle correlation in high-energy heavy-ion reactions at a few hundred MeV per nucleon

In this section the expression of the two-particle correlation function is derived. We apply it to heavy-ion reactions at a few hundred MeV/A. Contributions of the pion production can be neglected at this energy.

In the following we employ the simple Kapusta's nuclear fireball model[5.1] for the statistical system without interaction. This system is described by the grand partition function Ξ_0. Details of the fireball model will be presented in Appendix B.

The two-particle correlation function $C_b(p_1,p_2)$ at fixed impact parameter b is defined as

$$C_b(p_1,p_2) = [\frac{1}{\sigma_{in}} \frac{d\sigma}{d^3p_1 d^3p_2}]_b - [\frac{1}{\sigma_{in}} \frac{d\sigma}{d^3p_1}]_b [\frac{1}{\sigma_{in}} \frac{d\sigma}{d^3p_2}]_b \quad . \tag{5.1}$$

Here $[(d\sigma/d^3p)/\sigma_{in}]_b$ and $[(d\sigma/d^3p_1d^3p_2)/\sigma_{in}]_b$ are the single particle and the two-particle distributions at fixed impact parameter b , respectively. The correlation function can be obtained from the grand partition function $\Xi = \Xi_0 \cdot \Xi_{int}$ in the following. The fluctuation of the number n_b at fixed impact parameter b is given by

$$\langle n_b(n_b-1)\rangle - \langle n_b\rangle^2 = \int d^3p_1 d^3p_2 \; C_b(p_1,p_2) \quad , \tag{5.2}$$

and can be expressed in terms of Ξ of the system at the impact parameter b by using Eqs. (2.18), (3.14) and (4.1):

$$\lambda^2 \frac{\partial^2}{\partial\lambda^2} \log \Xi$$

$$= V \sum_{n=2} n(n-1)a_n^{(0)}\lambda^n + V\lambda^2 a_n^{int}$$

$$= \int d^3p_1 d^3p_2 \, [\, C_b^{(0)}(\mathbb{p}_1,\mathbb{p}_2) + C_b^{int}(\mathbb{p}_1,\mathbb{p}_2) \,] \quad , \tag{5.3}$$

where $C_b^{(0)}(\mathbb{p}_1,\mathbb{p}_2)$ and $C_b^{int}(\mathbb{p}_1,\mathbb{p}_2)$ are previously given in Eqs. (4.8) and (3.18), respectively. Thus we get

$$C_b(\mathbb{p}_1,\mathbb{p}_2) = C_b^{(0)}(\mathbb{p}_1,\mathbb{p}_2) + C_b^{int}(\mathbb{p}_1,\mathbb{p}_2) \quad . \tag{5.4}$$

The single particle distribution which we denote as $I_b(\mathbb{p})$ is obtained from the partition function Ξ, and can be written as

$$I_b(\mathbb{p}) = I_b^{(0)}(\mathbb{p}) + \int d^3p' \, C_b^{int}(\mathbb{p},\mathbb{p}') \quad , \tag{5.5}$$

where $I_b^{(0)}(\mathbb{p})$ is the single particle distribution obtained from the partition function Ξ_0 and is given in Eq. (3.17). Eq. (5.5) is obtained from the relation

$$\langle n_b \rangle = \lambda\frac{\partial}{\partial\lambda} (\log \Xi_0 + \log \Xi_{int})$$

$$= \int [\frac{1}{\sigma_{in}} \frac{d\sigma}{d^3p}]_b d^3p \quad . \tag{5.6}$$

From the definition of the function $R_b^{int}(\mathbb{p}_1,\mathbb{p}_2)$ at fixed b [Eq. (3.16)], Eq. (5.5) becomes

$$I_b(\mathbb{p}) = I_b^{(0)}(\mathbb{p}) \, [\, 1 + \varepsilon_b(\mathbb{p}) \,] \quad , \tag{5.7}$$

where

$$\varepsilon_b(\mathbb{p}) = \int d^3p' \; I_b^{(0)}(\mathbb{p}') \; R_b^{int}(\mathbb{p},\mathbb{p}') \quad . \tag{5.8}$$

To compare with the experiments, the single particle distribution $I_b(\mathbb{p})$ and the two-particle distribution

$$\left[\frac{1}{\sigma_{in}} \frac{d\sigma}{d^3p_1 d^3p_2}\right]_b = C_b(\mathbb{p}_1,\mathbb{p}_2) + I_b(\mathbb{p}_1) I_b(\mathbb{p}_2) \tag{5.9}$$

should be integrated over the impact parameter. The integrated two-particle correlation which we denote as $C(\mathbb{p}_1,\mathbb{p}_2)$ is given by

$$C(\mathbb{p}_1,\mathbb{p}_2) = \langle\, C_b(\mathbb{p}_1,\mathbb{p}_2) + I_b(\mathbb{p}_1) I_b(\mathbb{p}_2) \,\rangle_b$$

$$- \langle\, I_b(\mathbb{p}_1) \,\rangle_b \langle\, I_b(\mathbb{p}_2) \,\rangle_b \quad , \tag{5.10}$$

where

$$\langle\, Q_b \,\rangle_b \stackrel{d}{\equiv} \frac{1}{b_{max}^2} \int_0^{b_{max}} 2\pi b\, db \; Q_b \quad , \tag{5.11}$$

b_{max} being the maximum impact parameter. The function $I_b(\mathbb{p})$ and $C_b(\mathbb{p}_1,\mathbb{p}_2)$ are dependent of the impact parameter, because in these functions the quantities T, μ, and V vary with it. The explicit dependence is determined by solving the equation of state for the fireball.(See Appendix B)

We calculate $C(\mathbb{p}_1,\mathbb{p}_2)$ for the collision of equal-mass nuclei. In this case the temperature is shown to be independent of the impact parameter. So we can write

$$I_b^{(0)}(\mathbb{p}) = n_b^{(0)}\ \hat{I}^{(0)}(\mathbb{p}) \tag{5.12}$$

for the ideal gas, where $n_b^{(0)}$ is the total proton number in the fireball at the fixed impact parameter, and the function $\hat{I}^{(0)}(\mathbb{p})$ is independent of b. Eq. (3.21) is written as

$$R_b^{int}(\mathbb{p}_1,\mathbb{p}_2) = \frac{1}{V}\ \hat{R}^{int}(\mathbb{p}_1,\mathbb{p}_2) \quad , \tag{5.13}$$

where

$$\hat{R}^{int}(\mathbb{p}_1,\mathbb{p}_2) = 8\pi\ \frac{(p_1^0+p_2^0)\sqrt{s}}{4p_1^0p_2^0}\ \sum_S \sum_J\ (2J+1)R_J^S(p) \quad , \tag{5.14}$$

$\hat{R}^{int}(\mathbb{p}_1,\mathbb{p}_2)$ being independent of b. From Eqs. (5.7), (5.8) and (5.13) the single-particle distribution integrated over the impact parameter, which we denote as I(p), is obtained as follows:

$$I(\mathbf{p}) = I^{(0)}(\mathbf{p})[\, 1 + \hat{\varepsilon}(\mathbf{p})\,] \quad , \tag{5.15}$$

where

$$I^{(0)}(\mathbf{p}) = \langle n_b^{(0)} \rangle_b \, \hat{I}^{(0)}(\mathbf{p}) \quad , \tag{5.16}$$

and

$$\hat{\varepsilon}(\mathbf{p}) = \frac{1}{\hat{V}_0} \int d^3p' \, \hat{I}^{(0)}(\mathbf{p}') \, \hat{R}^{int}(\mathbf{p},\mathbf{p}') \quad . \tag{5.17}$$

Here $\hat{V}_0$ is related to V through the following relations;

$$V = \hat{V}_0 \, n_b^{(0)} \quad , \tag{5.18}$$

$$\hat{V}_0 = \frac{2}{\rho_c} \frac{n_b}{n_b^{(0)}} \quad , \tag{5.19}$$

where ρ_c is the density of the thermal system (i.e. the critical density in the fireball model[5.1]), and is one of parameters in our model. The ratio $n_b/n_b^{(0)}$ becomes independent of the impact parameter in the case of equal-mass nuclei.

Finally we define the normalized correlation function $R(\mathbf{p}_1,\mathbf{p}_2)$ as

$$R(\mathbf{p}_1,\mathbf{p}_2) = C(\mathbf{p}_1,\mathbf{p}_2)/I(\mathbf{p}_1)I(\mathbf{p}_2) \quad . \tag{5.20}$$

This function is obtained from Eqs. (5.10) and (5.15), and written as

$$R(\mathbf{p}_1,\mathbf{p}_2) = R_L + R^{HBT}(\mathbf{p}_1,\mathbf{p}_2) + R^{dyn}(\mathbf{p}_1,\mathbf{p}_2) \quad . \tag{5.21}$$

The first term in Eq. (5.21) is given by

$$R_L = \frac{< n_b^2 >_b}{< n_b >_b^2} - 1 \quad . \tag{5.22}$$

It represents the fluctuation of proton number due to its impact parameter dependence, and is independent of $\mathbf{p}_1$ and $\mathbf{p}_2$. To select high-multiplicity events we restrict $y_{max} \lesssim 0.7$, y_{max} being defined by

$$y_{max} = \frac{b_{max}}{R_p + R_T} \quad , \tag{5.23}$$

where $R_p(=R_T)$ is the radius of the projectile(target) nucleus. In this case, R_L can be negligible as shown in Figs. 3(a) and (b). The second term, $R^{HBT}(\mathbf{p}_1,\mathbf{p}_2)$, is due to the identical particle effect (Hanbury Brown-Twiss effect), and is expressed as

$$R^{HBT}(\mathbf{p}_1,\mathbf{p}_2) = \frac{C^{HBT}(\mathbf{p}_1,\mathbf{p}_2)}{[\ 1 + \hat{\varepsilon}(\mathbf{p}_1)\ ][\ 1 + \hat{\varepsilon}(\mathbf{p}_2)\ ]} \quad , \tag{5.24}$$

where

$$C^{HBT}(\mathbf{p}_1,\mathbf{p}_2) = -\frac{1}{2}\frac{1}{\langle n_b \rangle_b^2} \langle n_b^2 \exp^{-(\mathbf{p}_1-\mathbf{p}_2)^2/2\sigma'^2} \rangle_b \quad . \tag{5.25}$$

The b dependence of σ' can be determined by Eqs. (4.7) and (5.18). The last term in Eq. (5.21), $R^{dyn}(\mathbf{p}_1,\mathbf{p}_2)$, represents the dynamical correlation due to the nucleon-nucleon interactions, and is written as

$$R^{dyn}(\mathbf{p}_1,\mathbf{p}_2) = \frac{C^{dyn}(\mathbf{p}_1,\mathbf{p}_2)}{[\ 1 + \hat{\varepsilon}(\mathbf{p}_1)\ ][\ 1 + \hat{\varepsilon}(\mathbf{p}_2)\ ]} \quad , \tag{5.26}$$

where

$$C^{dyn}(\mathbf{p}_1,\mathbf{p}_2) = \frac{1}{\langle V \rangle_b} \hat{R}^{int}(\mathbf{p}_1,\mathbf{p}_2) \quad , \tag{5.27}$$

$\hat{R}^{int}(\mathbf{p}_1,\mathbf{p}_2)$ being given in Eq. (5.14).

Using Eq. (5.21), we calculate the proton-proton correlation function $R(\mathbf{p}_1,\mathbf{p}_2)$ for various reactions at 0.4 GeV/A in the laboratory system. At this energy the contribution of pion production can be neglected. In Fig. 4(a) the dependence of the correlation function on azimuthal angle between two protons for reaction Fe+Cu is shown at the same kinetic energy (T_L) and polar scattering angle (θ_L) for both protons. Asymmetry of the mass and the charge between Fe and Cu is neglected here. The functions $R^{dyn}(\mathbf{p}_1,\mathbf{p}_2)$, $R^{HBT}(\mathbf{p}_1,\mathbf{p}_2)$ and $R(\mathbf{p}_1,\mathbf{p}_2)$ are shown separately. We put tentatively $y_{max}=0.5$ and $\rho_c=\rho_0$ in Fig. 4(a); $y_{max}=0.5$ and $\rho_c=0.3\rho_0$ in Fig. 4(b). The quantity ρ_0 is the normal density of nuclear matter. The same correlation functions for reaction Ar+KCl are shown in Fig. 5(a) and (b) with the same parameters used in Fig. 4(a) and (b). The y_{max} dependence of $R(\mathbf{p}_1,\mathbf{p}_2)$ is shown in Figs. 6(a)(b) and 7(a)(b) for $\rho_c=\rho_0$ and $\rho_c=0.3\rho_0$ at the same T_L and θ_L as used in Fig. 4. We can see the value of R at the peak increases with y_{max}.

The ρ_c dependence of $R(\mathbf{p}_1,\mathbf{p}_2)$ is shown in Fig. 8(a) and (b) with the same θ_L and T_L as in Fig. 4. In the calculation we take account of the partial waves L<6[5.2]. The peak of R^{dyn} is due to the strong attractive force in the $^1S_0$ channel of proton-proton scattering. The results are almost well described with only the s-wave contribution as shown in Fig. 9, and agree qualitatively with Koonin's nonrelativistic model[5.3]. The relativistic effect decreases the correlation function by a few percent at the peak of R.

The θ_L and T_L dependence of $R(\mathbf{p}_1,\mathbf{p}_2)$ are shown in Figs. 10(a)(b) and 11(a)(b) with the same parameters as in Fig. 4(a). The dependence of $R(\mathbf{p}_1,\mathbf{p}_2)$ on projectile and target nuclei is also shown in Fig. 12(a)-(c).

At higher energies we must consider the contribution from the pion production. In the statistical model the proton-proton correlation becomes small at high energies. Because the density of pion increases at high energies and correspondingly that of proton decreases for fixed hadron density (See Appendix B). In the next section we discuss the pion contribution to the correlation function.

§6. Two-particle correlation in high-energy heavy-ion reactions at a few GeV per nucleon

In this section we generalize the formulas for the single particle distribution and the two-particle correlation function in the previous section so as to include the pion contribution and apply them to the heavy-ion reaction at higher energies. In section 2 we have formulated the grand partition function for the system composed of one species of particles by using the S matrix. Eqs. (2.7)∿(2.10) are readily extended for the system of more than two species of hadrons[6.1]. For example, we have the following results for the system of pions and nucleons:

$$\Xi = \Xi_0 \cdot \Xi_{int} \quad , \tag{6.1}$$

$$\Xi_0 = \Xi_0^{(N)} \cdot \Xi_0^{(\pi)} \quad , \tag{6.2}$$

$$\Xi_{int} = \exp\left[\sum_{m=0}^{\infty} \sum_{n=0}^{\infty} \lambda^n C_{nm} \right] \quad , \tag{6.3}$$

where

$$C_{nm} = (tr_{nm} e^{-\beta H})_c \qquad (n+m \geqq 2) \quad .$$

Here $\Xi_0^{(N)}$ and $\Xi_0^{(\pi)}$ are the ideal gas parts of the partition function Ξ for the nucleon and the pion, respectively. The quantity C_{nm} corresponds to C_ν in §2, and is the contribution of the connected diagram with m pions and n nucleons as shown in Fig. 13. From Eq. (6.3) one can obtain the diagrammatic expansion of $\log \Xi_{int}$ as shown in Fig. 14. In application to the heavy-ion reaction, contributions of C_{nm} $(n,m \geqq 3)$ to the grand partition function could be negligible. Thus Eq. (6.3) can be written as

$$\log \Xi_{int} = \lambda^2 C_{20} + \lambda C_{11} + C_{02} \quad . \tag{6.4}$$

The two-particle correlation function for hadrons A and B (A,B = nucleon or pion) at fixed impact parameter b is defined as

$$C_{AB,b}(\mathbf{p}_1,\mathbf{p}_2) = \left[\frac{1}{\sigma_{in}} \frac{d\sigma^{AB}}{d^3p_1 d^3p_2}\right]_b - \left[\frac{1}{\sigma_{in}} \frac{d\sigma^{A}}{d^3p_1}\right]_b \left[\frac{1}{\sigma_{in}} \frac{d\sigma^{B}}{d^3p_2}\right]_b \quad . \tag{6.5}$$

This correlation function can be obtained from the grand partition function by using the same procedure done in

Eqs. (5.2) - (5.4). We have

$$C_{AB,b}(p_1,p_2) = \delta_{AB}\, C^{(0)}_{AA,b}(p_1,p_2) + C^{int}_{AB,b}(p_1,p_2) \quad . \tag{6.6}$$

The first term $C^{(0)}_{AA,b}$, is the correlation due to the identical particle effect:

$$C^{(0)}_{AB,b}(p_1,p_2) = I^{(0)}_{A,b}(p_1)\; I^{(0)}_{A,b}(p_2)\; R^{(0)}_{AA,b}(p_1,p_2) \quad , \tag{6.7}$$

where $I^{(0)}_{A,b}(p)$ is the single particle distribution obtained from the partition function $\Xi^{(A)}_0$, namely

$$I^{(0)}_{A,b}(p) = \frac{g_A \lambda_A V}{(2\pi)^3} \quad e^{-\beta p^0} \quad , \tag{6.8}$$

$$\lambda_A = e^{-\beta\mu_A} \quad . \tag{6.9}$$

Here g_A and μ_A are the statistical weight of spin and the chemical potential of the hadron A, respectively. By assuming chemical equilibrium, μ_A is given by

$$\mu_A = \begin{cases} \mu & \text{(nucleon)} \\ 0 & \text{(pion)} \ , \end{cases} \tag{6.10}$$

where μ is the chemical potential corresponding to the baryon number conservation. See Appendix B for a detailed discussion. The quantity $R_{AA}^{(0)}(\mathbf{p}_1,\mathbf{p}_2)$ in Eq. (6.7) is

$$R_{AA,b}^{(0)}(\mathbf{p}_1,\mathbf{p}_2) = -\gamma_A \frac{1}{g_A} e^{-(\mathbf{p}_1-\mathbf{p}_2)^2/2\sigma'^2} \quad , \quad (6.11)$$

where

$$\gamma_A = \begin{cases} +1 & \text{(fermion)} \\ -1 & \text{(boson)} \end{cases} \quad . \qquad (6.12)$$

The second term of Eq. (6.6), $C_{AB,b}^{int}$, is the correlation due to the interaction between the hadrons A and B:

$$C_{AB,b}^{int}(\mathbf{p}_1,\mathbf{p}_2) = \kappa_{AB}\, I_{A,b}^{(0)}(\mathbf{p}_1)\, I_{B,b}^{(0)}(\mathbf{p}_2)\, R_{AB,b}^{int}(\mathbf{p}_1,\mathbf{p}_2) \quad , \qquad (6.13)$$

where

$$\kappa_{AB} = \kappa_{BA} = \begin{cases} 1 & \text{(A=B=nucleon or pion)} \\ 1/2 & \text{(A=pion, B=nucleon)} \end{cases} \qquad (6.14)$$

and

$$R^{int}_{AB,b}(\mathbf{p}_1,\mathbf{p}_2) = \frac{8\pi}{V} \frac{(p^0_1+p^0_2)\sqrt{s}}{4p^0_1 p^0_2 g_A g_B} \sum_S \sum_J (2J+1) R^S_J(p^0_1,p^0_2,p) \quad . \tag{6.15}$$

In the Eq. (6.15) $R^S_J(p^0_1,p^0_2,p)$ is expressed as

$$R^S_J(p^0_1,p^0_2,p) = \frac{1}{p^2} \sin\delta^S_J \left[\frac{2\beta p}{(p^0_1+p^0_2)} \cos\delta^S_J + \frac{d\delta^S_J}{dp} \sin\delta^S_J \right] \quad , \tag{6.16}$$

where δ^S_J is the scattering phase shift of the collision between A and B with total spin S and total angular momentum J.

Similarly the single particle distribution at fixed impact parameter b can be obtained as

$$I_{A,b}(\mathbf{p}) \stackrel{d}{\equiv} \left[\frac{1}{\sigma_{in}} \frac{d\sigma^A}{d^3p}\right]_b$$

$$= I^{(0)}_{A,b}(\mathbf{p})[\, 1 + \varepsilon_{A,b}(\mathbf{p})\,] \quad , \tag{6.17}$$

where

$$\varepsilon_{A,b}(\mathbf{p}) = \sum_B \kappa_{AB} \int d^3p' \; I^{(0)}_{B,b}(\mathbf{p}') R^{int}_{AB,b}(\mathbf{p},\mathbf{p}') \quad . \tag{6.18}$$

In order to compare with the experiments, we should integrate the single particle and the two-particle distributions over the impact parameter as in §5. In the following we treat the collision of equal-mass nuclei. In this case we can express the quantities $I^{(0)}_{A,b}(\mathbf{p})$ and $R^{int}_{AB,b}(\mathbf{p}_1,\mathbf{p}_2)$ as follows (See Eqs. (5.12) and (5.13)):

$$I^{(0)}_{A,b}(\mathbf{p}) = n^{(0)}_{A,b}\ \hat{I}^{(0)}_{A}(\mathbf{p}) \quad , \tag{6.19}$$

$$R^{int}_{AB,b}(\mathbf{p}_1,\mathbf{p}_2) = \frac{1}{V}\ \hat{R}^{int}_{AB}(\mathbf{p}_1,\mathbf{p}_2) \quad , \tag{6.20}$$

where $n^{(0)}_{A,b}$ is the total number of the hadron A in the fire-ball at fixed impact parameter b which is obtained from the partition function $\Xi^{(0)}_{A}$ and

$$\hat{I}^{(0)}_{A}(\mathbf{p}) = \frac{1}{4\pi m_A^3}\ \frac{\beta m_A}{K_2(\beta m_A)}\ e^{-\beta p^0} \quad , \tag{6.21}$$

$$\hat{R}^{int}_{AB}(\mathbf{p}_1,\mathbf{p}_2) = 8\pi\ \frac{(p_1^0+p_2^0)\sqrt{s}}{4p_1^0p_2^0g_Ag_B}\ \sum_S \sum_J\ (2J+1)R^S_J(p_1^0,p_2^0,p). \tag{6.22}$$

Here m_A is the mass of the hadron A and $K_2(x)$ is the modified Bessel function (See Appendix B). The quantities $\hat{I}_A^{(0)}(\mathbf{p})$ and $\hat{R}_{AB}^{int}(\mathbf{p}_1,\mathbf{p}_2)$ are independent of b. For convenience we define the following quantity;

$$\hat{r}_A^{(0)} = n_{A,b}^{(0)} / n_b^{(0)} \quad , \tag{6.23}$$

where $n_b^{(0)}$ is the total proton number and $\hat{r}_A^{(0)}$ becomes independent of b for the collision of equal-mass nuclei. Using Eq. (6.23) we can express Eq. (6.19) as

$$I_{A,b}^{(0)}(\mathbf{p}) = \hat{r}_A^{(0)} \; n_b^{(0)} \; \hat{I}_A^{(0)}(\mathbf{p}) \quad . \tag{6.24}$$

From Eqs. (6.17) (6.20) and (6.24) the integrated single particle distribution which we denote as $I_A(\mathbf{p})$ can be obtained as

$$I_A(\mathbf{p}) = \hat{r}_A^{(0)} \; \langle n_b^{(0)} \rangle \; \hat{I}_A^{(0)}(\mathbf{p}) \; [\; 1 + \hat{\varepsilon}_A(\mathbf{p}) \;] \quad , \tag{6.25}$$

where

$$\langle n_b^{(0)} \rangle = \frac{1}{\pi b_{max}^2} \int_0^{b_{max}} 2\pi b db \; n_b^{(0)} \quad , \tag{6.26}$$

b_{max} being the maximum impact parameter, and

$$\hat{\varepsilon}_A(\mathbf{p}) = \frac{1}{\hat{V}_0} \sum_B \kappa_{AB} \; \hat{r}_B^{(0)} \int d^3p' \; \hat{I}_B^{(0)}(\mathbf{p}') \; \hat{R}_{AB}^{int}(\mathbf{p},\mathbf{p}') \quad . \tag{6.27}$$

Here, as in §5,

$$\hat{V}_0 = V/n_b^{(0)} \tag{6.28}$$

$$= \frac{2}{\rho_c}\left(1 + \frac{3}{2}\hat{r}_{\pi+} \right) \frac{n_b}{n_b^{(0)}} \quad , \tag{6.29}$$

where

$$\hat{r}_{\pi+} = n_{\pi+} / n_b \quad , \tag{6.30}$$

$n_{\pi+}$ and n_b being the total π^+ and proton number in the fireball obtained from the partition function Ξ, and ρ_c the critical density. Eq. (6.28) is obtained from the constraint that the hadron density be ρ_c (See Appendix B).

Finally the integrated correlation function $C_{AB}(\mathbf{p}_1,\mathbf{p}_2)$ can be obtained from Eqs. (6.6), (6.7) and (6.13). We define the normalized correlation function $R_{AB}(\mathbf{p}_1,\mathbf{p}_2)$ as

$$R_{AB}(\mathbf{p}_1,\mathbf{p}_2) = \frac{C_{AB}(\mathbf{p}_1,\mathbf{p}_2)}{I_A(\mathbf{p}_1)\ I_B(\mathbf{p}_2)} \quad . \tag{6.31}$$

Using Eqs. (6.20) and (6.24) we get the final results;

$$R_{AB}(\mathbf{p}_1,\mathbf{p}_2) = R_L + R_{AB}^{HBT}(\mathbf{p}_1,\mathbf{p}_2) + R_{AB}^{dyn}(\mathbf{p}_1,\mathbf{p}_2) \quad . \tag{6.32}$$

The first term in Eq. (6.32) is the same quantity as Eq. (5.22)

$$R_L = \frac{\langle n_b^2 \rangle}{\langle n_b \rangle^2} - 1 \quad , \tag{6.33}$$

and can be negligible for high-multiplicity events with $y_{max} \lesssim 0.7$ (y_{max} being given by Eq. (5.23)). The second term due to Hanbury Brown-Twiss effect, $R_{AB}^{HBT}(\mathbf{p}_1,\mathbf{p}_2)$, is given by

$$R_{AB}^{HBT}(\mathbf{p}_1,\mathbf{p}_2) = \frac{C_{AB}^{HBT}(\mathbf{p}_1,\mathbf{p}_2)}{[1 + \hat{\varepsilon}_A(\mathbf{p}_1)]\,[1 + \hat{\varepsilon}_B(\mathbf{p}_2)]} \quad , \tag{6.34}$$

where

$$C_{AB}^{HBT}(\mathbf{p}_1,\mathbf{p}_2) = \delta_{AB}\,\frac{(-\gamma_A)}{g_A}\,\frac{1}{\langle n_b \rangle^2}\,\langle n_b^2 \exp^{-(\mathbf{p}_1-\mathbf{p}_2)^2/2\sigma'^2} \rangle \quad . \tag{6.35}$$

The b dependence of σ' can be determined by Eqs. (4.7) and (6.28). The last term in Eq. (6.32), $R_{AB}^{dyn}(\mathbf{p}_1,\mathbf{p}_2)$, is given by

$$R_{AB}^{dyn}(\mathbf{p}_1,\mathbf{p}_2) = \frac{C_{AB}^{dyn}(\mathbf{p}_1,\mathbf{p}_2)}{[1 + \hat{\varepsilon}_A(\mathbf{p}_1)]\,[1 + \hat{\varepsilon}_B(\mathbf{p}_2)]} \quad , \tag{6.36}$$

where

$$C^{dyn}_{AB}(\mathbf{p}_1,\mathbf{p}_2) = \frac{\kappa AB}{\langle V \rangle} \; \hat{R}^{int}_{AB}(\mathbf{p}_1,\mathbf{p}_2) \quad , \tag{6.37}$$

$\hat{R}^{int}_{AB}(\mathbf{p}_1,\mathbf{p}_2)$ being given by Eq. (6.21).

In the next section, using Eqs. (6.25) and (6.32), we calculate the single particle and two-particle distributions for pions and nucleons and compare them with experiments at higher energies.

§7. Numerical results and comparison with experimental data at higher energies

In this section we give the results of numerical calculations of Eqs. (6.25) and (6.32) and compare them with the experimental data at higher energies.

7.1) the proton-proton correlation

When the incident energy becomes larger than about 1 GeV/A , effect of the pion production to various quantities can not be negligible. Fig. 15(a)-(c) show the beam-energy dependence of the azimuthal angle distribution of the proton-proton correlation $R(p_1,p_2)$ for the reactions Ar + KCl, Fe + Cu and U + U. We employ the same parameters (ρ_c, y_{max}) and the same T_L and θ_L as those in Fig. 4(a) in §5 [$\rho_c=\rho_0$, $y_{max}=0.5$, $T_L=0.1$ GeV and $\theta_L=30°$]. For fixed hadron density, the density of pion increases with incident energy and correspondingly that of proton decreases. Therefore the correlation due to proton-proton interactions becomes smaller.

Preliminary experiments [7.1] on the proton-proton correlation in the reaction Ar + KCl at 1.8 GeV/A are compared with our calculation in Fig. 16. Asymmetry of the mass and charge between Ar and KCl is neglected here. A good fit is given at $\rho_c = \rho_0$ and $y_{max} = 0.4$ as shown by a solid curve.

As the selected data have large multiplicities of charged particles, one may put $y_{max} \leq 0.8$ in this experiments. Then, in order to get comparable values to the data, we must have at least $\rho_c \geq 0.5\rho_0$. For instance, a dashed curve is obtained with $\rho_c = 0.3\rho_0$ and $y_{max} = 0.8$. In Fig. 16 the result of Koonin[7.2] is also shown by a dotted line, which agrees qualitatively with ours.

7.2) the pion-pion correlation

Figs. 17(a)-(c) and 18(a)-(c) show the dependence of the correlation function on azimuthal angle between two positive (or negative) pions in the reactions Ar + KCl, Fe + Cu and U + U at 1.8 GeV/A in the laboratory system. Same values of the kinetic energy(T_L) and the polar angle(θ_L) are taken for both pions. We put tentatively $y_{max} = 0.5$ and $\rho_c = \rho_0$. It is shown that the correlation $R^{dyn}(p_1,p_2)$ due to pion-pion interactions is almost negligible at this energy. In the calculations we take account of the partial waves $L<5$[7.3]. The y_{max} and ρ_c dependences of $R(p_1,p_2)$ are shown in Figs. 19 and 20, respectively. The correlation R for various nuclei are also shown in Fig. 21. The qualitative difference among three reactions in Fig. 21 can be easily understood from the V dependence of σ' (See Eqs. (4.7) and (6.35)). Fig. 22(a)-(c) show the beam-energy dependence. For fixed hadron density, the increase of pion multiplicity means the increase of the volume V, so σ' becomes smaller at higher beam energies.

Fig. 23 shows the correlation function $R^{dyn}(p_1,p_2)$ for π^+ and π^- . The contribution of the ρ meson resonance is very small. This is caused by the larger mass of ρ meson than the threshold of $\pi^+\pi^-$ scattering.

7.3) the pion-nucleon interaction

In the simple fireball model formulated in Appendix B.1 which we call ideal-gas model from now on, the system contains Δ resonances with zero width instead of employing realistic pion- nucleon interaction. In our model the interaction is introduced in terms of experimental scattering phase shifts with $L<5$[7.4] . So it is very interesting to compare our model with the ideal-gas model. Of course if we neglect the other interactions among pions and nucleons except the one in the I=J=3/2 channel and take the width of the Δ resonance to be zero, our model becomes equivalent to the ideal-gas model.

Using Eqs. (B.24)-(B.30) in Appendix B, we calculate the average multiplicity of π^+ per proton, the entropy per baryon and the chemical potential. The results are given in Table I. For comparison we also show in the parentheses the same quantities with the ideal-gas model. The values in Table I are independent of projectile and target nuclei. In our model the multiplicity of pion is slightly larger than the one in the ideal-gas model. Therefore the entropy per baryon of our model is also larger. The increase of pion multiplicity in our model results from the finiteness of width of the resonance. Low-mass side of the tail of the Δ resonance yields a finite contribution to the multiplicity at rather low energy of 0.8 GeV/A.

Figs. 24 and 25 show the proton and pion inclusive distributions for the reaction Ar+KCl at 0.8 GeV/A calculated by using Eq. (6.25). The dashed lines are obtained by the ideal-gas model. The data are from Ref. 7.5. The parameter y_{max} is determined so as to fit the experimental proton spectra. To fit to the pion spectra, calculated values are multiplied by the factor 1/2 - 1/3. All models based on the equilibrium assumption give rather higher pion multiplicities than observed for values of ρ_c below or equal to ρ_0. Except the normalization, our calculations fit better to the data than the ideal-gas model does in the low-energy region. This feature can be easily understood. The peak of pion spectra in the ideal-gas model is caused by the decay of Δ. As stated above, a lower mass part of the tail of Δ makes the position of the peak of pion spectra shift to lower energy.

§8. Conclusions

The nonrelativistic proton-proton correlation functions R and C for heavy-ion collisions at low beam-energies have been investigated by Koonin in terms of the soft Reid potential. We express these functions relativistically with the scattering phase shifts by using the S-matrix formulation of statistical mechanics in §5.

There are two parameters in our model; the critical density ρ_c (density of the thermal system)[Eq.(5.19) and Eq.(B.11)] and the maximum value of the impact parameter y_{max} [Eq.(5.23)]. The former is considered to be independent of the kind of colliding nuclei and their energies, but the latter may vary with different experimental situations.
We have studied the proton-proton correlation function at 400 MeV/A, using some fixed values of the parameters. The correlation $R(p_1,p_2)$ has a peak due to the strong attractive force in the $^1S_0$ channel of the proton-proton scattering. The other interactions are almost negligible in this energy region. The value of R at the peak increases with y_{max} and ρ_c. Furthermore the correlation R increases as the volume of the thermal system becomes larger. The latter is a general feature of the statistical model.

The relativistic effect decreases the correlation function by a few percent at the peak of R. The results agree qualitatively with Koonin's one by choosing appropriate values of the parameters. The pion contrbution is neglected at this energy.

In §6, in order to investigate the heavy-ion reactions at higher energies in which pion production can not be negligible, we have generalized the formulas for the single particle distribution and two-particle correlation function given in §5. To our knowledge, there has been no investigation on the heavy-ion reaction which includes the pion-nucleon and pion-pion interactions relativistically. The hydrodynamical model does not include the pion explicitly. In the nuclear cascade model the treatment of the interactions between the produced pions and the nucleons is insufficient. In §7 using the experimental data of the pion-pion, the pion-nucleon and the nucleon-nucleon scattering phase shifts, we have calculated relativistically the proton-proton and pion-pion correlations and the inclusive distributions of protons and pions.

The proton-proton correlation R decreases with incident beam-energy in our model. A good fit to experimental data has been obtained with suitable parameters. From our analyses, we find that the reasonable value of ρ_c should satisfy the condition, $\rho_c \gtrsim 0.5\rho_0$.

The contribution of the ρ meson resonance for $\pi^+\pi^-$ correlation is very small because of its larger mass than the threshold of $\pi^+\pi^-$ scattering.

The simple fireball model uses the Δ resonance with zero width instead of employing realistic pion-nucleon interaction, and so its treatment is insufficient. In our model the interaction is taken into account exactly by using the experimental phase shifts of pion-nucleon scattering. Indeed our calculation for the pion inclusive cross section in the reaction Ar + KCl at 0.8 GeV/A fits better to the data in the low-energy region than the simple fireball model does. This favourable feature in our model is caused by the low-mass tail of Δ resonance. We emphasize that, in the high-energy heavy-ion reactions, the Δ resonance should be treated as a real one with the width experimentally observed.

For three-particle correlation function, etc., the terms C_{nm} $(n,m\geq 3)$ become essential. The investigation on these contribution to the grand partition function will appear in the forthcoming paper.

Contribution of Coulomb interaction is neglected in our calculations. It is considered to be small between the particles with high momenta[8.1]. Effects of the composite particle (deuteron, alpha, etc.) production are also neglected. Our results may be altered to some extent in the region where the Coulomb effects and/or the composite particle production cannot be ignored.

Acknowledgements

The author is most grateful to Professor S. Takagi and Dr. H. Yokomi for many lively discussions, kind hospitality and careful reading through the manuscript. He would like to thank Professor T. Sawada, Dr. O. Miyamura and members of Department of Applied Mathematics, Faculty of Engineering Science, Osaka University, for useful discussions and continuous encouragements. Also he thanks Dr. R. Ihara for valuable discussion on experimental data and others.

Above all, he wishes to express his gratitude to Dr. M. Iwasaki and Dr. S. Nishiyama of Department of Physics, Kochi University, for critical discussions and helpful advices.

All the numerical calculations for this work have been carried out on the Computer System at the Computation Center of Osaka University.

Appendix A

Formal Theory of Scattering and the Derivation of Eq. (2.13)

Using the operators G and G_0 given by Eq. (2.12), we define the following operators which are functions of the complex energy E;

$$\Omega = 1 + GH_I = GG_0^{-1} \quad ,$$

$$T = H_I + H_I G H_I = H_I \Omega \quad ,$$

$$S = \Omega^{-1*}\Omega \quad , \tag{A.1}$$

where $\Omega^*(E) \equiv \Omega(E^*)$. Following identities can be derived easily from these definitions:

$$\Omega^{-1} = 1 - G_0 H_I = G_0 G^{-1} \quad , \tag{A.2}$$

$$T = H_I + H_I G_0 T \quad , \tag{A.3}$$

$$S = 1 + (G_0 - G_0^+)T \quad , \tag{A.4}$$

$$S^{-1} = 1 - (G_0 - G_0^+)T^+ \quad , \tag{A.5}$$

$$G^+ = G^* \quad , \quad G_0^+ = G_0^* \quad , \quad T^+ = T^* \quad . \tag{A.6}$$

When the variable E approaches the real axis, Eqs. (A.4) and (A.5) become

$$S = 1 - 2\pi i\delta(E-H_0)T \quad , \tag{A.7}$$

$$S^{-1} = 1 + 2\pi i\delta(E-H_0)T^+ \quad . \tag{A.8}$$

The operator S formally given by (A.1) is actually related to the S-matrix describing the actual scattering processes. From the definition (A.1) the following relation can be derived easily

$$\mathrm{tr}(S^{-1}\frac{\overleftrightarrow{\partial}}{\partial E}\,S) = 2i\mathrm{Im}\ \mathrm{tr}(\Omega^{-1}\frac{\overleftrightarrow{\partial}}{\partial E}\,\Omega) \quad . \tag{A.9}$$

Using Eqs. (A.1) and (A.2) and utilizing the fact

$$G - G_0 = GH_IG_0 = G_0H_IG \quad ,$$

one can obtain the relation;

$$\mathrm{tr}(\Omega^{-1}\frac{\overleftrightarrow{\partial}}{\partial E}\,\Omega) = -2\ \mathrm{tr}(G - G_0) \quad . \tag{A.10}$$

From Eqs. (A.9) and (A.10) we have the final result:

$$\mathrm{tr}(S^{-1}\,\frac{\overleftrightarrow{\partial}}{\partial E}\,S) = -4i\ \mathrm{Im}\ \mathrm{tr}(G - G_0) \quad . \tag{A.11}$$

Appendix B

The Statistical Model with a Simplified Participant-Spectator Geometry

In this appendix we give the brief review of the statistical model with a simplified participant-spectator geometry which has been applied to relativistic heavy-ion reactions and discuss the generalization of this model so as to include the hadron-hadron interactions.

B.1) A simplified participant-spectator geometry

Consider the collision of two heavy ions at a given impact parameter b (Fig. B-1). A certain part of projectile nucleus will meet a certain part of target nucleus. Since the energy of collision is very high, the systems P and T shown in Fig. B-1 will fly off after the collision with essentially unchanged velocity. Thus the system P(T) can be called the projectile(target) spectators. Residual parts of each nucleus, however, will hit together. If the incident energy is large enough, many hadrons(pions, kaons, etc.) can be produced and they together with hitting nucleons are called participants. This clean-cut participant-spectator model stated above is confirmed experimentally. Of course, from more detailed investigation this simple geometrical description may be altered to some extent. In the following we discuss the participants only. The system composed of these participants has been called " nuclear-fireball ".

B.2) The nuclear-fireball model

In the nuclear-fireball model the thermal equilibrium is assumed for the fireball composed of many hadrons. This fireball includes the hadronic resonances (Δ, N^*, ρ, K^*, etc.), so in this model the hadron-hadron interactions are partially taken into account in terms of resonance approximation.

The grand partition function of this thermal system can be written as

$$\Xi^{(0)}(\beta, \mu_i, V) = \prod_i \Xi_i^{(0)}(\beta, \mu_i, V) \quad , \qquad \text{(B.1)}$$

where

$$\beta^{-1} = T \quad , \qquad \lambda_i = e^{\beta\mu_i} \quad . \qquad \text{(B.2)}$$

Here T, V and μ_i are the temperature, the volume and the chemical potential of the i-th hadron. Assuming chemical equilibrium, we have

$$\mu_i = B_i \mu_B + S_i \mu_S \quad , \tag{B.3}$$

where B_i and S_i are the baryon number and the strangeness of the i-th hadron, respectively. Thus all chemical potentials, μ_i, can be expressed in terms of two chemical potential μ_B and μ_S corresponding to the baryon number and strangeness conservation, respectively. The Gell-Mann-Nishijima relation for an isospin averaged Q=A/2 system yields Q=(B+S)/2, where Q is the total charge and A the atomic number. Thus if one conserves B and S, Q is automatically conserved on the average.

In the Boltzmann statistics, $\Xi_i^{(0)}$ can be expressed as

$$\log \Xi_i^{(0)} = \lambda_i V \frac{g_i}{(2\pi)^3} \int d^3p \; e^{-\beta p^0} \quad , \tag{B.4}$$

$$= \lambda_i V \frac{g_i m_i^3}{2\pi^2} \frac{K_2(\beta m_i)}{\beta m_i} \; , \tag{B.5}$$

where g_i is the internal degree of freedom(spin and isospin) and m_i the mass of a particle of type i, and

$$p^0 = \sqrt{p^2 + m_i^2} \quad .$$

$K_n(x)$ is the n-th Bessel function. From this partition function the number and the energy of the i-th hadron can be obtained as follows:

$$N_i^{(0)} = \lambda_i V \frac{g_i m_i^3}{2\pi^2} \frac{K_2(\beta m_i)}{\beta m_i} \quad , \tag{B.6}$$

$$E_i^{(0)} = N_i \frac{1}{\beta} [3 + m_i \frac{K_1(\beta m_i)}{K_2(\beta m_i)}] \quad . \tag{B.7}$$

For a given impact parameter we can calculate the mass W_{FB}, the baryon number B_{FB}, and the strangeness S_{FB} of the fireball uniquely by the kinematics and the geometry. The unknown parameters are β, V, μ_B, and μ_S. They are determined by the equations for the conservation of the energy, the baryon number and the strangeness, and the constraint that the hadron number density of the fireball be ρ_c (the critical density):

$$\sum_i E_i^{(0)} = W_{FB} \quad , \tag{B.8}$$

$$\sum_i B_i N_i^{(0)} = B_{FB} \quad , \tag{B.9}$$

$$\sum_i S_i N_i^{(0)} = S_{FB} \quad , \tag{B.10}$$

$$\frac{1}{V}\sum_i N_i^{(0)} = \rho_c \quad . \tag{B.11}$$

The charm particle production will not be considered in this paper but it is straightforward to include it.

The inclusive spectra of the i-th hadron in the fire-ball frame at the fixed impact parameter are then given by

$$\left(\frac{dN_i^{(0)}}{d^3p}\right)_b = \lambda_i V \frac{g_i}{(2\pi)^3} e^{-\beta p0} \tag{B.12}$$

$$= N_i^{(0)} \frac{1}{4\pi m_i^3} \frac{\beta m_i}{K_2(\beta m_i)} e^{-\beta p0} \quad . \tag{B.13}$$

If the a-th hadron will decay and produce the i-th hadron, one must add this contribution to Eq. (B.12);

$$\left(\frac{dN_i^{(0)}}{d^3p}\right)_b = (B.12) + \sum_a \left(\frac{dN}{d^3p}\right)_b^{a\to i} \tag{B.14}$$

For the case of two-body decay ($a\to i + i'$), we approximate the distributions of the i-th and i'-th hadron to be isotropic. Then this contribution becomes

$$p^0 \left(\frac{dN}{d^3p}\right)_b^{a\to i} = \int d^3p_a \left(\frac{dN_a^{(0)}}{d^3p_a}\right)_b \frac{1}{4\pi p_c} \delta(E-E_c)$$

$$= \frac{m_a}{2p_c} \frac{\lambda_a V g_a}{(2\pi)^3} \frac{1}{\beta^2} \frac{1}{p} \left[e^{-\beta x}(1+\beta x)\right]_{x=E_a^+}^{x=E_a^-} \quad . \qquad (B.15)$$

Here

$$p_c = (m_a^4 + m_i^4 + m_{i'}^4 - 2m_a^2 m_i^2 - 2m_a^2 m_{i'}^2 - 2m_i^2 m_{i'}^2)^{1/2}/2m_a$$

$$E_c = (p_c^2 + m_i^2)^{1/2} \quad ,$$

$$E = (E_a p^0 - p_a . p)/m_a \quad ,$$

$$E_a^{\pm} = m_a(E_c p^0 \pm p_c p)/m_i^2 \quad . \qquad (B.16)$$

The inclusive cross section in the laboratory system (Lab) is given by

$$\left(\frac{dN_i^{(0)}}{dT_L d\Omega_L}\right)_b = p_L p_0 \left(\frac{dN_i^{(0)}}{d^3p}\right)_b \quad , \qquad (B.17)$$

where

$$p^0 = \gamma_{FB}(p_L^0 - \beta_{FB} p_L \cos\theta_L) \quad ,$$

$$T_L = p_L^0 - m_i \quad ,$$

$$\gamma_{FB} = (1 - \beta_{FB}^2)^{-1/2} \quad . \tag{B.18}$$

Here β_{FB} is the velocity of the fireball and θ_L the emission angle in the Lab system. After integrating Eq. (B.17) over the impact parameter, we obtain the final expression for inclusive distribution of the i-th hadron:

$$\frac{dN_i^{(0)}}{dT_L d\Omega_L} = \frac{1}{\sigma_T^{in}} \int_0^{b_{max}} 2\pi b db \left(\frac{dN_i^{(0)}}{dT_L d\Omega_L}\right)_b$$

$$= \frac{1}{y_{max}^2} \int_0^{y_{max}} 2y dy \left(\frac{dN_i^{(0)}}{dT_L d\Omega_L}\right)_y \quad , \tag{B.19}$$

where

$$\sigma_T^{in} = (R_p + R_T)^2 \quad , \tag{B.20}$$

$$y = \frac{b}{R_p + R_T} \quad , \quad y_{max} = \frac{b_{max}}{R_p + R_T} \quad . \tag{B.21}$$

Here b_{max} is the maximum impact parameter and $R_p(R_T)$ the radius of the projectile(target) nucleus. In the simple nuclear-fireball model stated above, there are two free parameters ρ_c and y_{max}.

Some results from the model are shown in Figs. 24, 25, B-2 and B-3. Note that the experimental proton spectra in the low energy region should not be compared directly with the nuclear-fireball model unless one includes the Coulomb effects. The fireball model describes successfully at least the gross feature of inclusive distributions. Particularly it fits better to the selected data with high-multiplicities as shown in Fig. B-3 and Refs. 92)-94). However, the model fails to reproduce the observed pion production rate (See section 7.3). All models based on the equilibrium assumption give rather higher pion multiplicity than observed. Some reasons for this situation has been considered: (i) The energetic pions produced at the early stage of the fireball carry out a considerable energy, or a compression energy term which lower the temperature of the system may be added to the fireball model. (ii) A significant amount of pion absorption by the spectator nuclei may occur. (iii) The incident energy is not enough to reach the thermal equilibrium for pion component of the fireball because of its small particle number.

B.3) A generalized nuclear-fireball model

We generalize the nuclear-fireball model stated in B.2 so as to include the hadron-hadron interactions. In the generalized model , instead of resonance approximation, all interactions among hadrons are taken into account and so the fireball contains no resonance as an elementary particle. In the following, for the simplicity of discussion, we treat the system composed of pions and nucleons.

The grand partition function of this system has been already given by Eqs. (6.1)-(6.3):

$$\Xi(\beta,\mu,V) = \Xi_0(\beta,\mu,V) \quad \Xi_{int}(\beta,\mu,V) \quad . \tag{B.22}$$

Here, as in §6, we neglect the term $C_{nm}(n,m\geqq 3)$. Thus Ξ_{int} can be written as

$$\log \Xi_{int} = \lambda^2 C_{20} + \lambda C_{11} + C_{02} \quad . \tag{B.23}$$

By using these partition functions, the multiplicities of nucleon and pion can be obtained as follows:

$$N_N = N_N^{(0)} + N_N^{(int)} \quad , \tag{B.24}$$

$$N_\pi = N_\pi^{(0)} + N_\pi^{(int)} \quad , \tag{B.25}$$

where

$$N_N^{(0)} = C_{10} \quad , \qquad N_\pi^{(0)} = C_{01} \quad ,$$

$$N_N^{(int)} = \lambda C_{11} + 2\lambda^2 C_{20} \quad ,$$

$$N_\pi^{(int)} = \lambda C_{11} + 2C_{02} \quad . \tag{B.26}$$

The quantity $N_N^{(0)}$ and $N_\pi^{(0)}$ are already given by Eq. (B.6). Similarly the total energy of the system can be expressed as

$$E = - \left[\frac{\partial}{\partial\beta} \log \Xi \right]_\lambda \quad . \tag{B.27}$$

The unknown parameters in this case are β, μ and V. These are determined by the following relations like as Eqs. (B.8)-(B.11):

$$E = W_{FB} \quad , \tag{B.28}$$

$$N_N = B_{FB} \quad , \tag{B.29}$$

$$\frac{1}{V}(N_N + N_\pi) = \rho_c \quad . \tag{B.30}$$

Using thus determined parameters, we can calculate the inclusive cross section and the two-particle correlation function by Eqs. (6.25) and (6.32).

References

Theory

(I) Review articles

1) A. Goldhaber and H.H. Heckman, Ann. Rev. Nucl. Sci. 28 (1978) 161.

2) Proc. Eighth Intern. Conf. on High Energy Physics and Nuclear Structure (Vancouver, August 1979), Nucl. Phys. A335 (1980) 481,491.

3) Proc. Hakone Seminar on High-Energy Nuclear Interactions and Properties of Dense Nuclear Matter (Hakone, Japan, July 1980).

4) Proc. Intern. Conf. on Nuclear Physics (Berkeley, 24-30 August 1980), Nucl. Phys. A354 (1981) 3, 375, 395.

5) Proc. Ninth Intern. Conf. on High Energy Physics and Nuclear Structure (Versailles, 6-10 July 1981), Nucl. Phys. A374 (1982) 447, 475, 489.

6) S. Das Gupta and A.Z. Mekjian, Phys. Rep. 72 (1981) 131.

(II) Statistical model

(fireball)

7) G.D. Westfall et al., Phys. Rev. Lett. 37 (1976) 1202;
J.I. Kapusta, Phys. Rev. C16 (1977) 1493;
J. Gosset et al., Phys. Rev. C16 (1977) 629;
A.Z. Mekjian, Nucl. Phys. A312 (1978) 491;
I. Montvay and J. Zimanyi, Nucl. Phys. A316 (1979) 490;
A. Sandoval et al., Phys. Rev. C21 (1980) 1321;
R. Stock et al., Phys. Rev. Lett. 44 (1980) 1243.

(firestreak)

8) W.D. Myers, Nucl. Phys. A296 (1978) 177;

J. Gosset, J.I. Kapusta and G.D. Westfall, Phys. Rev. C18 (1978) 844;

K.L. Wolf et al., Phys. Rev. Lett. 42 (1979) 1448.

(2-fireball)

9) S. Das Gupta, Phys. Rev. Lett. 41 (1978) 1450.

(microcanonical)

10) J. Knoll, Phys. Rev. C20 (1979) 773; Nucl. Phys. A343 (1980) 511;

E. Forest, S. Das Gupta and C.S. Lam, Phys. Rev. C21 (1980) 1989;

S. Bohrmann and J. Knoll, Nucl. Phys. A356 (1981) 498;

S. Bohrmann, Phys. Lett. 107B (1981) 269;

J. Cugnon, J. Knoll and J. Randrup, Nucl. Phys. A360 (1981) 444;

J. Knoll and J. Randrup, Phys. Lett. 103B (1981) 264;

F. Asai, Nucl. Phys. A365 (1981) 519;

F. Asai and M. Sano, Prog. Theor. Phys. 66 (1981) 251.

(entropy, composite particle)

11) T. Nakai, O. Miyamura and H. Yokomi, Prog. Theor. Phys. 63 (1980) 2136.

12) A. Mekjian, Phys. Rev. Lett. 38 (1977) 640; Phys. Lett. 89B (1980) 177;

R. Bond et al., Phys. Lett. 71B (1977) 43;

13) P.J. Siemens and J.O. Rasmussen, Phys. Rev. Lett. 42 (1979) 880;

P.J. Siemens and J.I. Kapusta, Phys. Rev. Lett. 43 (1979) 1486;

I.M. Mishustin et al., Phys. Lett. 95B (1980) 361;

J.I. Kapusta, Phys. Rev. C21 (1980) 1301.

14) K.A. Olive, Phys. Lett. 89B (1980) 299.

15) H. Sato and K. Yazaki, Phys. Lett. 98B (1981) 153;

J. Randrup and S.E. Koonin, Nucl. Phys. A356 (1981) 223;

B.K. Jennings et al., Phys. Rev. C25 (1982) 278.

(expansion)

16) A.Z. Mekjian, Phys. Rev. C17 (1978) 1051;

N.K. Glendenning and Y. Karant, Phys. Rev. Lett. 40 (1978) 374; Phys. Rev. C21 (1980) 1501;

S.I.A. Garpman et al., Phys. Lett. 86B (1979) 133; 87B (1979) 1.

(non-equilibrium)

17) J. Randrup, Nucl. Phys. A314 (1979) 429;

H.J. Pirner and B. Schürmann, Nucl. Phys. A316 (1979) 461;

R. Malfliet, Phys. Rev. Lett. 44 (1980) 864; Nucl. Phys. A363 (1981) 429;

B. Schürmann et al., Nucl. Phys. A360 (1981) 435.

(others)

18) J. Zimanyi et al., Phys. Rev. Lett. 43 (1979) 1705.

19) G. Mantzouranis, Phys. Rev. C18 (1978) 2227.

(III) Hydrodynamical model

20) A.E. Glassgold, W. Heckrotte and K.M. Watson, Ann. Phys.(N.Y.) 6 (1959) 1.

21) W. Scheid, H. Müller and W. Greiner, Phys. Rev. Lett. 32 (1974) 741;

J. Hofmann et al., Phys. Rev. Lett. 36 (1976) 88; Nuovo Cimento 33A (1976) 343.

22) C.Y. Wong and T.A. Welton, Phys. Lett. 49B (1974) 243;

C.Y. Wong et al., Nucl. Phys. A253 (1975) 469.

23) M.I. Sobel et al., Nucl. Phys. A251 (1975) 502;

H.G. Baumgardt et al., Z. Phys. A273 (1975) 359.

24) A.A. Amsden et al., Phys. Rev. Lett. 35 (1975) 905; 38 (1977) 1055;
Phys. Rev. C15 (1977) 2059; C17 (1978)2080;
G. Bertsch and A.A. Amsden, Phys. Rev. C18 (1978) 1293.

25) M. Iwasaki and S. Takagi, Prog. Theor. Phys. 61 (1979) 475; 55 (1976) 949.

26) Y. Kitazoe et al., Nuovo Cimento Lett. 13 (1975) 139; Prog. Theor. Phys. 56 (1976) 860; J. Phys. Soc. Japan 44 (1978) Suppl. 386;
Y. Kitazoe and M. Sano, Nuovo Cimento Lett. 22 (1978) 153.

27) K.K. Gudima and V.D. Toneev, Sov. J. Nucl. Phys. 27 (1978) 351.

28) J.P. Bondorf et al., Nucl. Phys. A296 (1978) 320.

29) H. Stöcker et al., Z. Phys. A286 (1978) 121; A290 (1979) 297; A293 (1979) 173; A294 (1980) 125; Phys. Lett. 81B (1979) 303; Phys. Rev. Lett. 44 (1980) 725; 47 (1981) 1807;
L.P. Csernai et al., Z. Phys. A296 (1980) 173; Phys. Lett. 99B (1981) 85;
G. Buchwald et al., Z. Phys. A303 (1981) 111.

30) P. Danielewicz, Nucl. Phys. A314 (1979) 465.

31) P.L. Jain et al., Phys. Lett. 88B (1979) 189.

32) A.M. Gleeson and S. Raha, Phys. Rev. C21 (1980) 1065.

33) H.H.K. Tang and C.-Yin Wong, Phys. Rev. C21 (1980) 1846.

34) A.J. Sierk and J.R. Nix, Phys. Rev. C22 (1980) 1920.

35) H.W. Barz et al., Z. Phys. A302 (1981) 73.

36) J.I. Kapusta and D. Strottman, Phys. Rev. C23 (1981) 1282;
J.R. Nix and D. Strottman, Phys. Rev. C23 (1981) 2548;
J.I. Kapusta, Phys. Rev. C24 (1981) 2545.

(IV) Microscopic model

(linear cascade)

37) J. Hüfner and J. Knoll, Nucl. Phys. A290 (1977) 460;

J. Randrup, Phys. Lett. 76B (1978) 547;

J. Knoll and J. Randrup, Nucl. Phys. A324 (1979) 445.

(internuclear cascade)

38) E.A. Remler and A.P. Sathe, Ann. Phys.(N.Y.) 91 (1975) 295.

39) J.P. Bondorf et al., Phys. Lett. 65B (1976) 217; Z. Phys. A279 (1976) 385.

40) A.A. Amsden et al., Phys. Rev. Lett. 38 (1977) 1055.

41) J.D. Stevenson, Phys. Rev. Lett. 41 (1978) 1702.

42) Y. Yariv and Z. Fraenkel, Phys. Rev. C20 (1979) 2227.

43) J. Cugnon, Phys. Rev. C22 (1980) 1885;

J. Cugnon et al., Nuovo Cimento lett. 28 (1980) 55; Nucl. Phys. A352 (1981) 505; A360 (1981) 444;

G. Bertsch and J. Cugnon, Phys. Rev. C24 (1981) 2514.

44) E.C. Halbert, Phys. Rev. C23 (1981) 295.

(classical many-body)

45) A.R. Bodmer and C.N. Panos, Phys. Rev. C15 (1977) 1342; C22 (1980) 1025; Nucl. Phys. A356 (1981) 517.

46) L. Wilets et al., Nucl. Phys. A282 (1977) 341; A301 (1978) 359;

D.J.E. Callaway et al., Nucl. Phys. A327 (1979) 250.

47) A.A. Amsden et al., Phys. Rev. Lett. 38 (1977) 1055.

48) Y. Kitazoe et al., Nuovo Cimento Lett. 32 (1981) 337.

(V) Knock-out model

49) I.A. Schmidt and R. Blankenbecler, Phys. Rev. D15 (1977) 3321.

50) M. Chemtob, Nucl. Phys. A314 (1979) 387;
M. Chemtob and B. Schurmann, Nucl. Phys. A336 (1980) 505;
B. Schürmann and M. Chemtob, Z. Phys. A294 (1980) 371.

51) G.F. Bertsch, Phys. Rev. C15 (1977) 713.

52) S.E. Koonin, Phys. Rev. Lett. 39 (1977) 680;
R.L. Hatch and S.E. Koonin, Phys. Lett. 81B (1979) 1.

53) B.K. Jain, Phys. Rev. C22 (1980) 583.

(VI) Glauber-Eikonal model

54) R.J. Glauber and G. Matthiae, Nucl. Phys. B21 (1970) 135.

55) J. Randrup, Nucl. Phys. A316 (1979) 509.

56) B. Jakobsson et al., Phys. Lett. 82B (1979) 35.

57) B. Schürmann, Phys. Rev. C20 (1979) 1607.

58) M. Iwasaki et al., Prog. Theor. Phys. 63 (1980) 2005.

(VII) Participant-Spectator geometry

59) J.D. Bowman, W.J. Swiatecki and C.F. Tsang, LBL Report-2908 (1973).

60) R. Beckmann et al., Phys. Lett. 105B (1981) 411;
N. Mobed et al., Phys. Lett. 106B (1981) 371;

61) S.I.A. Garpman, Phys. Lett. 106B (1981) 367.

(VIII) Fragments

62) H. Feshbach and K. Hung, Phys. Lett. 47B (1973) 300;
A.S. Goldhaber, Phys. Lett. 53B (1974) 306.

63) J.P. Bondorf et al., Phys. Rev. Lett. 41 (1978) 391;
S.A. Chin and A.K. Kerman, Phys. Rev. Lett. 43 (1979) 1292;
R.A. Malfliet and Y. Karant, Phys. Lett. 86B (1979) 251;
P.A. Deutchmann and L.W. Townsend, Phys. Rev. Lett. 45 (1980) 1622.

64) B. Bertsch, Phys. Rev. Lett. 46 (1981) 472.

65) S. Fredriksson and M. Jandel, Phys. Rev. Lett. 48 (1982) 14.

(IX) Pion condensation, pion multiplicity

66) M. Gyulassy and W. Greiner, Z. Phys. A277 (1976) 391.

67) J. Knoll et al., Nucl. Phys. A308 (1978) 500.

68) M. Ta-chung, Phys. Rev. Lett. 42 (1979) 1331.

69) M. Wakamatsu, Nuovo Cimento 56A (1980) 336.

70) S. Krewald and J.W. Negele, Phys. Rev. C21 (1980) 2385;
P. Hecking and H.J. Pirner, Nucl. Phys. A333 (1980) 514.

71) B. Friedman et al., Nucl. Phys. A372 (1981) 483.

72) B. Jakobsson et al., Phys. Lett. 82B (1979) 35.

73) M. Gyulassy and S.K. Kauffmann, Phys. Rev. Lett. 40 (1978) 298;
Y. Afek et al., Phys. Rev. Lett. 41 (1978) 849;
J.P. Vary, Phys. Rev. Lett. 40 (1978) 295.

(X) Two-particle correlation

74) T. Nakai and H. Yokomi, Prog. Theor. Phys. 66 (1981) 1328;
M. Biyajima, O. Miyamura and T. Nakai, Phys. Lett. 77B (1978) 425.

75) S.E. Koonin, Phys. Lett. 70B (1977) 43;
F.B. Yano and S.E. Koonin, Phys. Lett. 78B (1978) 556.

76) J. Randrup, Nucl. Phys. A316 (1979) 509.

77) L.P. Csernai and W. Greiner, Phys. Lett. 99B (1981) 85.

78) M. Gyulassy et al., Phys. Rev. C20 (1979) 2267;
M. Gyulassy, Phys. Rev. Lett. 48 (1982) 454.

(XI) K, Λ and $\bar{p}$ production

79) J. Randrup and C.M. Ko, Nucl. Phys. A343 (1980) 519;
J. Randrup, Phys. Lett. 99B (1981) 9.

80) F. Asai, H. Sato and M. Sano, Phys. Lett. 98B (1981) 19;
F. Asai and M. Sano, Prog. Theor. Phys. 66 (1981) 251.

81) K.A. Olive, Phys. Lett. 95B (1980) 355.

(XII) Coulomb effects, n/p ratio

82) K.G. Libbrecht and S.E. Koonin, Phys. Rev. Lett. 43 (1979) 1581.
J. Cugnon and S.E. Koonin, Nucl. Phys. A355 (1981) 477;
M. Gyulassy and S.K. Kauffmann, Nucl. Phys. A362 (1981) 503;
M. Bawin and J. Cugnon, Phys. Rev. C25 (1982) 387.

83) J.D. Stevenson, Phys. Rev. Lett. 45 (1980) 1773; 41 (1978) 1702.

(XIII) Other topics

(selection for central collision)

84) C.-Y. Wong, Phys. Lett. 88B (1979) 39.

(event shape)

85) J. Kapusta and D. Strottman, Phys. Lett. 106B (1981) 33.

86) M. Gyulassy, K.A. Frankel and H. Stocker, Phys. Lett. 110B (1982) 185.

Experiment

(I) Review articles

87) A. Goldhaber and H.H. Heckman, Ann. Rev. Nucl. Sci. 28 (1978) 161.

88) S. Nagamiya et al., J. Phys. Soc. Japan 44 (1978) Suppl. 378; Nucl. Phys. A335 (1980) 517; Phys. Rev. C24 (1981) 971.

89) Proc. Hakone Seminar on High-Energy Nuclear Interactions and Properties of Dense Nuclear Matter (Hakone, Japan, July 1980).

90) Nuclear Science Annual Report, LBL-8151 (1977-1978).

91) Workshop on Nuclear Dynamics, LBL-10688 (1980).

(II) High-multiplicity events

92) R. Stock et al., Phys. Rev. Lett. 44 (1980) 1243.

93) S. Nagamiya et al., Phys. Rev. Lett. 45 (1980) 602.

94) R. Ihara, Phys. Lett. 106B (1981) 179.

95) A. Sandoval et al., Phys. Rev. Lett. 45 (1980) 874.

96) J.J. Lu et al., Phys. Rev. Lett. 46 (1981) 898.

(III) Inclusive spectra

97) H.H. Gutbrod et al., Phys. Rev. Lett. 37 (1976) 667;
J. Gosset et al., Phys. Rev. C16 (1977) 629;
A. Sandoval et al., Phys. Rev. C21 (1980) 1321.

98) S. Nagamiya et al., Phys. Lett. 81B (1979) 147;
I. Tanihata et al., Phys. Lett. 87B (1979) 349;

99) M.M. Gazzaly et al., Phys. Lett. 79B (1978) 325.

100) H.H. Heckman et al., Phys. Rev. C17 (1978) 1651.

(IV) Coulomb, n/p ratio

101) W. Schimmerling et al., Phys. Rev. Lett. 43 (1979) 1985;
R.A. Cecil et al., Phys. Rev. C24 (1981) 2013.

102) J. Chiba et al., Phys. Rev. C20 (1979) 1332;
K. Nakai et al., Phys. Rev. C20 (1979) 2210;
W. Benenson et al., Phys. Rev. Lett. 43 (1979) 683;
K.L. Wolf et al., Phys. Rev. Lett. 42 (1979) 1448.

(V) Two-particle correlation

103) I. Tanihata et al., Phys. Rev. 97B (1980) 363;
A.L. Sagle et al., Ref. 89) p.360;
F. Zarbakhsh et al., Phys. Rev. Lett. 46 (1981) 1268.

104) S.Y. Fung et al., Phys. Rev. Lett. 41 (1978) 1592

105) G.M. Chernov et al., Nucl. Phys. A280 (1977) 478;
BWDKLMT collaboration, Sov. J. Nucl. Phys. 32 (1980) 711;
MATEKBB collaboration, Sov. J. Nucl. Phys. 32 (1980) 819.

106) R. Ihara, Phys. Lett. 106B (1981) 179.

(VI) Participant-Spectator

107) J.D. Stevenson et al., Phys. Rev. Lett. 47 (1981) 990.

108) K.B. Bhalla et al., Phys. Lett. 82B (1979) 216;
A. Sandoval et al., Phys. Rev. Lett. 45 (1980) 874.

(VII) Fragments

109) E.M. Friedlander et al., Phys. Rev. Lett. 45 (1980) 1084;
P.L. Jain and G. Das, Phys. Rev. Lett. 48 (1982) 305;
H.B. Barber et al., Phys. Rev. Lett. 48 (1982) 856.

110) H.G. Baumgardt et al., J. Phys. G7 (1981) L175.

111) K. Van Bibber et al., Phys. Rev. Lett. 43 (1979) 840.

112) W.G. Meyer and H.H. Gutbrod, Phys. Rev. C22 (1980) 179.

113) D.E. Greiner et al., Phys. Rev. Lett. 35 (1975) 152;
J.B. Cumming et al., Phys. Rev. C17 (1978) 1632;
G.D. Westfall et al., Phys. Rev. Lett. 43 (1979) 1859.

(IX) Pion multiplicity

114) A. Sandoval et al., Phys. Rev. Lett. 45 (1980) 874;
J.J. Lu et al., Phys. Rev. Lett. 46 (1981) 898;
S.Y. Fung et al., Phys. Rev. Lett. 41 (1978) 1592.

115) S.Y. Fung et al., Phys. Rev. Lett. 40 (1978) 292.

116) P.J. McNulty et al., Phys. Rev. Lett. 38 (1977) 1519;
P.J. Lindstrom et al., Phys. Rev. Lett. 40 (1978) 93;
R. Kullberg et al., Phys. Rev. Lett. 40 (1978) 289.

(X) Λ production

117) J.W. Harris et al., Phys. Rev. Lett. 47 (1981) 229.

(XI) Shock wave, abnormal nuclei

118) H.G. Baumgardt et al., Z. Phys. A273 (1975) 359.

119) P.B. Price and J. Stevenson, Phys. Rev. Lett. 34 (1975) 409;
A.M. Poskanzer et al., Phys. Rev. Lett. 35 (1975) 1701;
R.J. Holt et al., Phys. Rev. Lett. 36 (1976) 183.

120) B. Jakobsson, R. Kullberg and I. Otterlund, Nucl. Phys. A276 (1977) 523.

121) P.L. Jain et al., Phys. Lett. 88B (1979) 189.

§1. 1.1) G.F. Chapline et al., Phys. Rev. D8 (1973) 4302.

1.2) A.B. Migdal, Rev. Mod. Phys. 50 (1978) 107;

W. Weise et al., Phys. Rep. 27 (1976) 1.

1.3) T.D. Lee, Rev. Mod. Phys. 47 (1975) 267.

1.4) P.D. Morley and M.B. Kislinger, Phys. Rep. 51 (1979) 63.

1.5) S. Fredriksson and M. Jandel, Phys. Rev. Lett. 48 (1982) 14.

1.6) Refs. 87)-121).

1.7) Refs. 7)-19).

1.8) Refs. 59)-61).

1.9) Refs. 20)-36).

1.10) Refs. 37)-48).

1.11) Refs. 49)-58), 62)-65) and 84)-86).

1.12) Refs. 1)-6).

1.13) Refs. 74)-78).

1.14) Refs. 66)-73).

1.15) Refs, 11)-15).

1.16) Ref. 29).

1.17) Refs. 79)-80).

1.18) Ref. 81).

1.19) Refs. 92)-94).

1.20) R. Dashen, S. Ma and H.J. Bernstein, Phys. Rev. 187 (1969) 345.

1.21) S.E. Koonin, Phys. Lett. 70B (1977) 43.

1.22) J.I. Kapusta, Phys. Rev. C16 (1977) 1493.

1.23) A.L. Sagle et al., in Proceedings of the Hakone Seminar, Japan (1980) p.360;

F. Zarbakhsh et al., Phys. Rev. Lett. 46 (1981) 1268.

1.24) S. Nagamiya et al., Phys. Lett. 81B (1979) 147;
I. Tanihata et al., Phys. Lett. 87B (1979) 349.

§2. 2.1) R. Dashen, S. Ma and H.J. Bernstein, Phys. Rev. 187 (1969) 345.
2.2) We employ the treatment of invariant phase space in:
M. Chaichian et al., Nucl. Phys. B92 (1975) 445.

§3. 3.1) M. Chaichian et al., Nucl. Phys. B92 (1975) 445.

§4. 4.1) R. Hanbury Brown and R.Q. Twiss, Nature 178 (1956) 1046.

§5. 5.1) J.I. Kapusta, Phys. Rev. C16 (1977) 629.
5.2) R.A. Arndt et al., Phys. Rev. C15 (1977) 1002.
5.3) S. E. Koonin, Phys. Lett. 70B (1977) 43.

§6. 6.1) R. Dashen, S. Ma and H.J. Bernstein, Phys. Rev. 187 (1969) 345.

§7. 7.1) A.L. Sagle et al., in Proceedings of the Hakone Seminar, Japan (1980) p.360;
F. Zarbakhsh et al., Phys. Rev. Lett. 46 (1981) 1268.
7.2) S.E. Koonin, Phys. Lett. 70B (1977) 43.
7.3) J.L. Petersen, "The $\pi\pi$ Interaction" CERN 77-04 (1977).
7.4) L. David Roper and R.M. Wright, Phys. Rev. 138 (1965) B190.
7.5) S. Nagamiya et al., Phys. Lett. 81B (1979) 147;
I. Tanihata et al., Phys. Lett. 87B (1979) 349.

§8. 8.1) Refs. 82)-83).

Table I. Calculated values of the chemical potential(μ), the π^+ to proton(P) ratio and the entropy per baryon(B) for various incident energies(t_i). Values estimated from the ideal-gas model are shown in parentheses. All these values are independent on projectile and target nuclei.

t_i (GeV/A)	0.8	1.8	2.1
T (MeV)	76	109	115
μ (GeV)	0.86 (0.82)	0.61 (0.66)	0.57 (0.64)
π / P	0.15 (0.11)	0.49 (0.36)	0.56 (0.42)
S / B	5.3 (5.0)	8.1 (7.5)	8.7 (8.0)

Figure Captions

Fig. 1. A typical diagram in the Feynman-Dyson expansion of Eq. (2.4) which corresponds to a term in Eq. (2.6). The momenta κ_ν, κ_ν', ... mean various sets of momenta of ν particles. The connected part of ν particles occurs m_ν times in the figure.

Fig. 2. A connected diagram corresponding to $C_\nu(\kappa_\nu)$. The ν particles with momenta $\mathbf{k}_1$, $\mathbf{k}_2$, ..., $\mathbf{k}_\nu$ are interacting with each other.

Fig. 3. Dependence upon the maximum impact parameter y_{max} of the correlation R_L for the reaction (a) Fe+Cu and (b) Ar+KCl.

Fig. 4. Proton-proton correlations in the reaction Fe+Cu at 0.4 GeV/A. Variable ϕ_L is the difference between the azimuthal angles of two scattered protons. The scattering angle θ_L and the kinetic energy T_L are fixed for both protons at $30°$ and 0.1 GeV in the laboratory system, respectively. The parameter y_{max} and the critical density ρ_c are chosen as $y_{max}=0.5$ and (a) $\rho_c=\rho_0$ and (b) $\rho_c=0.3\rho_0$, ρ_0 being the normal density of nuclear matter.

Fig. 5. Proton-proton correlations in the reaction Ar+KCl at 0.4 GeV/A. T_L and θ_L are the same as in Fig. 4. The parameter y_{max} and ρ_c are chosen as $y_{max}=0.5$ and (a) $\rho_c=\rho_0$ and (b) $\rho_c=0.3\rho_0$.

Fig. 6. Dependence upon y_{max} of ϕ_L distributions of the proton-proton correlation function R in the reaction Fe+Cu at 0.4 GeV/A with the parameter (a) $\rho_c=\rho_0$ and (b) $\rho_c=0.3\rho_0$. T_L and θ_L are the same as in Fig. 4.

Fig. 7. Dependence upon y_{max} of the proton-proton correlation function R in the reaction Ar+KCl at 0.4 GeV/A with the parameter (a) $\rho_c=\rho_0$ and (b) $\rho_c=0.3\rho_0$. T_L and θ_L are the same as in Fig. 4.

Fig. 8. Dependence upon ρ_c of ϕ_L distributions of the proton-proton correlation function R in the reaction (a) Fe+Cu and (b) Ar+KCl at 0.4 GeV/A with the parameter $y_{max}=0.5$. T_L and θ_L are the same as in Fig. 4.

Fig. 9. Contributions to the correlation function R^{dyn} from various partial waves of proton-proton scattering in the reaction Fe+Cu at 0.4 GeV/A. T_L and θ_L are the same as in Fig. 4. The parameters are taken as $y_{max}=0.5$ and $\rho_c=\rho_0$. The values for $^3P_0$ and

$^3P_1$ partial waves are multiplied by factor 10^2.

Fig. 10. Proton-proton correlation function R with various kinetic energies of two protons in the reaction (a) Fe+Cu and (b) Ar+KCl at 0.4 GeV/A. Same value of the kinetic energy T_L is taken for both protons. The scattering angle θ_L is fixed at 30° for both protons. The parameters y_{max} and ρ_c are the same as in Fig. 9.

Fig. 11. Proton-proton correlation function R with various scattering angles θ_L in the reaction (a) Fe+Cu and (b) Ar+KCl at 0.4 GeV/A. Same value of the scattering angle θ_L is taken for both protons. The kinetic energy T_L is fixed at 0.1 GeV for both protons. The parameters y_{max} and ρ_c are the same as in Fig. 9.

Fig. 12. Proton-proton correlation functions for various combinations of colliding nuclei at 0.4 GeV/A; (a) R , (b) R^{HBT} and (c) R^{dyn}. T_L and θ_L are the same as in Fig. 4. The parameters y_{max} and ρ_c are the same as in Fig. 9.

Fig. 13. A connected diagram corresponding to C_{nm}. Here n and m are the number of nucleons and pions, respectively.

Fig. 14. Diagrammatic expansion of log Ξ_{int}.

Fig. 15. Proton-proton correlation function R with various incident energies in the reaction (a) Ar+KCl , (b) Fe+Cu and (c) U+U. The scattering angle θ_L and the kinetic energy T_L are fixed at 30° and 0.1 GeV for both protons, respectively. The parameters are taken as $y_{max}=0.5$ and $\rho_c=\rho_0$.

Fig. 16. Comparison of the experimental data on the proton-proton correlation function $R(\Delta p)$ with our calculation, where $\Delta p=|p_1-p_2|/2$. Reaction is Ar+KCl collision at 1.8 GeV/A. Kinematical variables are fixed as $p=|p_1+p_2|/2=1.0$ GeV/c and $\theta_L=13.45°$. The parameters are set as $\rho_c=\rho_0$ and $y_{max}=0.4$ for the solid curve, $\rho_c=0.3\rho_0$ and $y_{max}=0.8$ for the dashed curve. Koonin's result for $\tau=0$ and $r_0=2$ fm is also shown by the dotted curve for comparison.

Fig. 17. Azimuthal angle (ϕ_L) distributions of $\pi^+\pi^+$ (or $\pi^-\pi^-$) correlation functions in the reaction (a) Ar+KCl , (b) Fe+Cu and (c) U+U at 1.8 GeV/A. The scattering angle θ_L and the kinetic energy T_L are fixed for both pions at 30° and 0.1 GeV in the laboratory system, respectively. The parameters are taken as

$y_{max}=0.5$ and $\rho_c=\rho_0$. The correlation function R^{dyn} is almost zero.

Fig. 18. $\pi^+\pi^+$ correlation functions in the reaction (a) Ar+KCl , (b) Fe+Cu and (c) U+U at 1.8 GeV/A for $T_L=1.0$ GeV. Same values T_L and θ_L are taken for both pions. Here θ_L, y_{max} and ρ_c are the same as in Fig. 17.

Fig. 19. Dependence upon y_{max} of $\pi^+\pi^+$ correlation function R in the reaction Ar+KCl at 1.8 GeV/A. T_L and θ_L are the same as in Fig. 18. The parameter ρ_c is taken as $\rho_c=\rho_0$.

Fig. 20. Dependence upon ρ_c of $\pi^+\pi^+$ correlation function R in the reaction Ar+KCl at 1.8 GeV/A. T_L and θ_L are the same as in Fig. 18. The parameter y_{max} is chosen as $y_{max}=0.5$.

Fig. 21. $\pi^+\pi^+$ correlation function R for various combinations of colliding nuclei at 1.8 GeV/A. T_L, θ_L, y_{max} and ρ_c are the same as in Fig. 18.

Fig. 22. $\pi^+\pi^+$ correlation function R with various incident energies in the reaction (a) Ar+KCl ,(b) Fe+Cu

and (c) U+U . T_L, θ_L, y_{max} and ρ_c are the same as in Fig. 18.

Fig. 23. Azimuthal angle distributions of $\pi^+\pi^-$ correlation function R^{dyn} in the reaction Ar+KCl at 1.8 GeV/A. T_L, θ_L, y_{max} and ρ_c are the same as in Fig. 18. The values of R^{dyn} are multiplied by factor 10^2.

Fig. 24. Inclusive cross section of proton in the reaction Ar+KCl at 0.8 GeV/A with various scattering angles in the laboratory system. Our results are shown by the solid curves with the parameters ρ_c=ρ_0 and y_{max} =0.5. For comparison, calculations by Kapusta's simple fireball model with the same parameters ρ_c and y_{max} are also shown by the dashed curves.

Fig. 25. Same as Fig. 24 for pions.

Fig. B-1. Participant-spectator geometry. Parts P and T are the projectile and target spectator, respectively. The figure is drawn in the c.m. system.

Fig. B-2. Neutron inclusive cross section for the reaction Ne+U at 337 MeV/A compared with the simple fireball model (ρ_c = ρ_0). Data are from ref. 101.

Fig. B-3. Inclusive cross section of charged particles for Fe on Al, Cu and W at 1.88 GeV/A. The results from the simple fireball model are drawn by the solid curves with the parameters $\rho_c = \rho_0$ and $y_{max} = 0.7$ (Al), 0.5(Cu) and 0.3(W). Almost the same results are obtained for $\rho_c = \rho_0$ and $y_{max} = 0.8$(Al), 0.6(Cu) and 0.4(W). Data are from ref. 94.

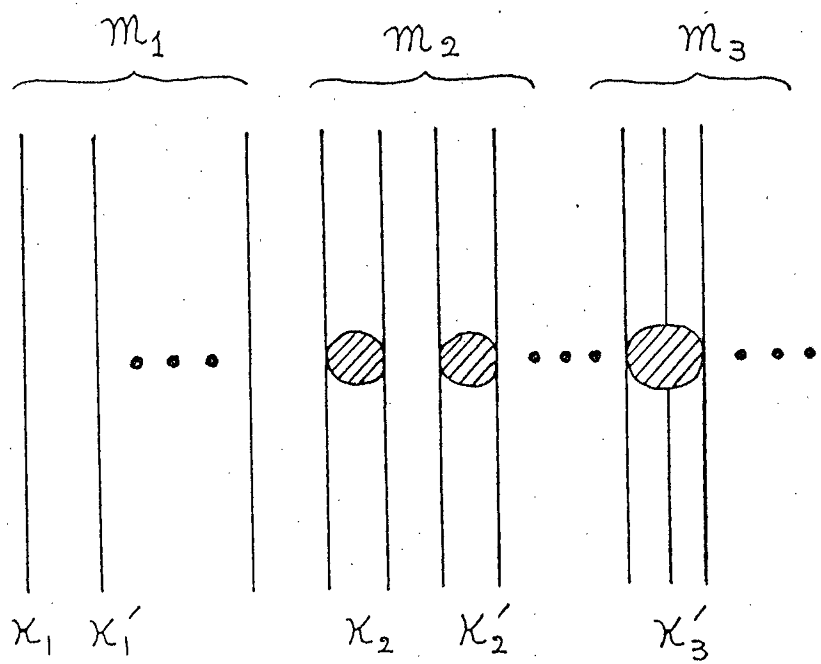
$\mathfrak{m}_1$
$\mathfrak{m}_2$
$\mathfrak{m}_3$
κ_1 κ_1'
κ_2 κ_2'
κ_3'

Fig. 1

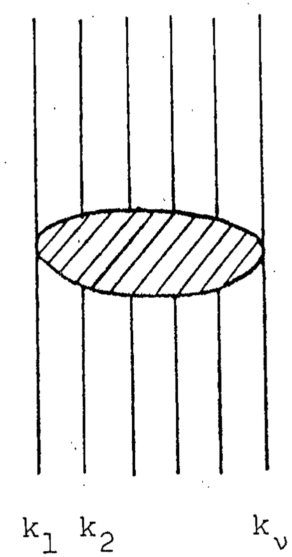
k_1 k_2 k_ν

Fig. 2

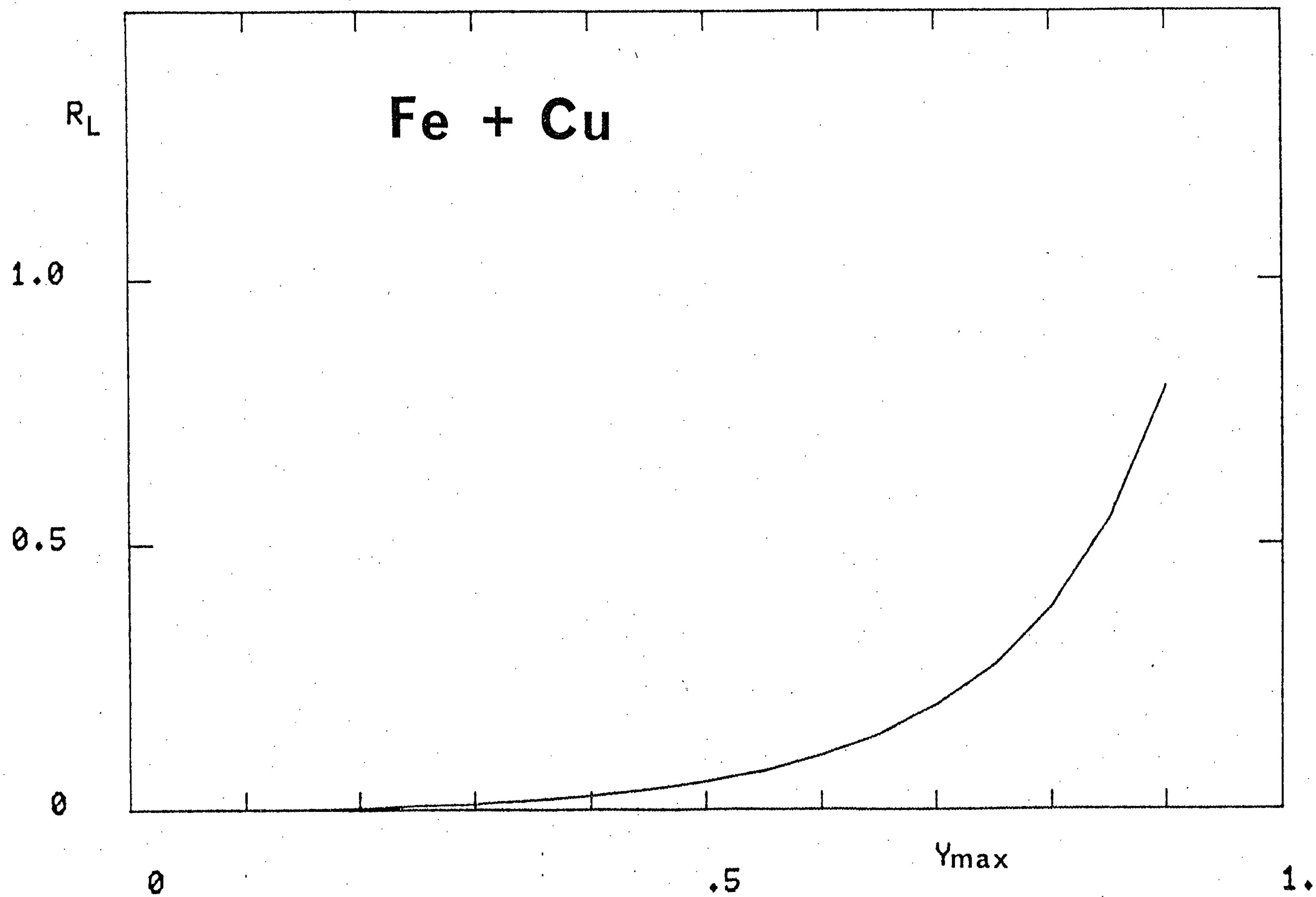

Fig. 3(a)

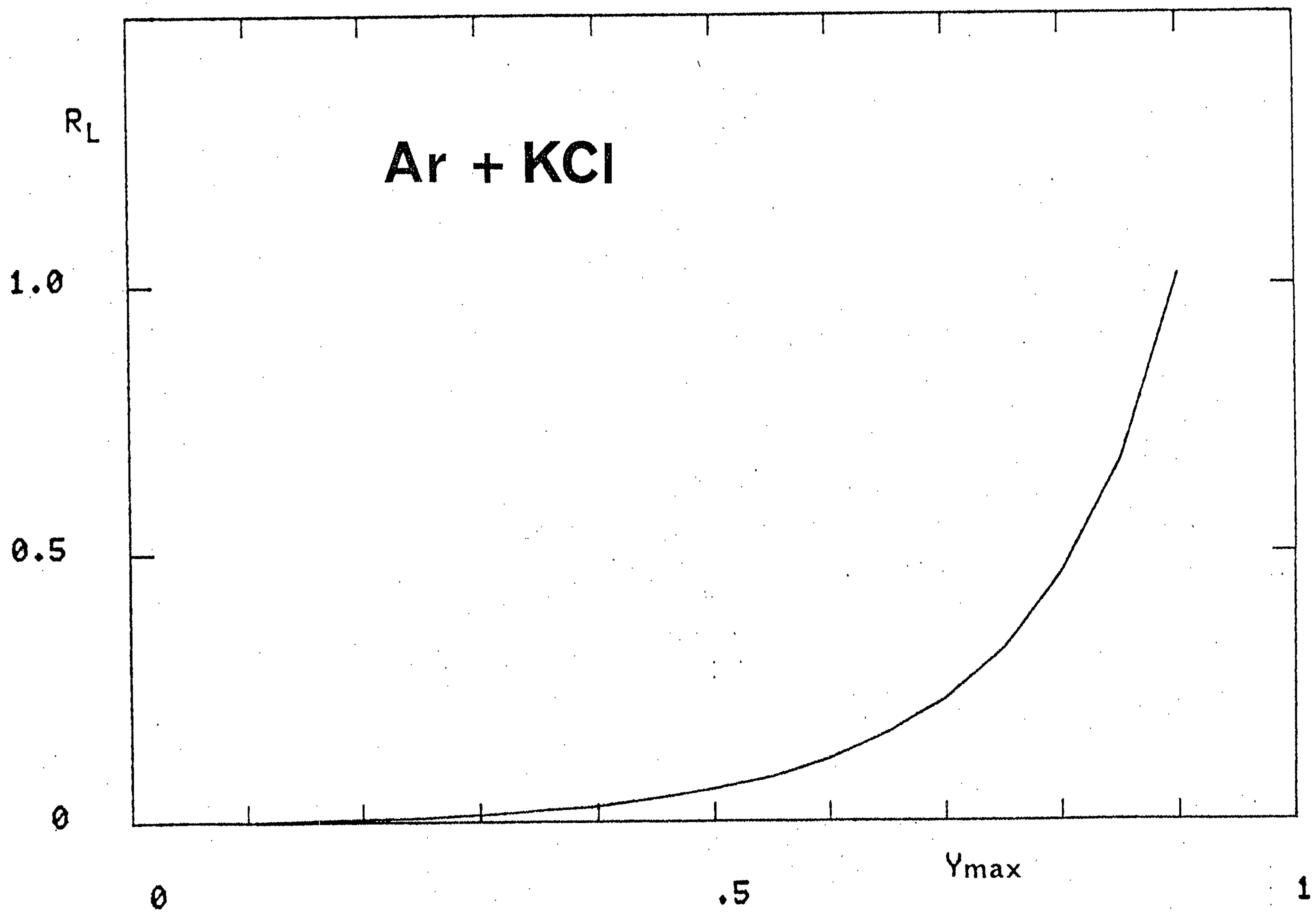

Fig. 3(b)

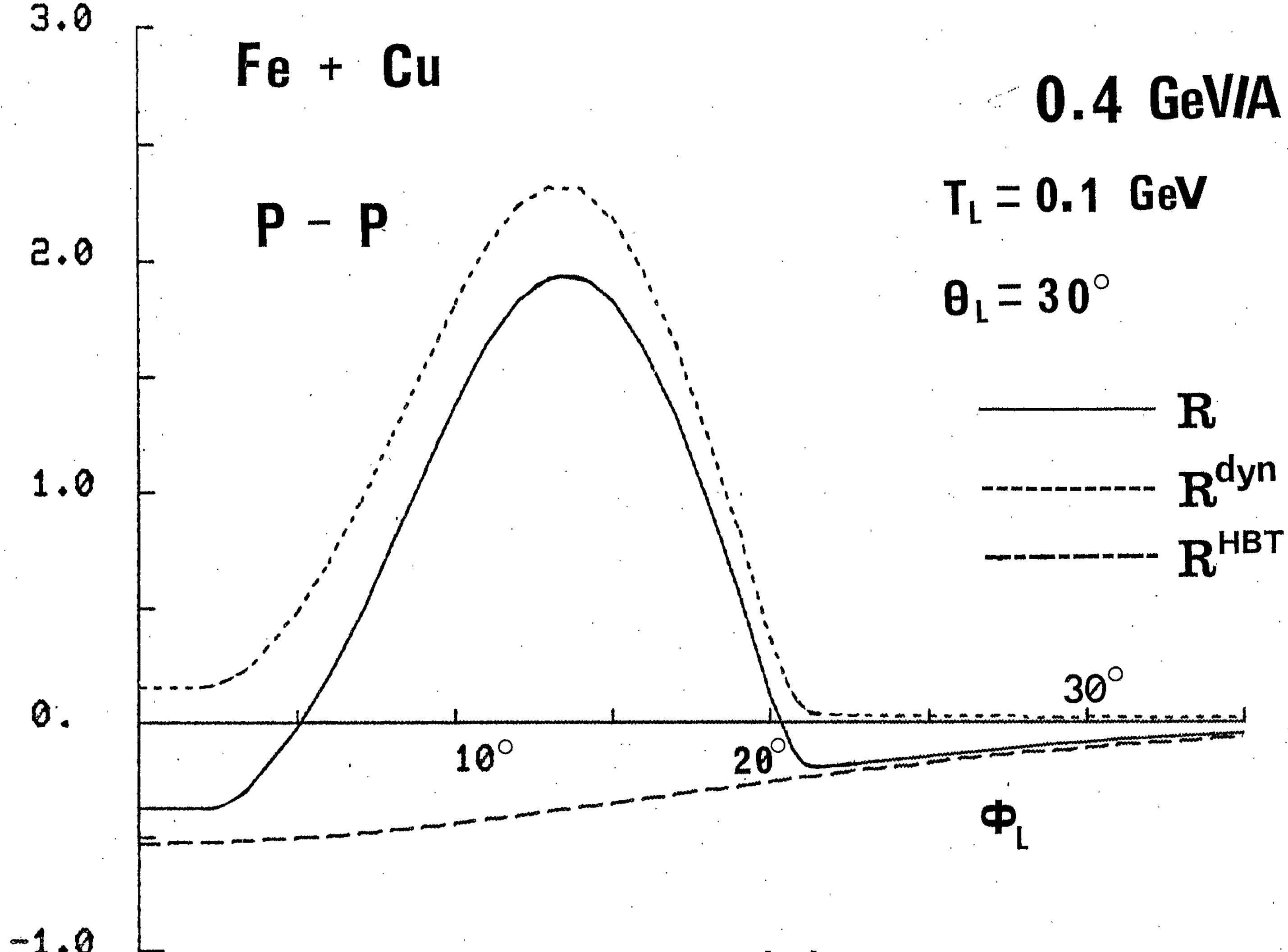

3.0
2.0
1.0
0.
-1.0
Fe + Cu
P - P
0.4 GeV/A
$T_L = 0.1$ GeV
$\theta_L = 30°$
R
R^{dyn}
R^{HBT}
10°
20°
30°
Φ_L

Fig. 4(a)

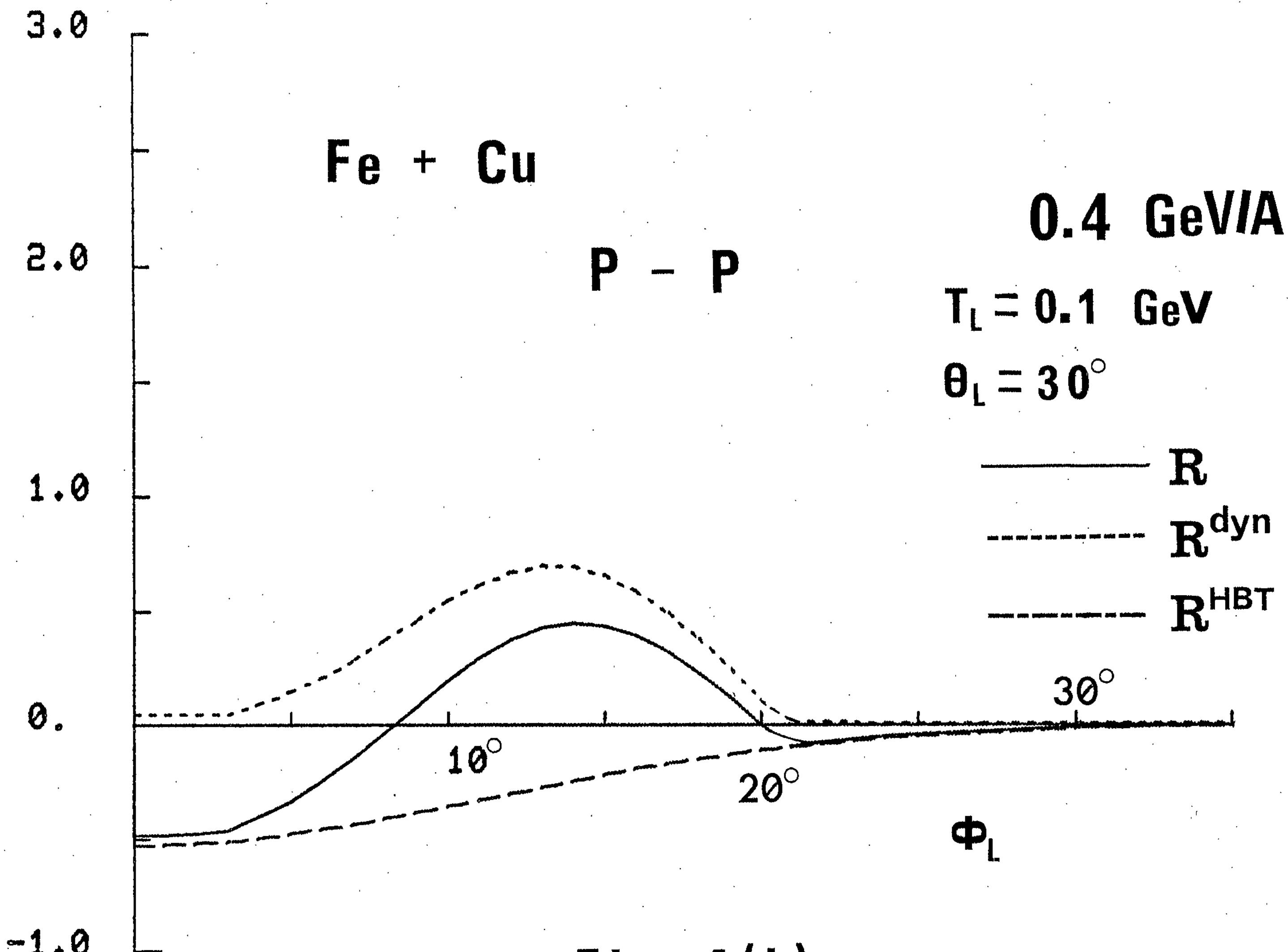
3.0
2.0
1.0
0.
-1.0
Fe + Cu
P - P
0.4 GeV/A
$T_L = 0.1$ GeV
$\theta_L = 30^\circ$
R
R^{dyn}
R^{HBT}
10°
20°
30°
Φ_L

Fig. 4(b)

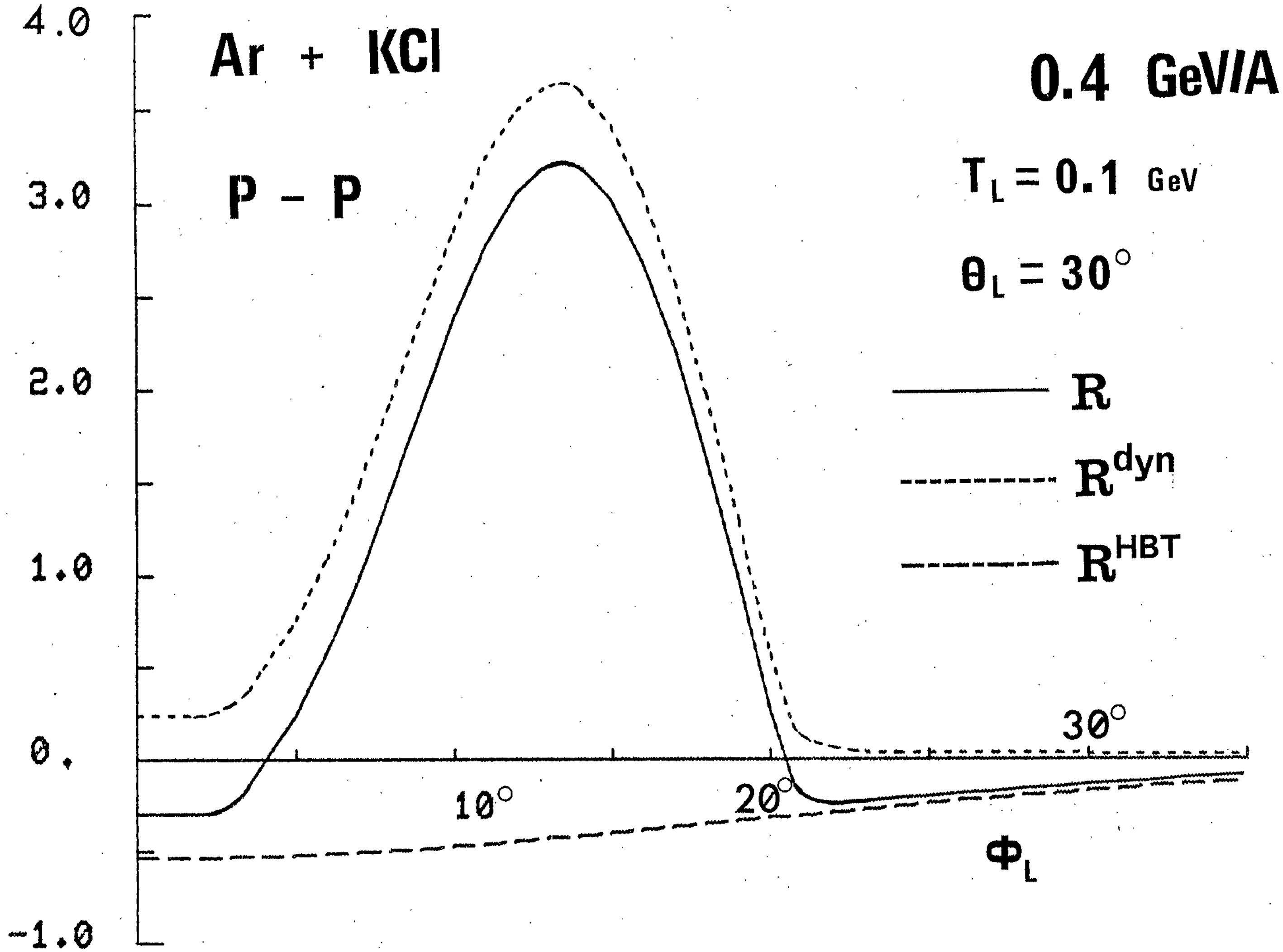
4.0
3.0
2.0
1.0
0.
-1.0
Ar + KCl
P - P
0.4 GeV/A
T_L = 0.1 GeV
θ_L = 30°
R
R^dyn
R^HBT
10°
20°
30°
Φ_L

Fig. 5(a)

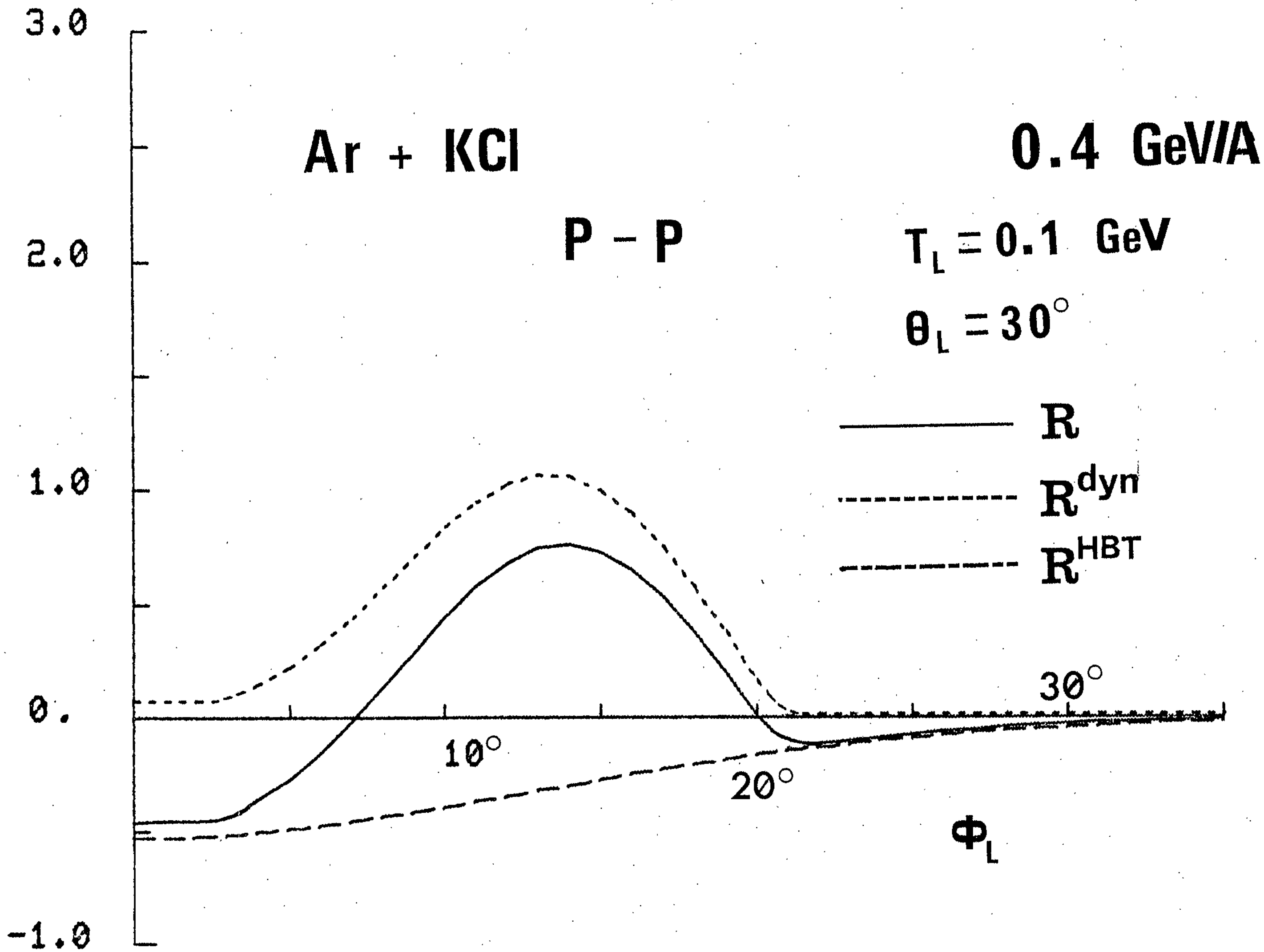

3.0
2.0
1.0
0.
-1.0
Ar + KCl
0.4 GeV/A
P - P
T_L = 0.1 GeV
θ_L = 30°
R
R^dyn
R^HBT
10°
20°
30°
Φ_L

Fig. 5(b)

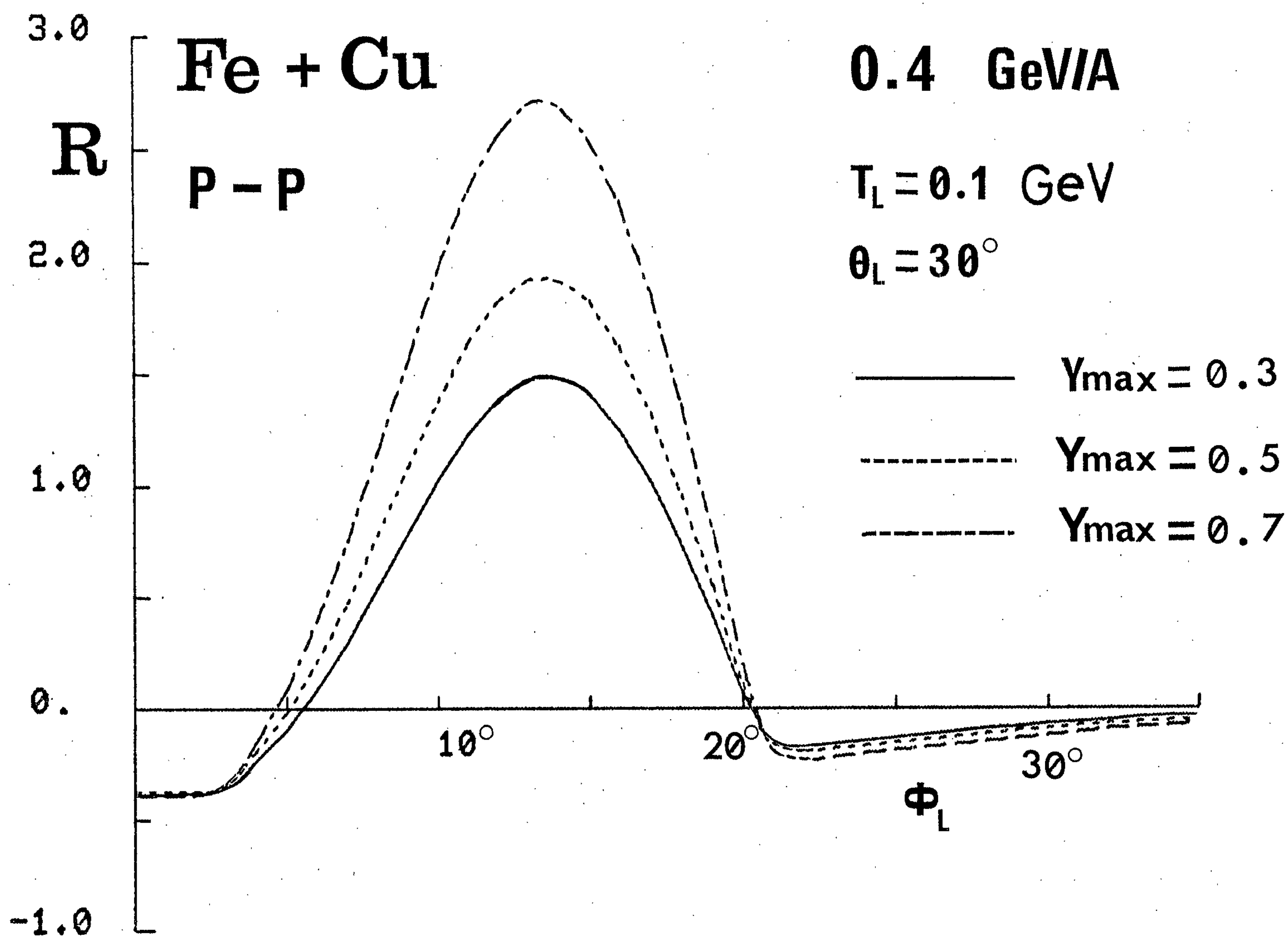

Fe + Cu
0.4 GeV/A
R
P - P
$T_L = 0.1$ GeV
$\theta_L = 30°$
Ymax = 0.3
Ymax = 0.5
Ymax = 0.7
3.0
2.0
1.0
0.
-1.0
10°
20°
30°
Φ_L

Fig. 6(a)

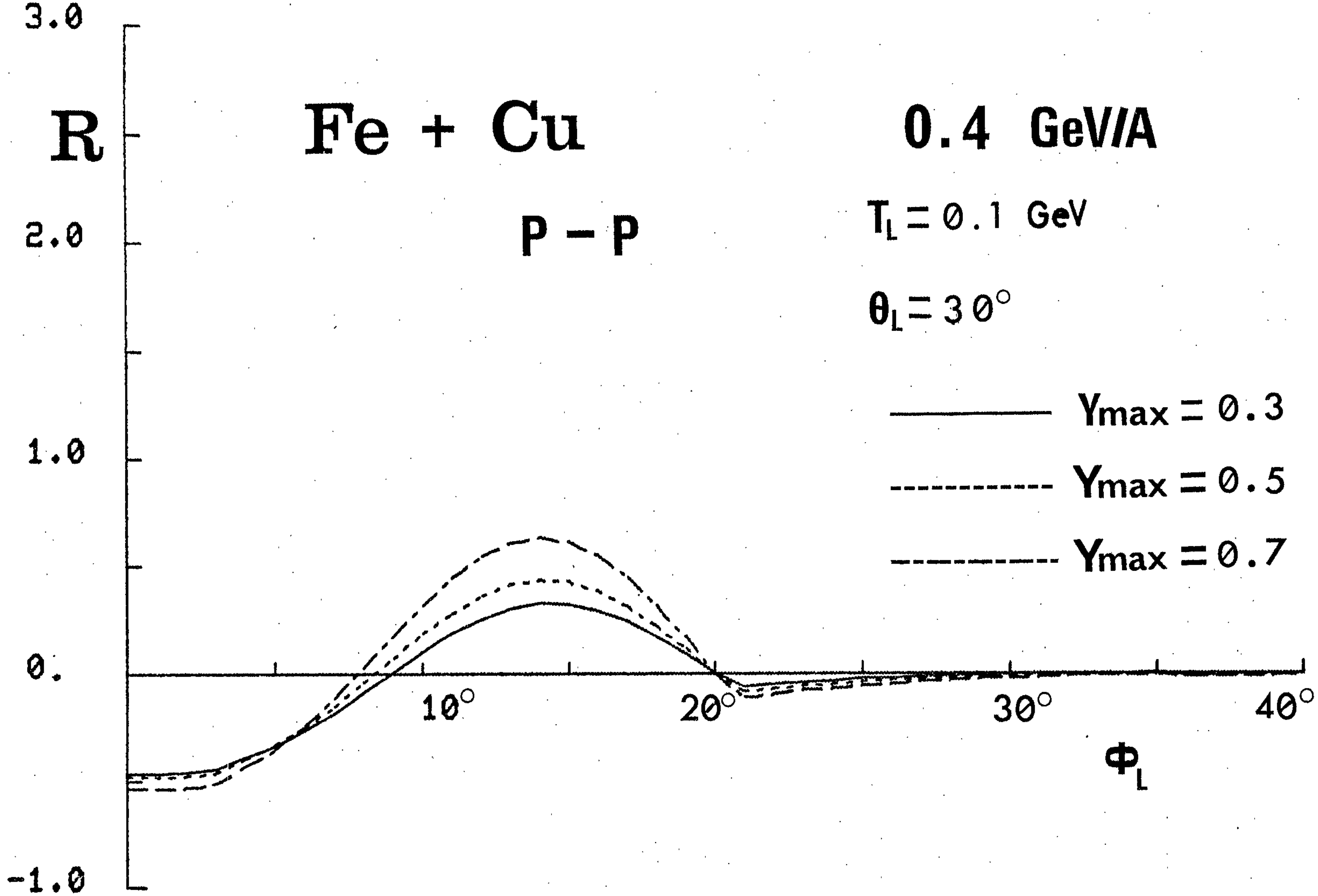

3.0
2.0
1.0
0.
-1.0
R
Fe + Cu
0.4 GeV/A
P - P
T_L = 0.1 GeV
θ_L = 30°
Ymax = 0.3
Ymax = 0.5
Ymax = 0.7
10°
20°
30°
40°
Φ_L

Fig.6(b)

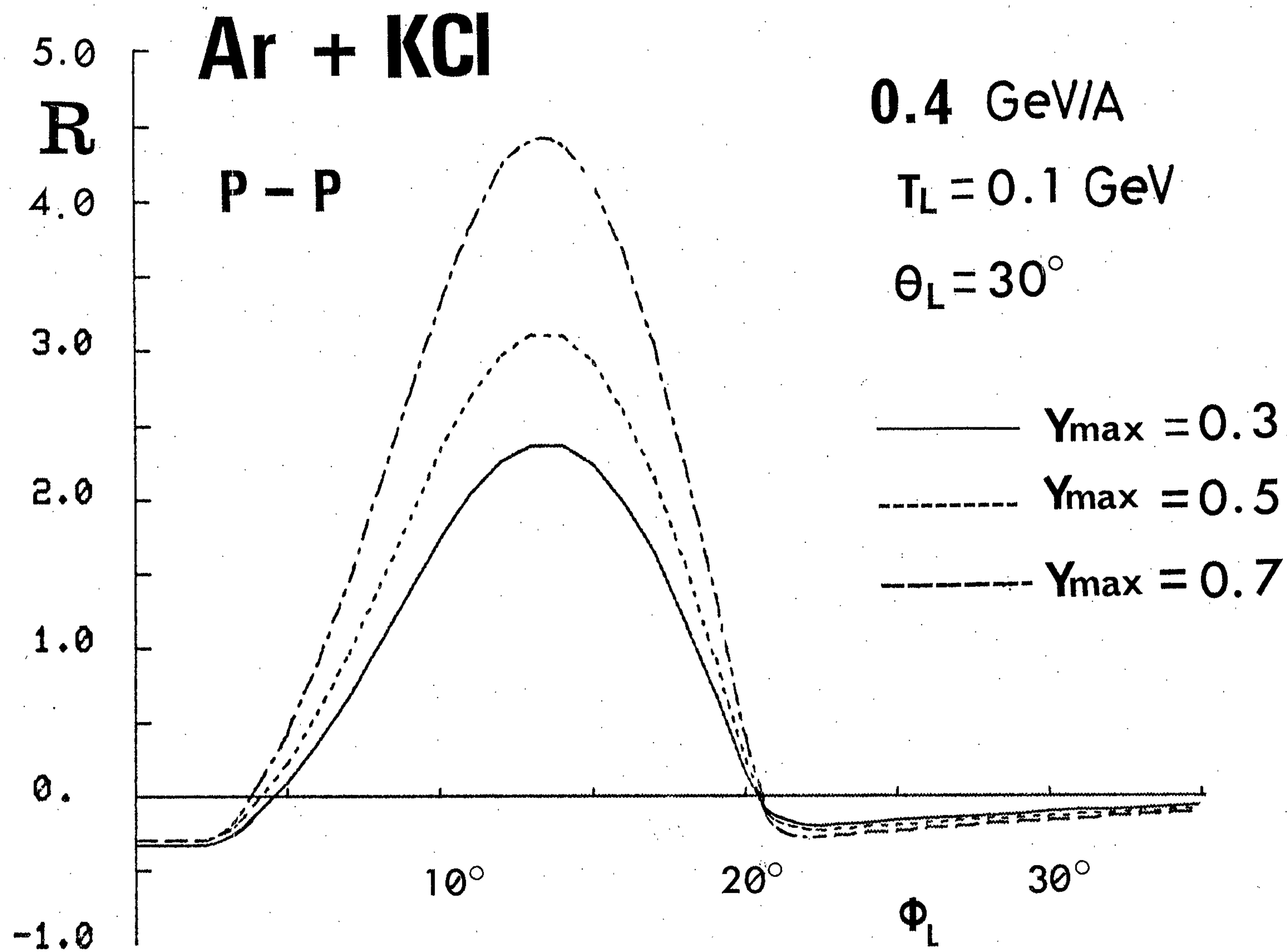
Ar + KCl
R
P – P
0.4 GeV/A
$T_L = 0.1$ GeV
$\theta_L = 30°$
$Y_{max} = 0.3$
$Y_{max} = 0.5$
$Y_{max} = 0.7$
5.0
4.0
3.0
2.0
1.0
0.
-1.0
10°
20°
30°
Φ_L

Fig. 7(a)

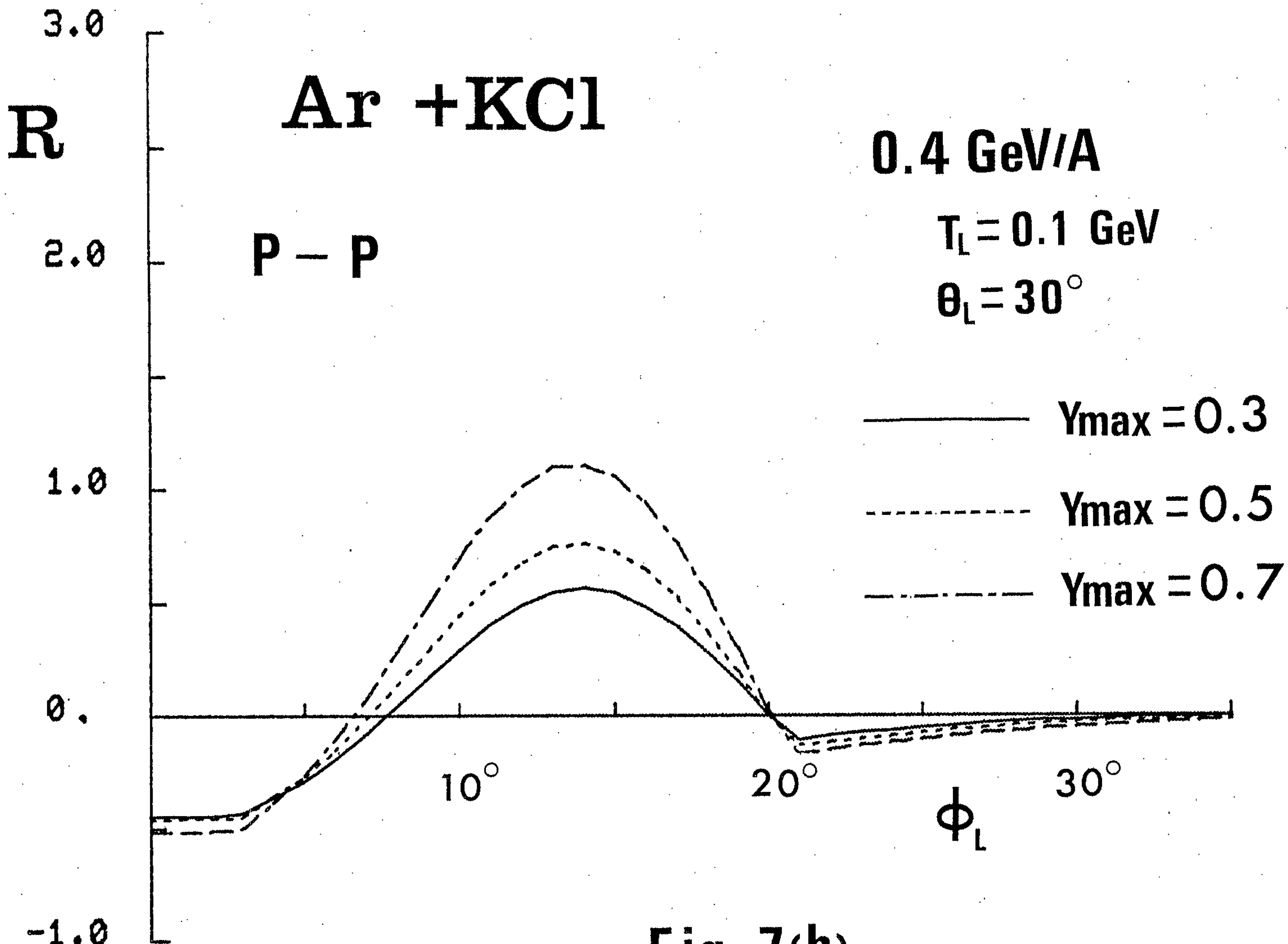
3.0
2.0
1.0
0.
-1.0
R
Ar +KCl
P – P
0.4 GeV/A
$T_L = 0.1$ GeV
$\theta_L = 30°$
Ymax = 0.3
Ymax = 0.5
Ymax = 0.7
10°
20°
30°
ϕ_L

Fig. 7(b)

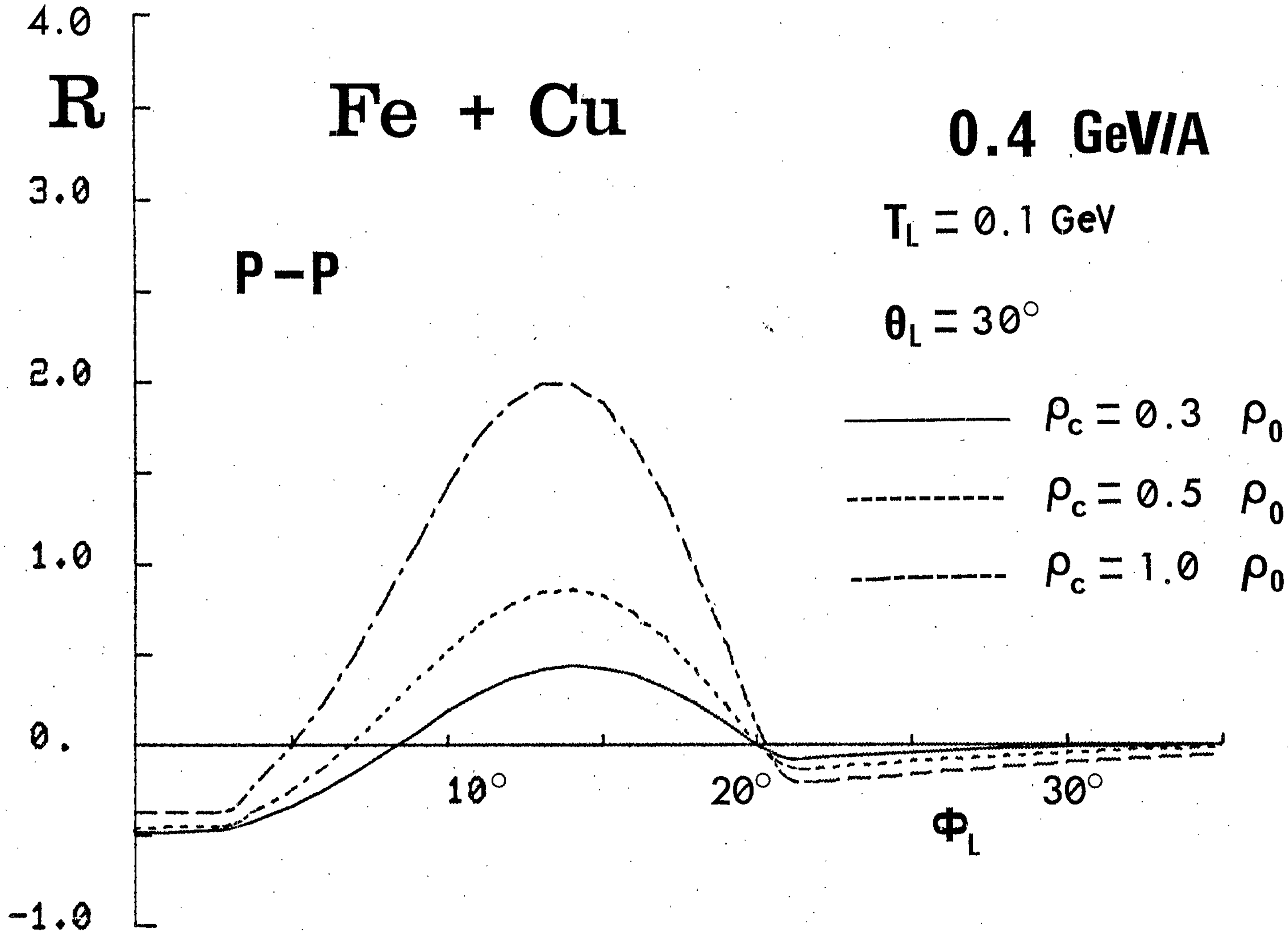

4.0
R
Fe + Cu
0.4 GeV/A
3.0
$T_L = 0.1$ GeV
P−P
$\theta_L = 30°$
2.0
$\rho_c = 0.3\ \rho_0$
$\rho_c = 0.5\ \rho_0$
1.0
$\rho_c = 1.0\ \rho_0$
0.
10°
20°
30°
Φ_L
−1.0

Fig. 8(a)

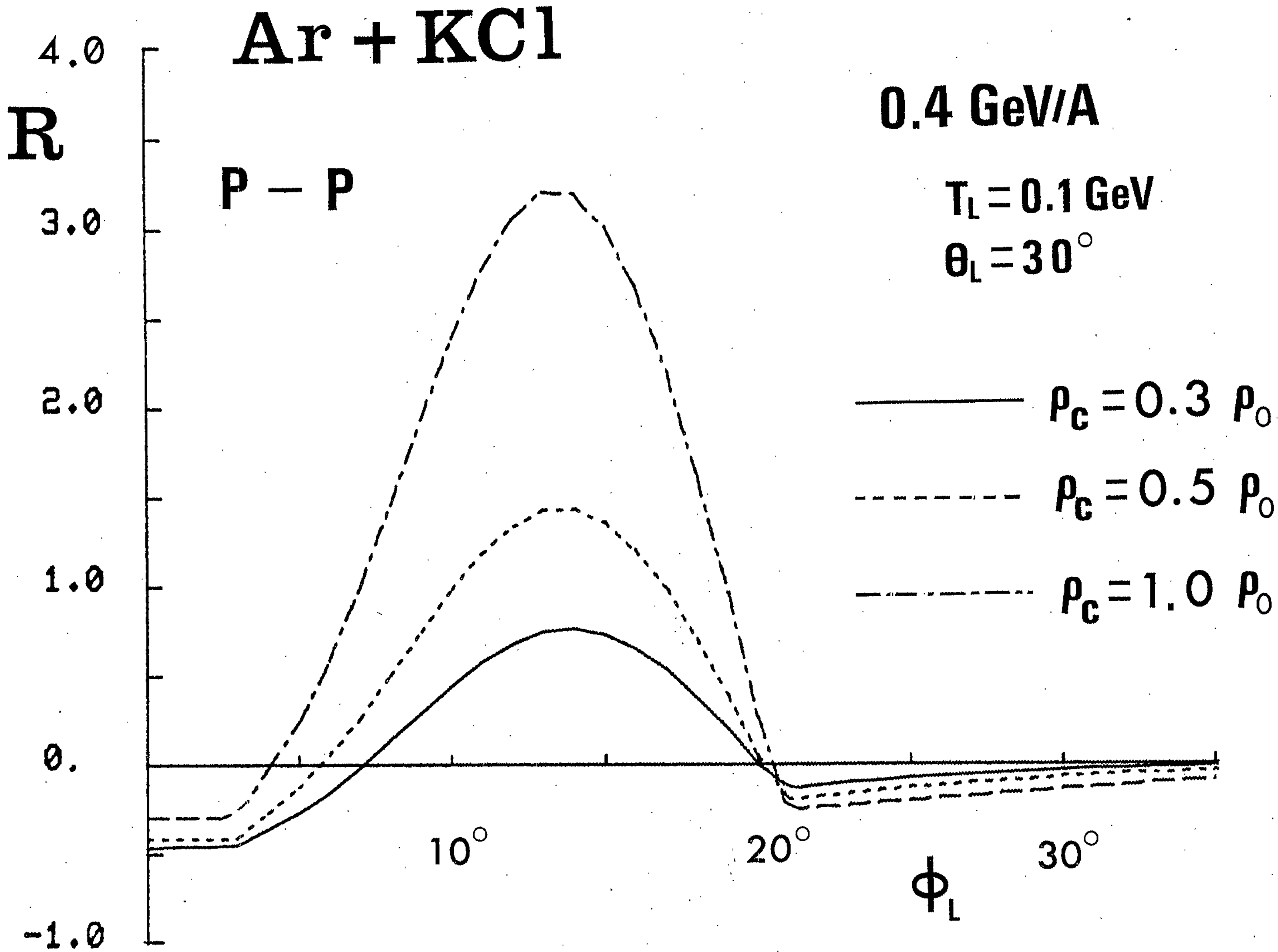

Ar + KCl
R
P − P
0.4 GeV/A
$T_L = 0.1$ GeV
$\theta_L = 30°$
$\rho_c = 0.3\ \rho_0$
$\rho_c = 0.5\ \rho_0$
$\rho_c = 1.0\ \rho_0$
4.0
3.0
2.0
1.0
0.
-1.0
10°
20°
30°
ϕ_L

Fig. 8(b)

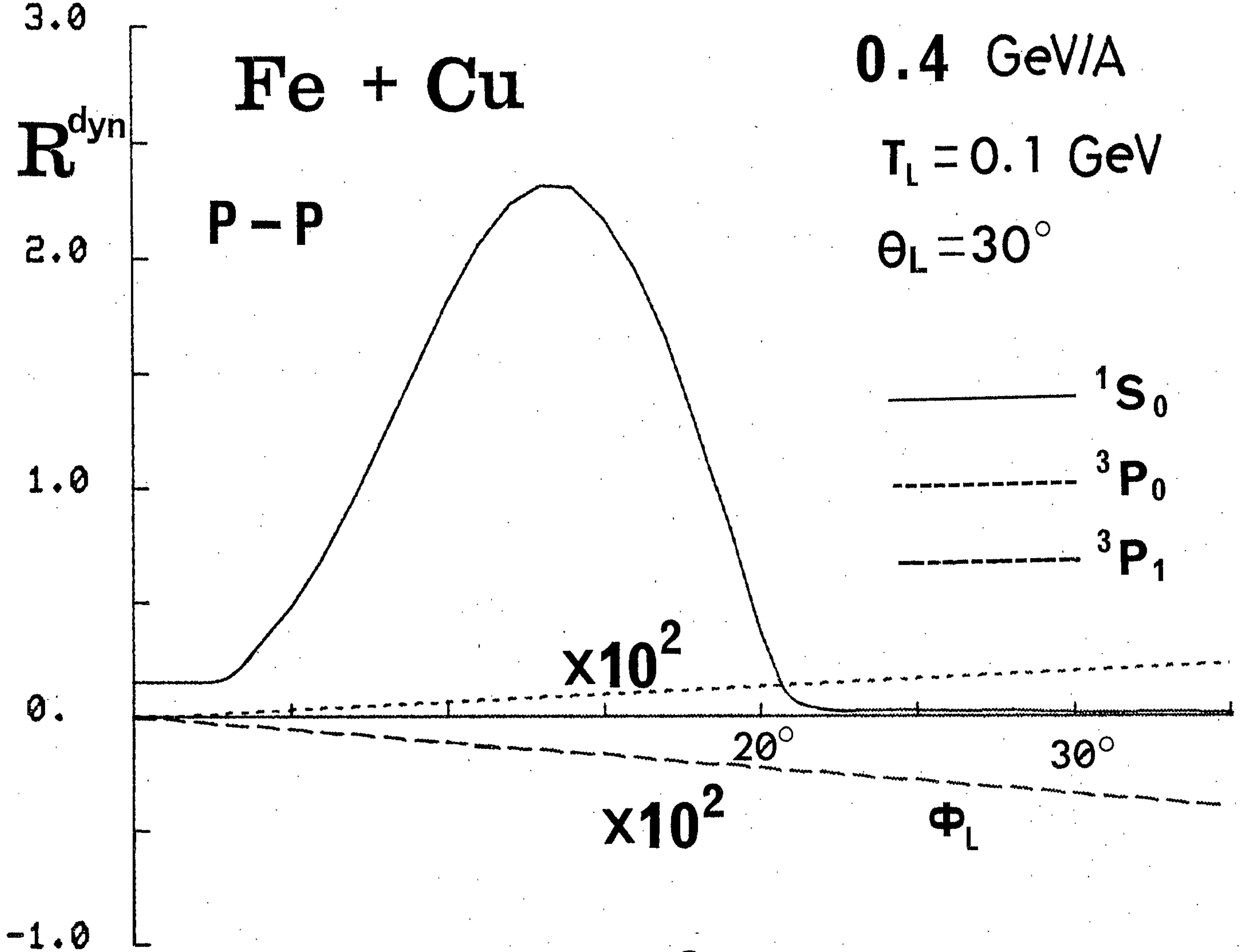
3.0
2.0
1.0
0.
-1.0
Fe + Cu
R^dyn
P – P
0.4 GeV/A
T_L = 0.1 GeV
Θ_L = 30°
¹S₀
³P₀
³P₁
x10²
x10²
20°
30°
Φ_L

Fig. 9

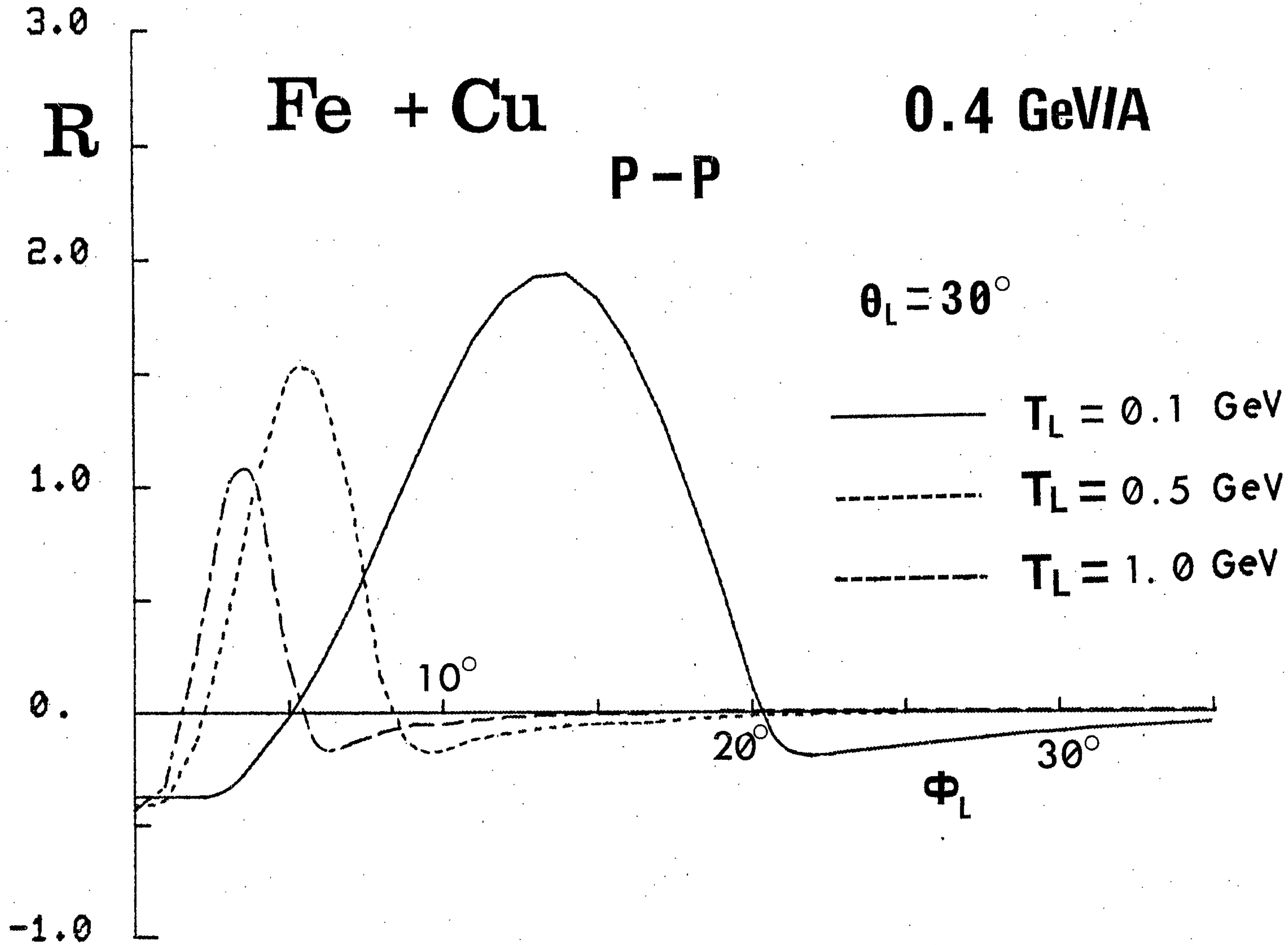

3.0
2.0
1.0
0.
-1.0
R
Fe + Cu
0.4 GeV/A
P - P
$\theta_L = 30°$
$T_L = 0.1$ GeV
$T_L = 0.5$ GeV
$T_L = 1.0$ GeV
10°
20°
30°
Φ_L

Fig.10(a)

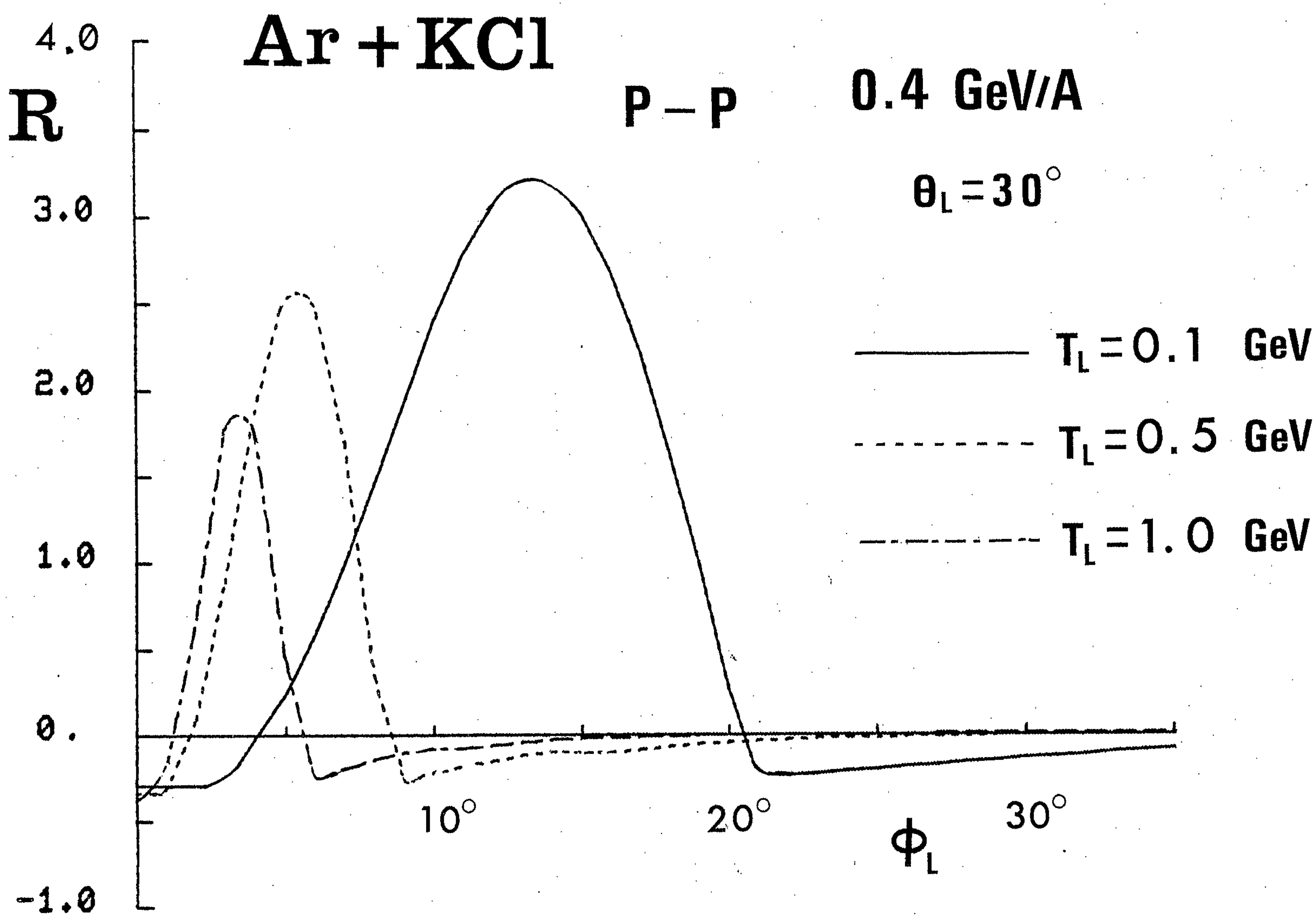
Ar + KCl
P – P
0.4 GeV/A
θL = 30°
R
4.0
3.0
2.0
1.0
0.
-1.0
10°
20°
30°
φL
TL = 0.1 GeV
TL = 0.5 GeV
TL = 1.0 GeV

Fig. 10(b)

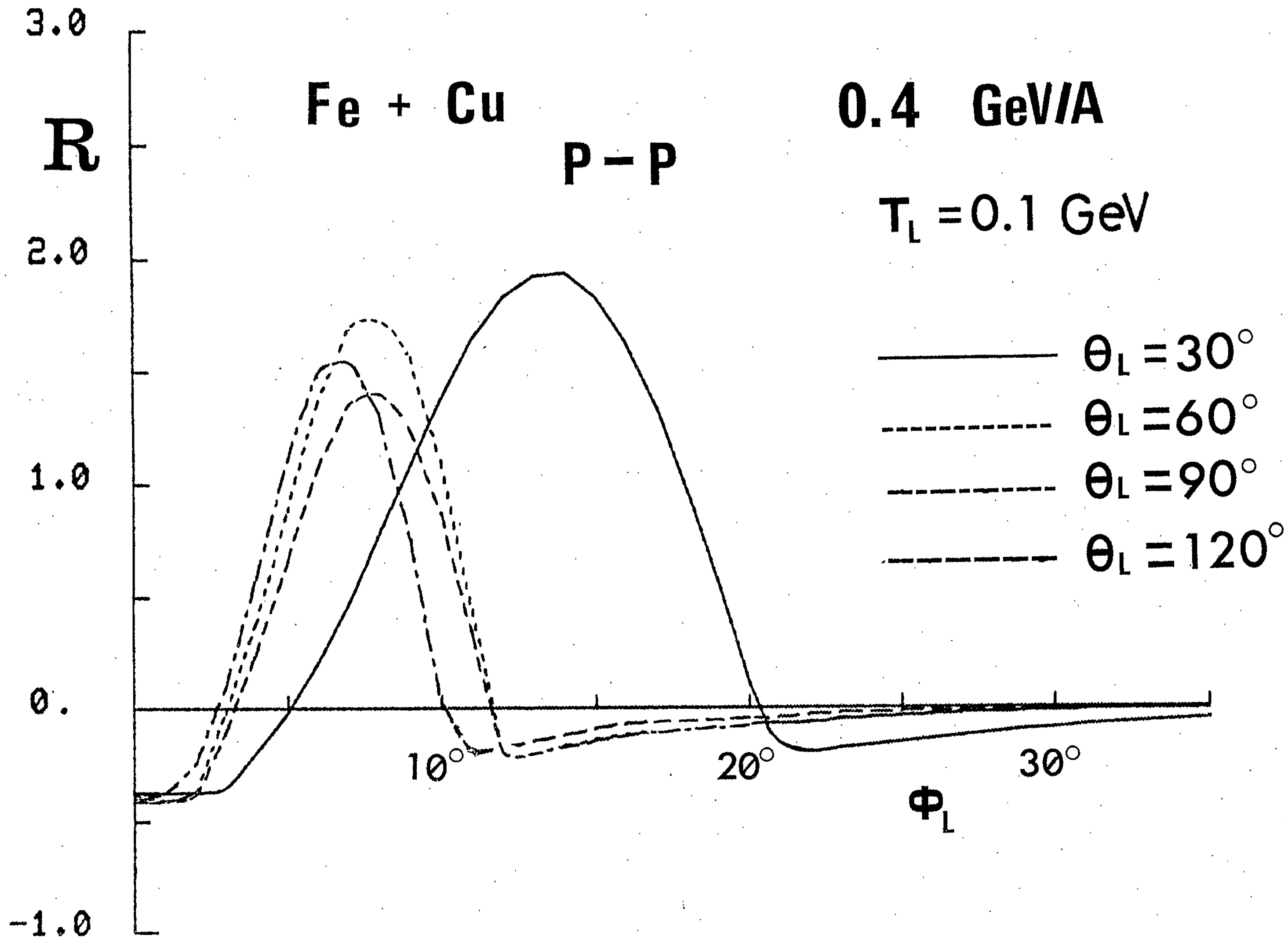
3.0
2.0
1.0
0.
-1.0
R
Fe + Cu
P - P
0.4 GeV/A
T_L =0.1 GeV
$\theta_L = 30°$
$\theta_L = 60°$
$\theta_L = 90°$
$\theta_L = 120°$
10°
20°
30°
Φ_L

Fig.11(a)

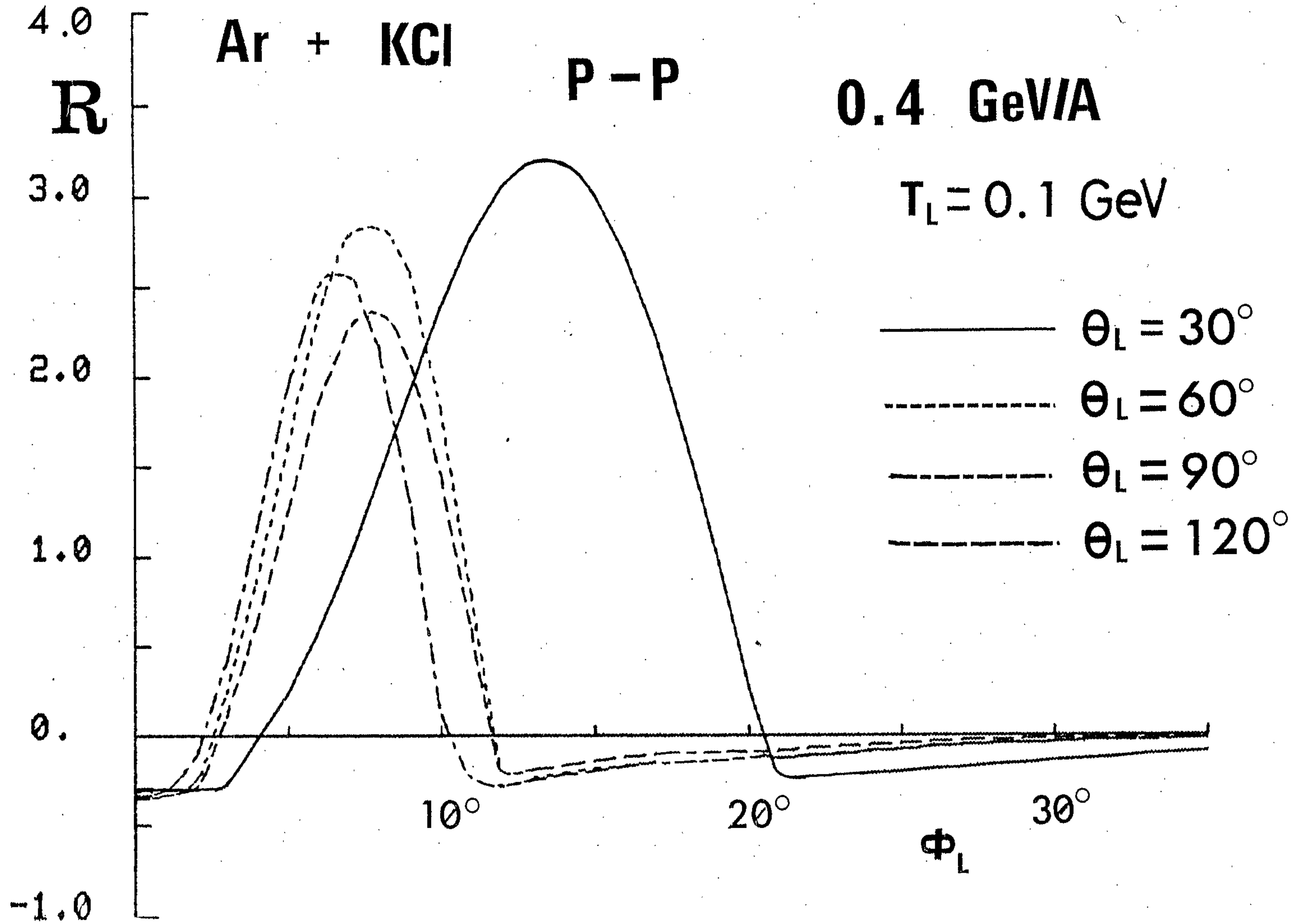
4.0
3.0
2.0
1.0
0.
-1.0
R
Ar + KCl
P - P
0.4 GeV/A
$T_L = 0.1$ GeV
$\theta_L = 30°$
$\theta_L = 60°$
$\theta_L = 90°$
$\theta_L = 120°$
10°
20°
30°
Φ_L

Fig. 11(b)

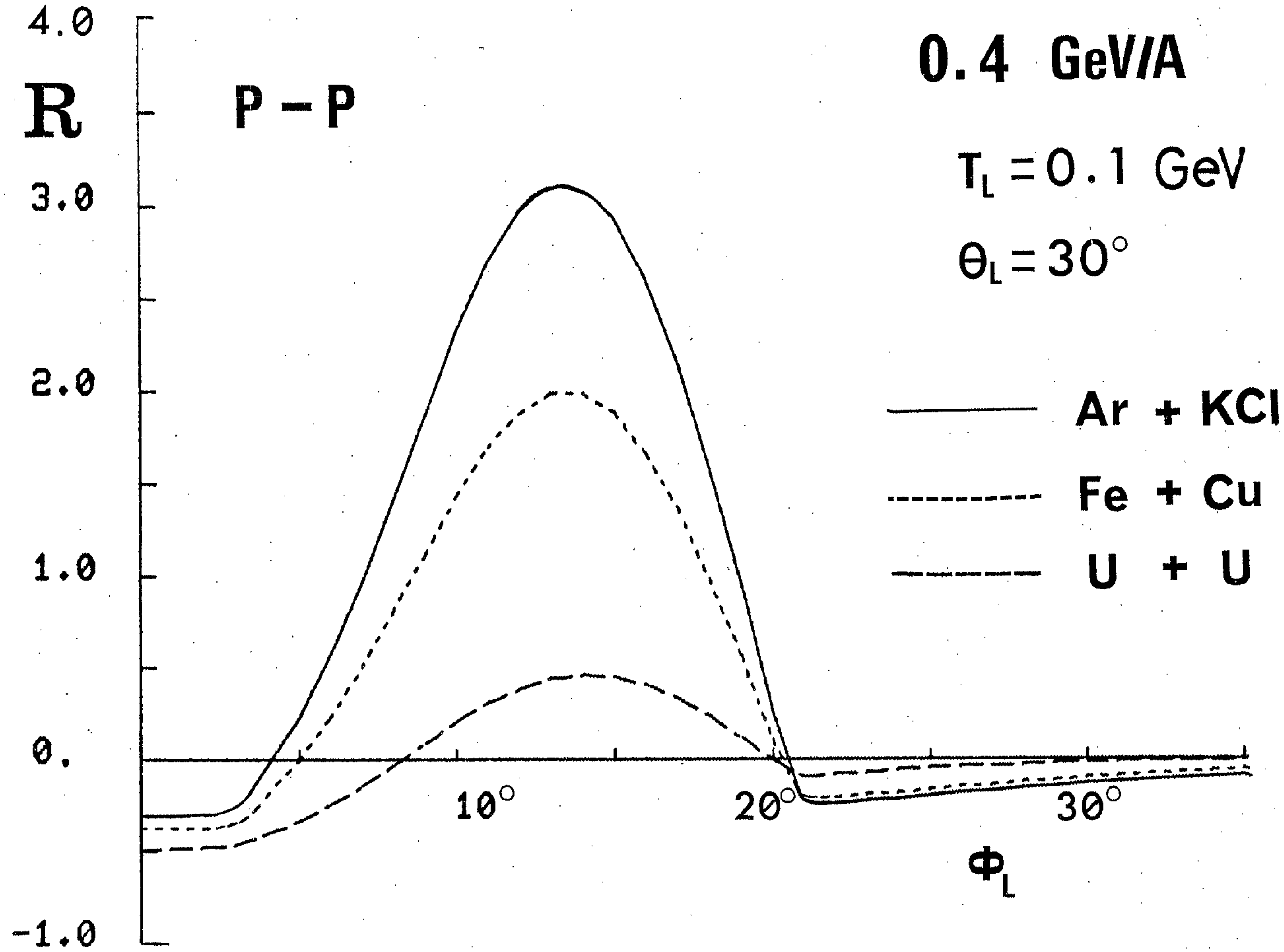
4.0
R
P – P
3.0
2.0
1.0
0.
-1.0
10°
20°
30°
Φ_L
0.4 GeV/A
$T_L = 0.1$ GeV
$\theta_L = 30°$
Ar + KCl
Fe + Cu
U + U

Fig. 12(a)

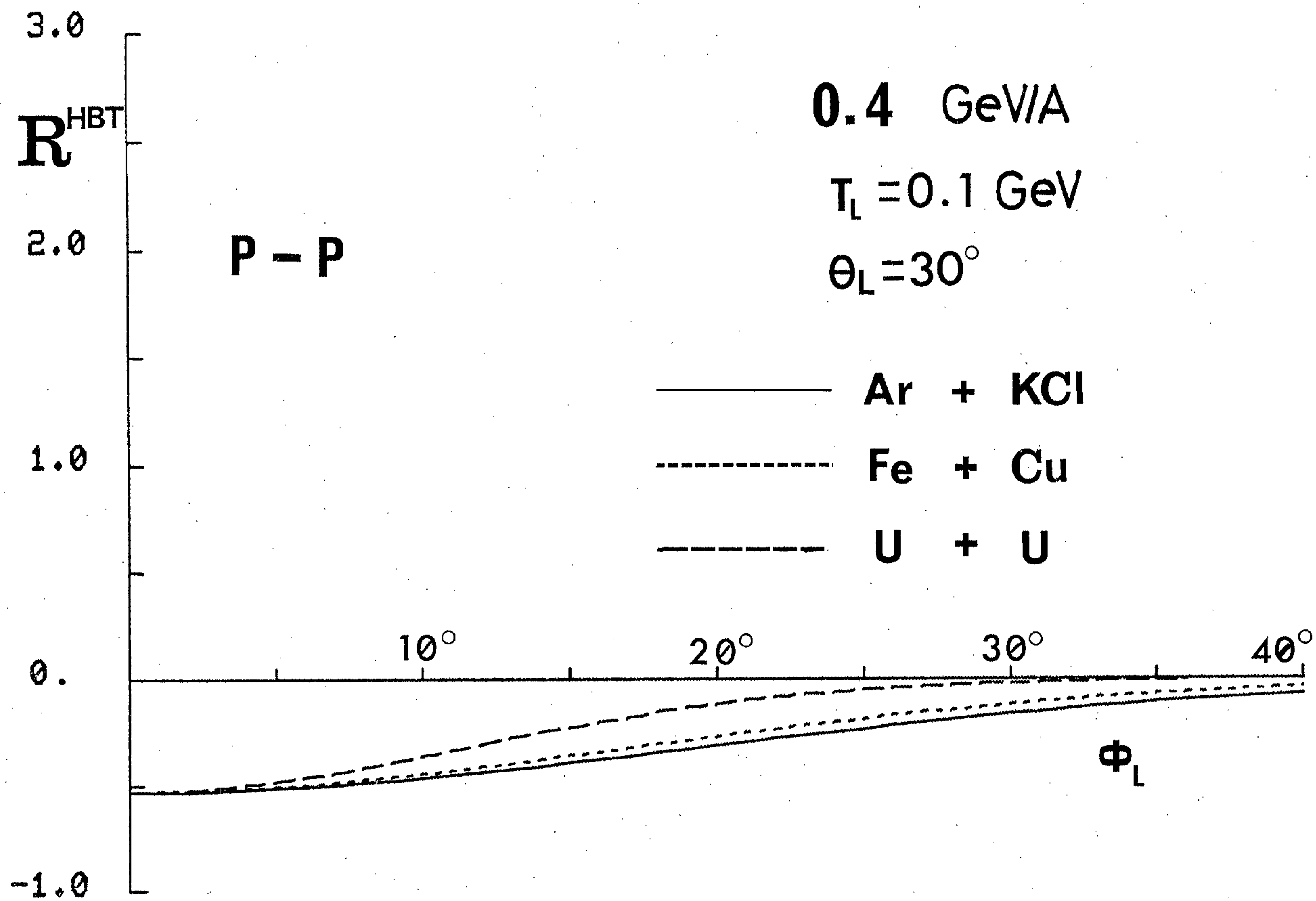

3.0
2.0
1.0
0.
-1.0
R^{HBT}
P – P
0.4 GeV/A
T_L =0.1 GeV
θ_L=30°
Ar + KCl
Fe + Cu
U + U
10°
20°
30°
40°
Φ_L

Fig.12(b)

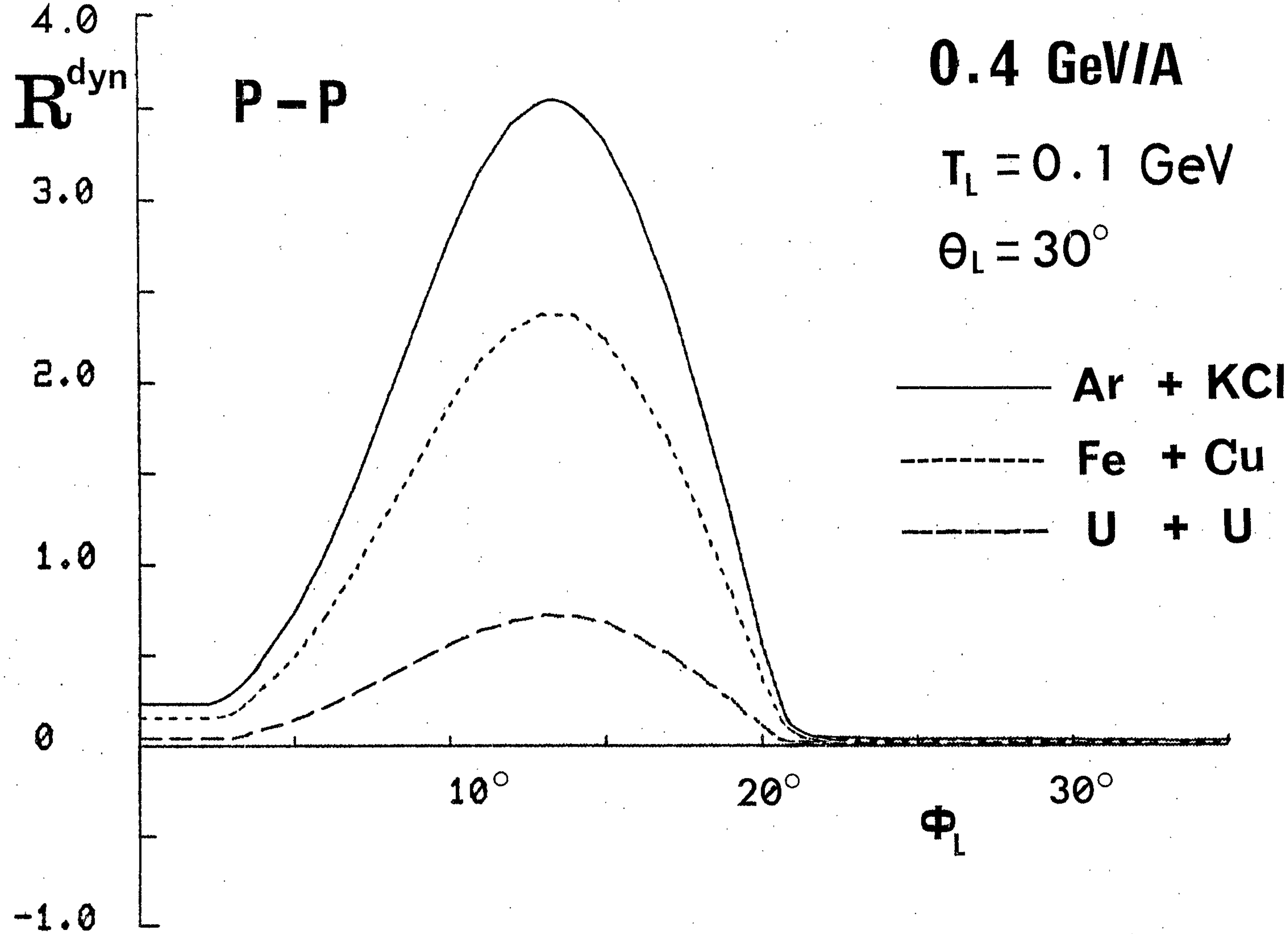

4.0
3.0
2.0
1.0
0
-1.0
R^{dyn}
P - P
0.4 GeV/A
$T_L = 0.1$ GeV
$\theta_L = 30°$
Ar + KCl
Fe + Cu
U + U
10°
20°
30°
Φ_L

Fig.12(c)

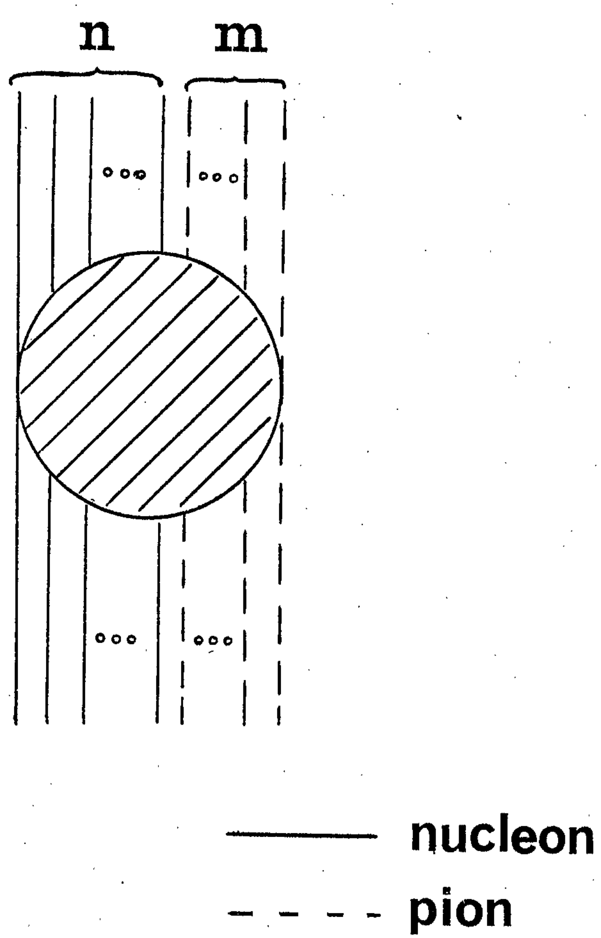

Fig. 13

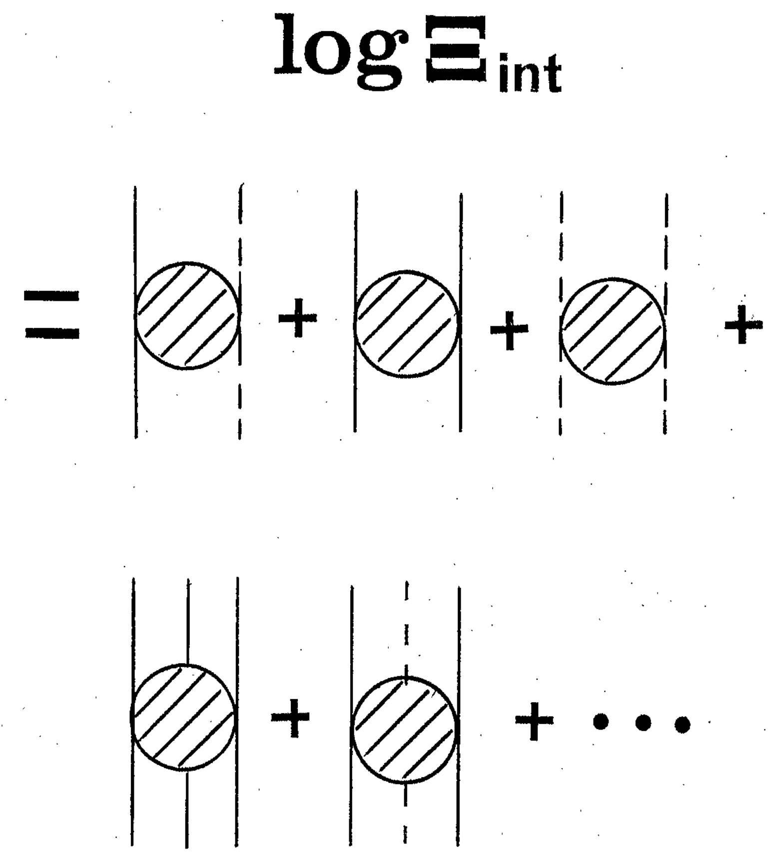

Fig. 14

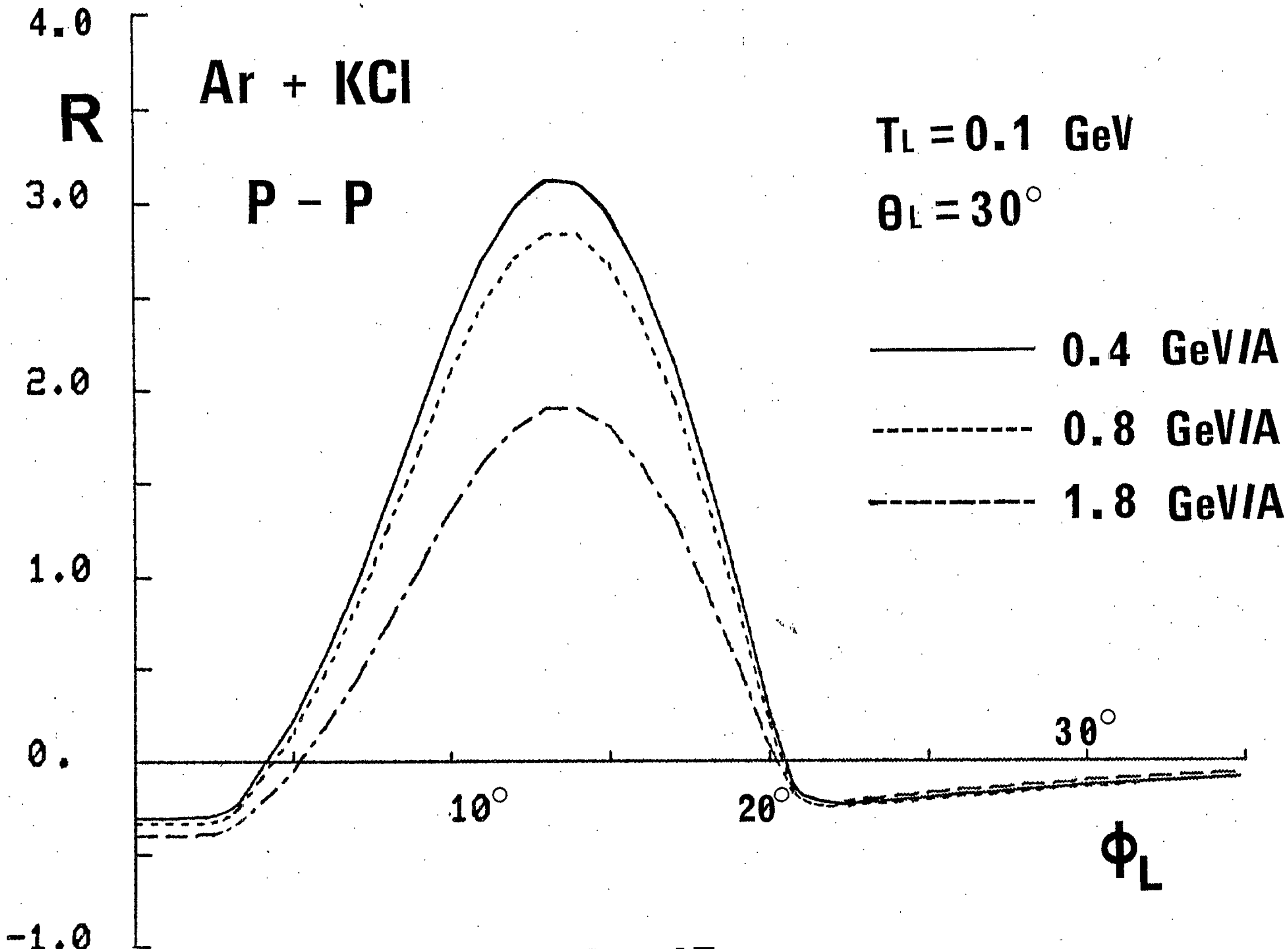

4.0
3.0
2.0
1.0
0.
-1.0
R
Ar + KCl
P - P
$T_L = 0.1$ GeV
$\theta_L = 30^\circ$
0.4 GeV/A
0.8 GeV/A
1.8 GeV/A
10°
20°
30°
ϕ_L

Fig.15(a)

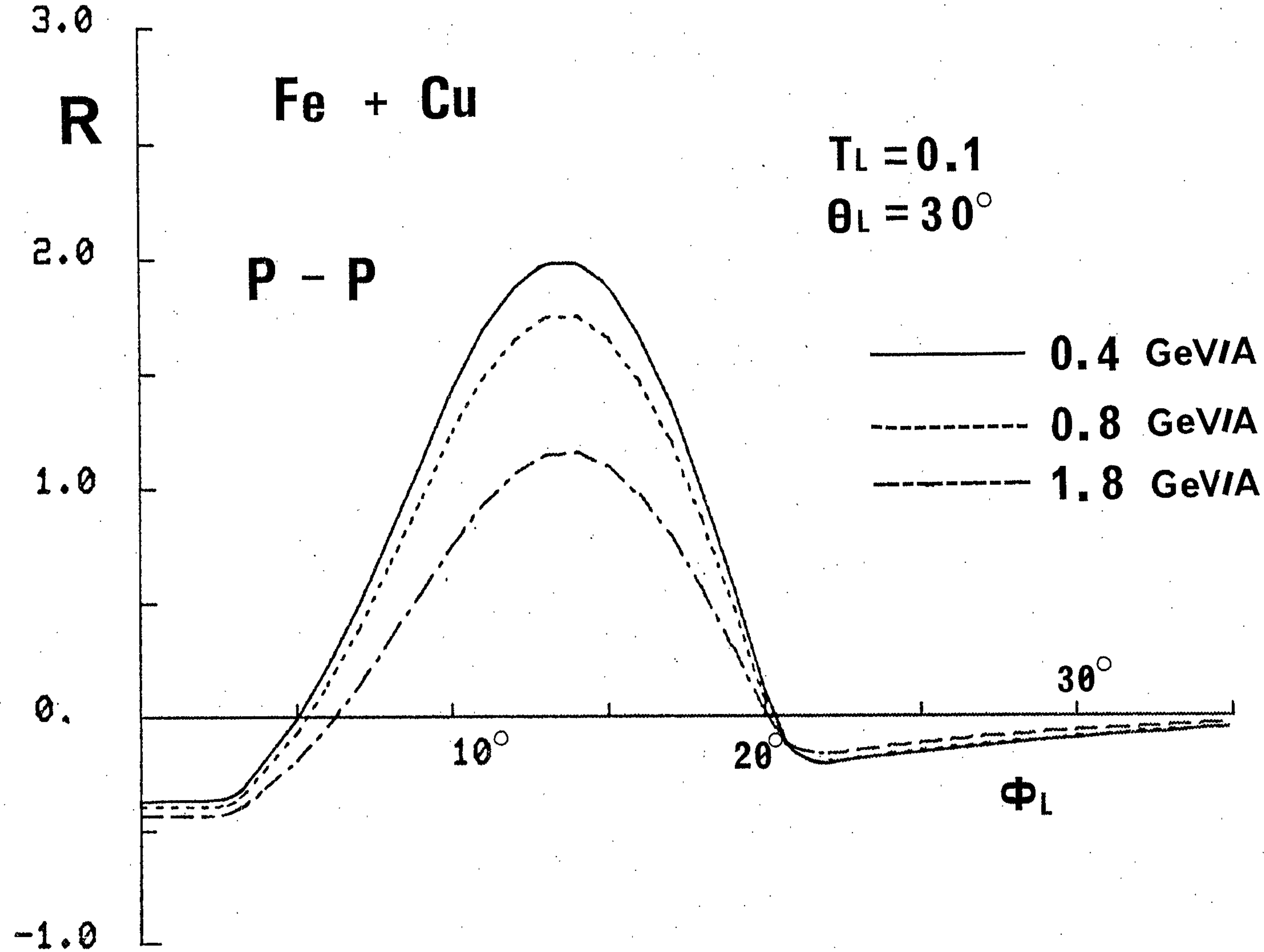
3.0
2.0
1.0
0.
-1.0
R
Fe + Cu
P - P
$T_L = 0.1$
$\theta_L = 30^\circ$
0.4 GeV/A
0.8 GeV/A
1.8 GeV/A
10°
20°
30°
Φ_L

Fig.15(b)

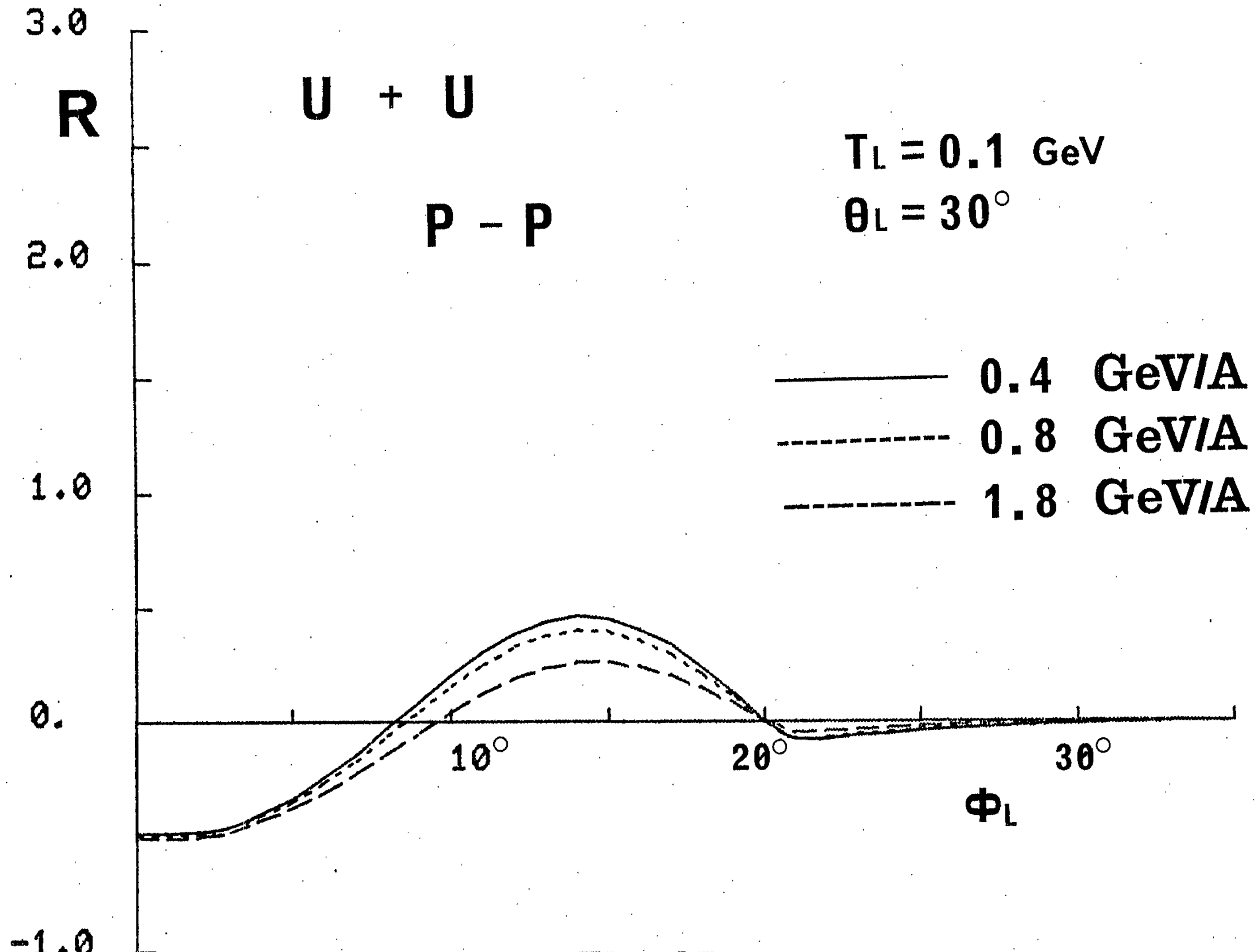
3.0
R
U + U
P - P
$T_L = 0.1$ GeV
$\theta_L = 30^\circ$
2.0
0.4 GeV/A
0.8 GeV/A
1.8 GeV/A
1.0
0.
10°
20°
30°
Φ_L
-1.0

Fig.15(c)

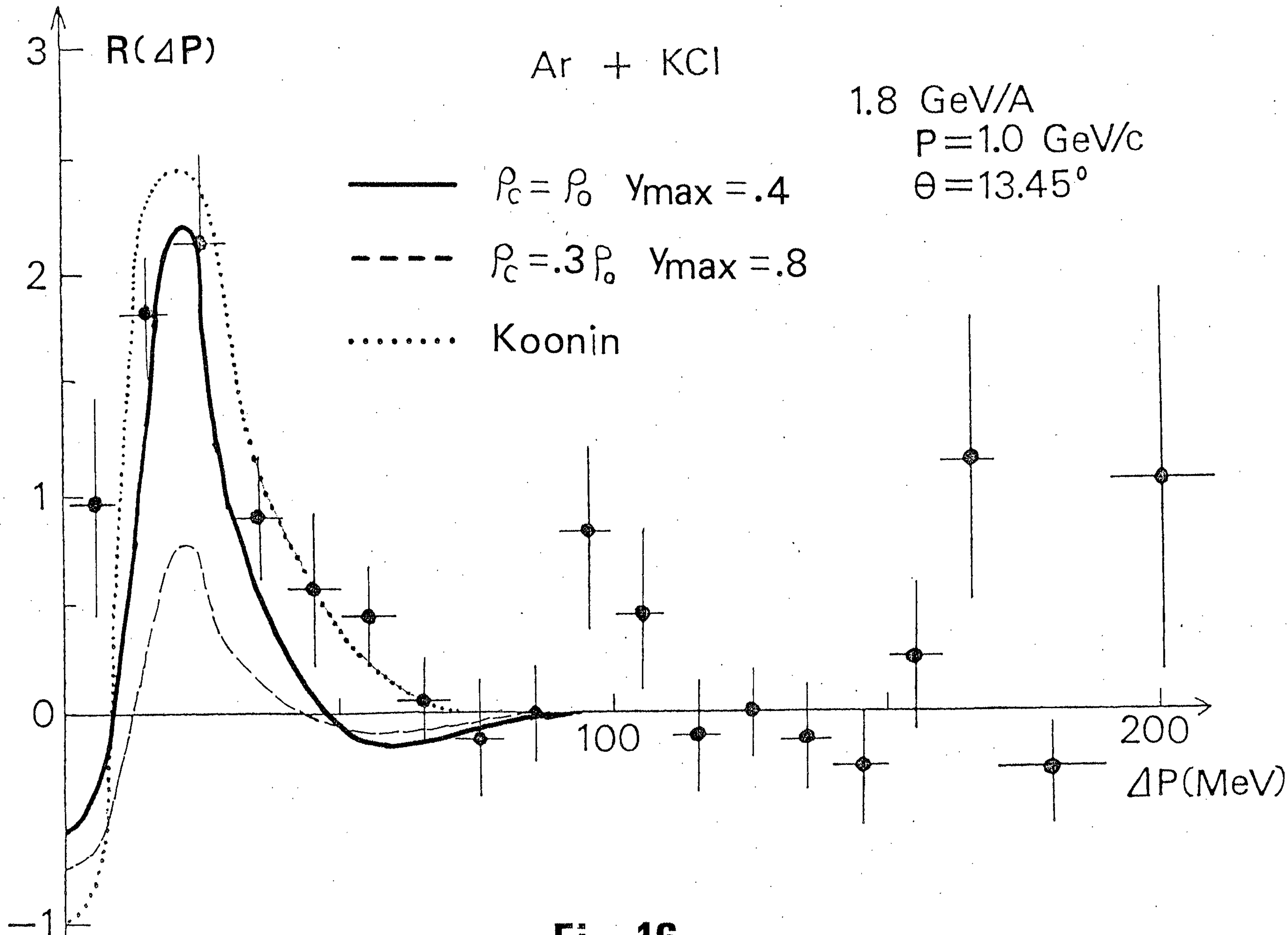

R(ΔP)
3
2
1
0
−1
Ar + KCl
1.8 GeV/A
P = 1.0 GeV/c
θ = 13.45°
$\rho_c = \rho_o$ $y_{max} = .4$
$\rho_c = .3\rho_o$ $y_{max} = .8$
Koonin
100
200
ΔP(MeV)

Fig. 16

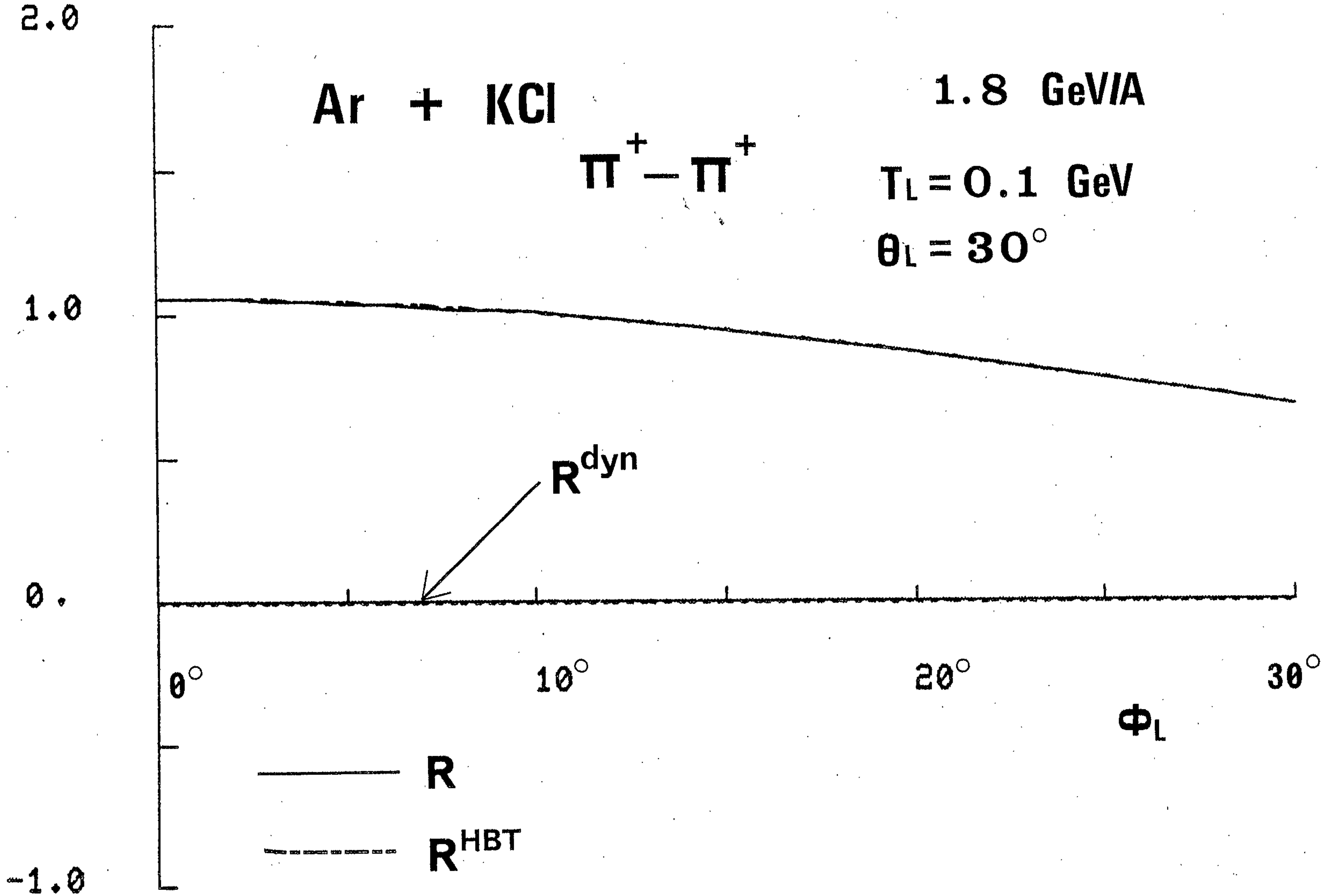

2.0
1.0
0.
-1.0
Ar + KCl
1.8 GeV/A
$\pi^+-\pi^+$
$T_L = 0.1$ GeV
$\theta_L = 30^\circ$
R^{dyn}
0°
10°
20°
30°
Φ_L
R
R^{HBT}

Fig.17(a)

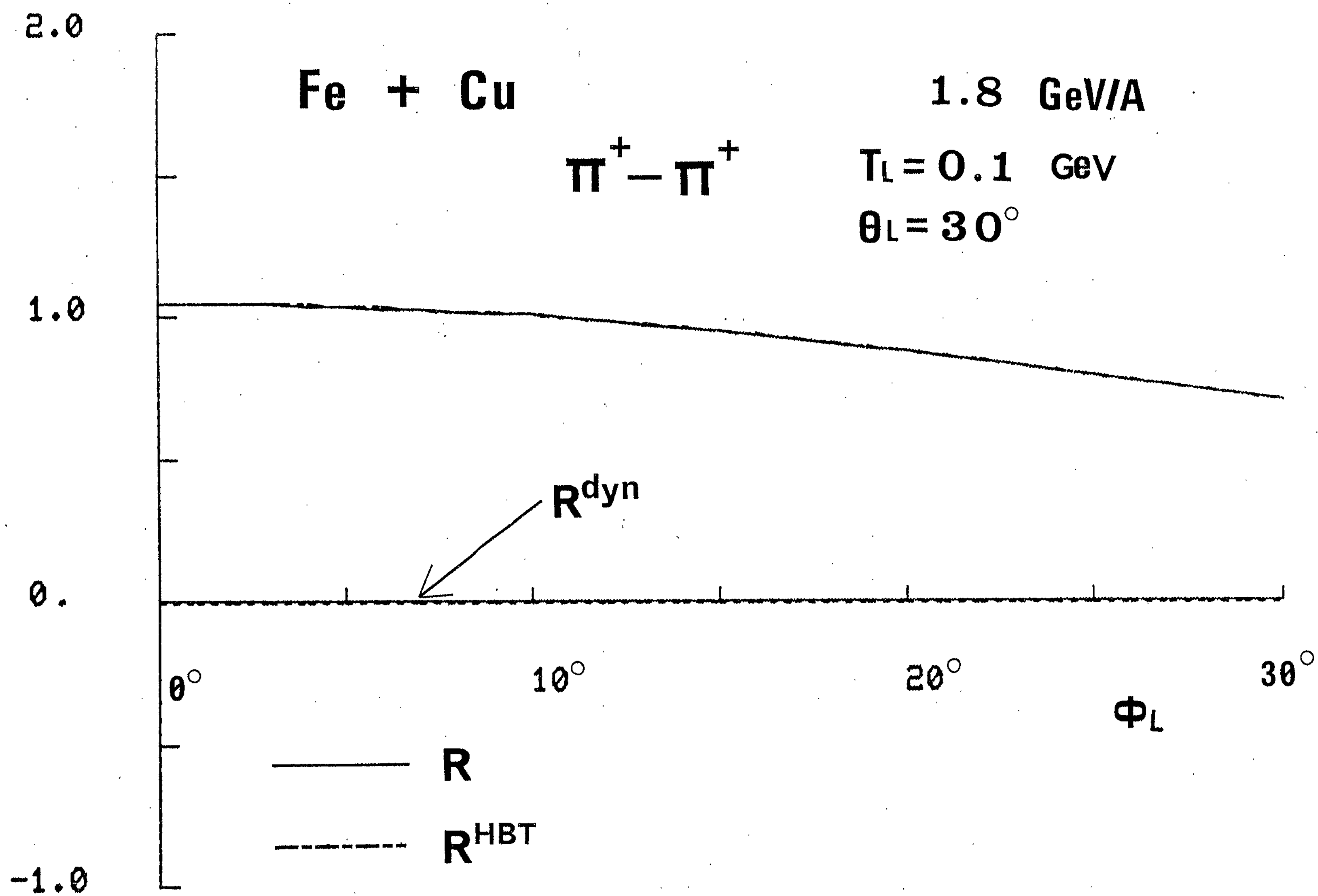

Fig.17(b)

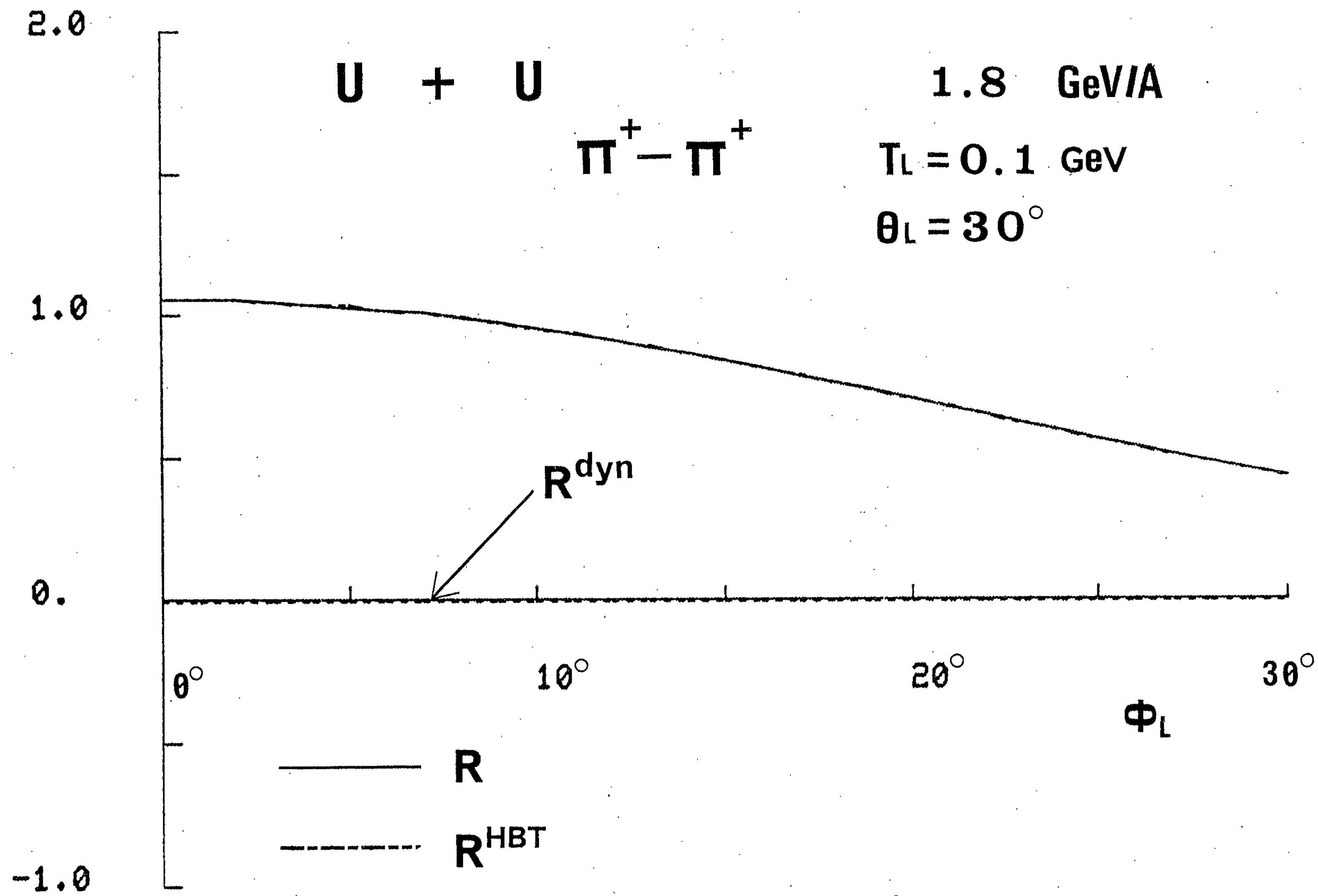

Fig.17(c)

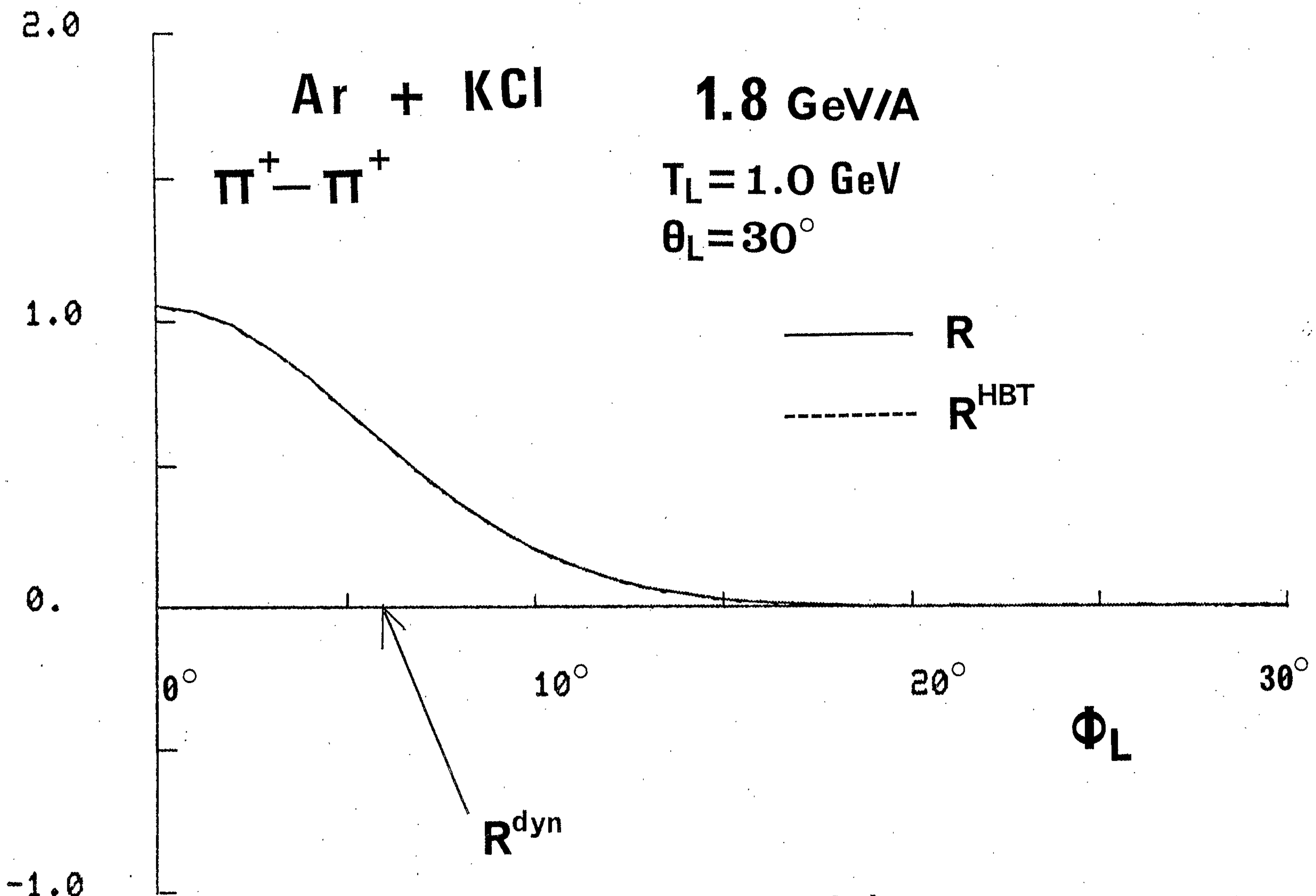

Fig.18(a)

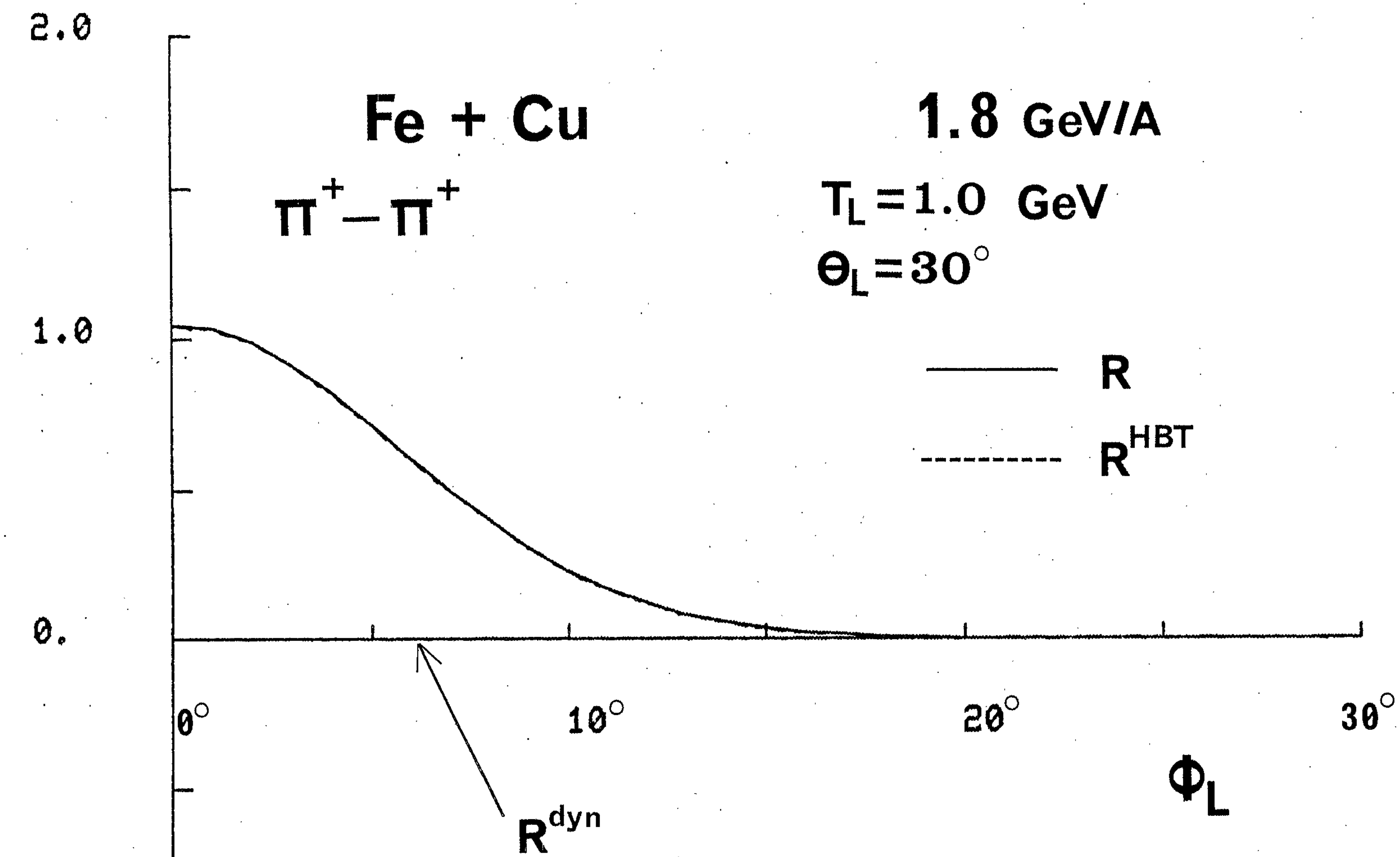

Fig.18(b)

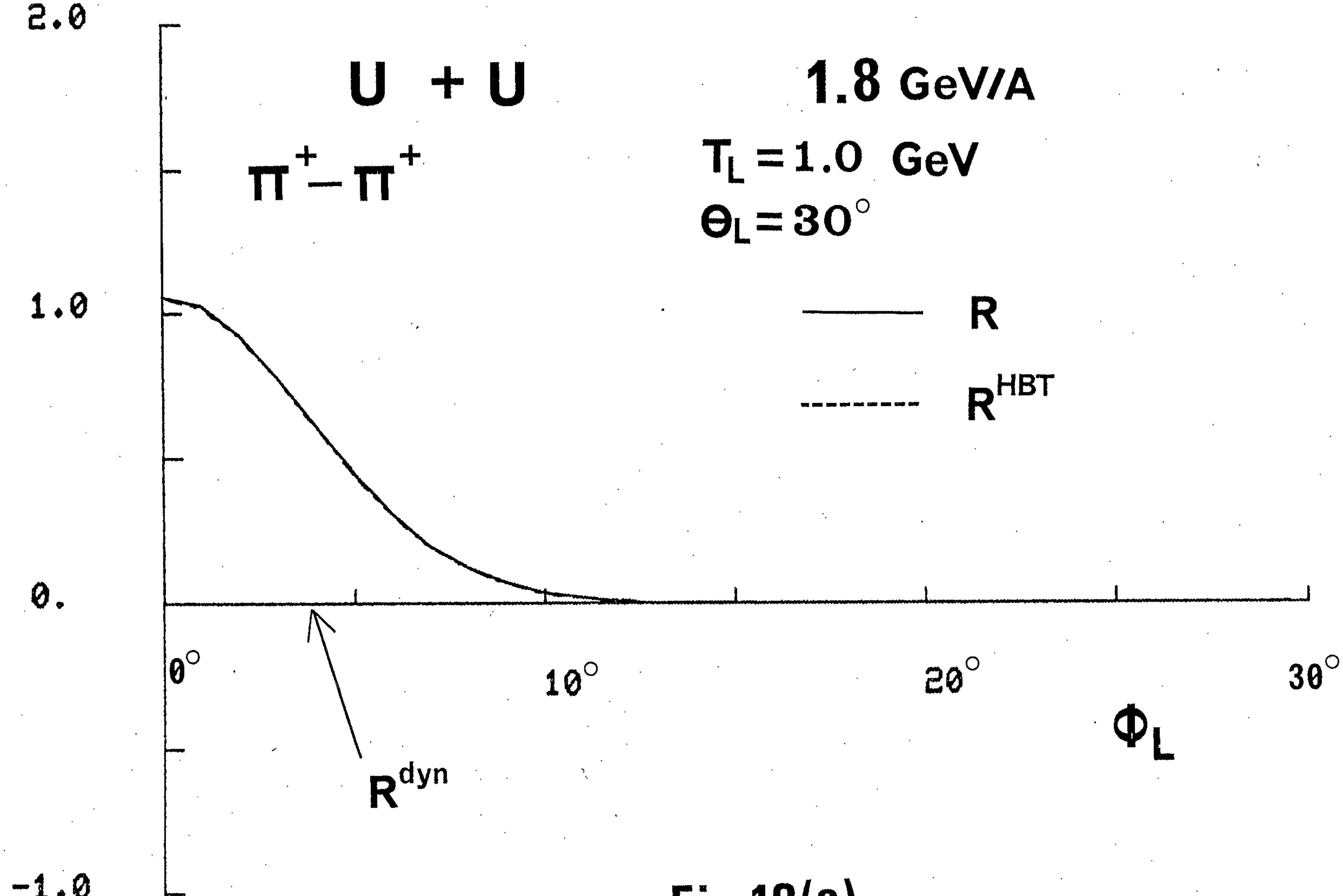
2.0
1.0
0.
-1.0
U + U
1.8 GeV/A
π⁺–π⁺
$T_L = 1.0$ GeV
$\Theta_L = 30°$
R
R^{HBT}
R^{dyn}
0°
10°
20°
30°
Φ_L

Fig.18(c)

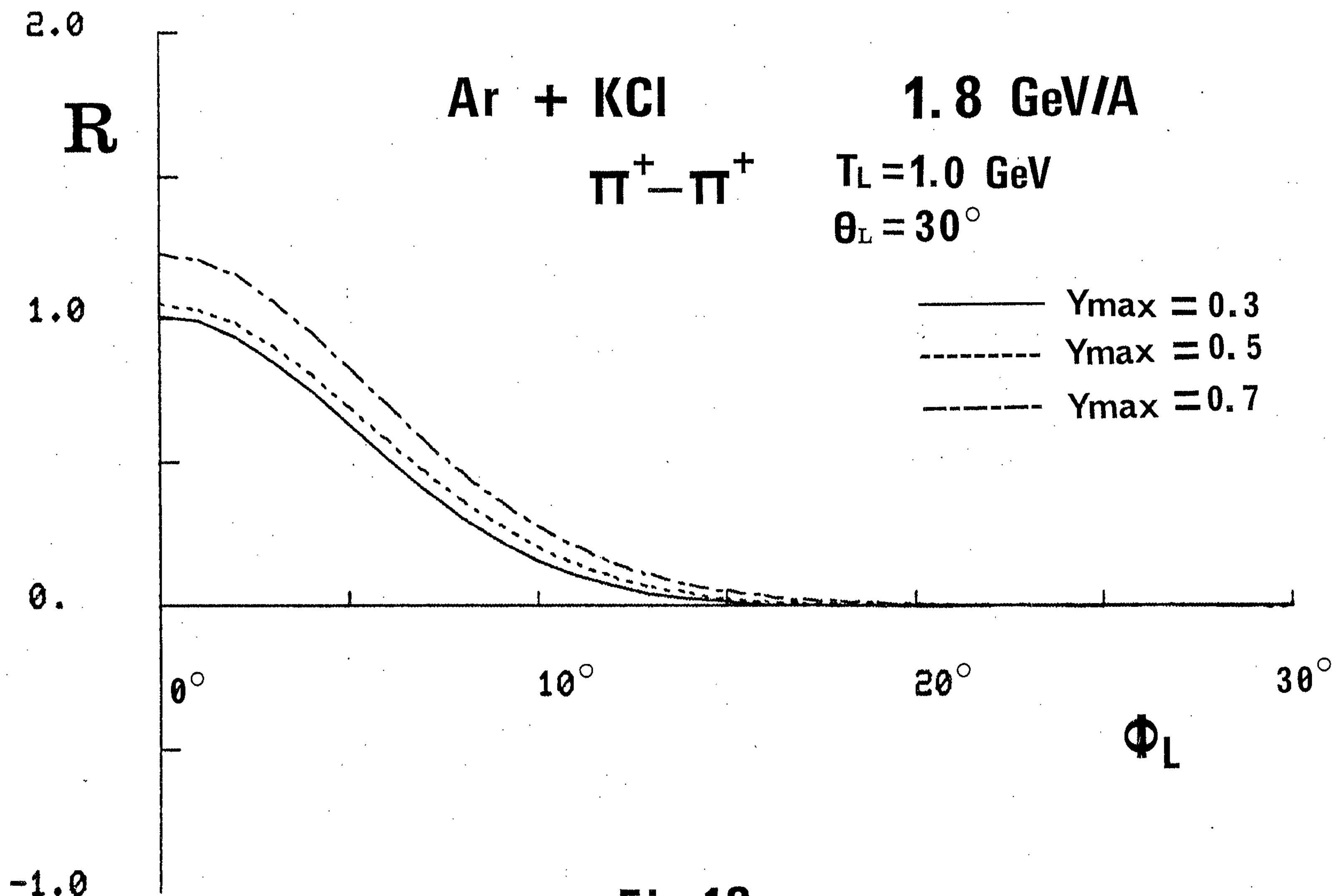
2.0
R
Ar + KCl
1.8 GeV/A
π⁺–π⁺
T_L =1.0 GeV
θ_L = 30°
1.0
Ymax = 0.3
Ymax = 0.5
Ymax = 0.7
0.
0°
10°
20°
30°
Φ_L
-1.0

Fig.19

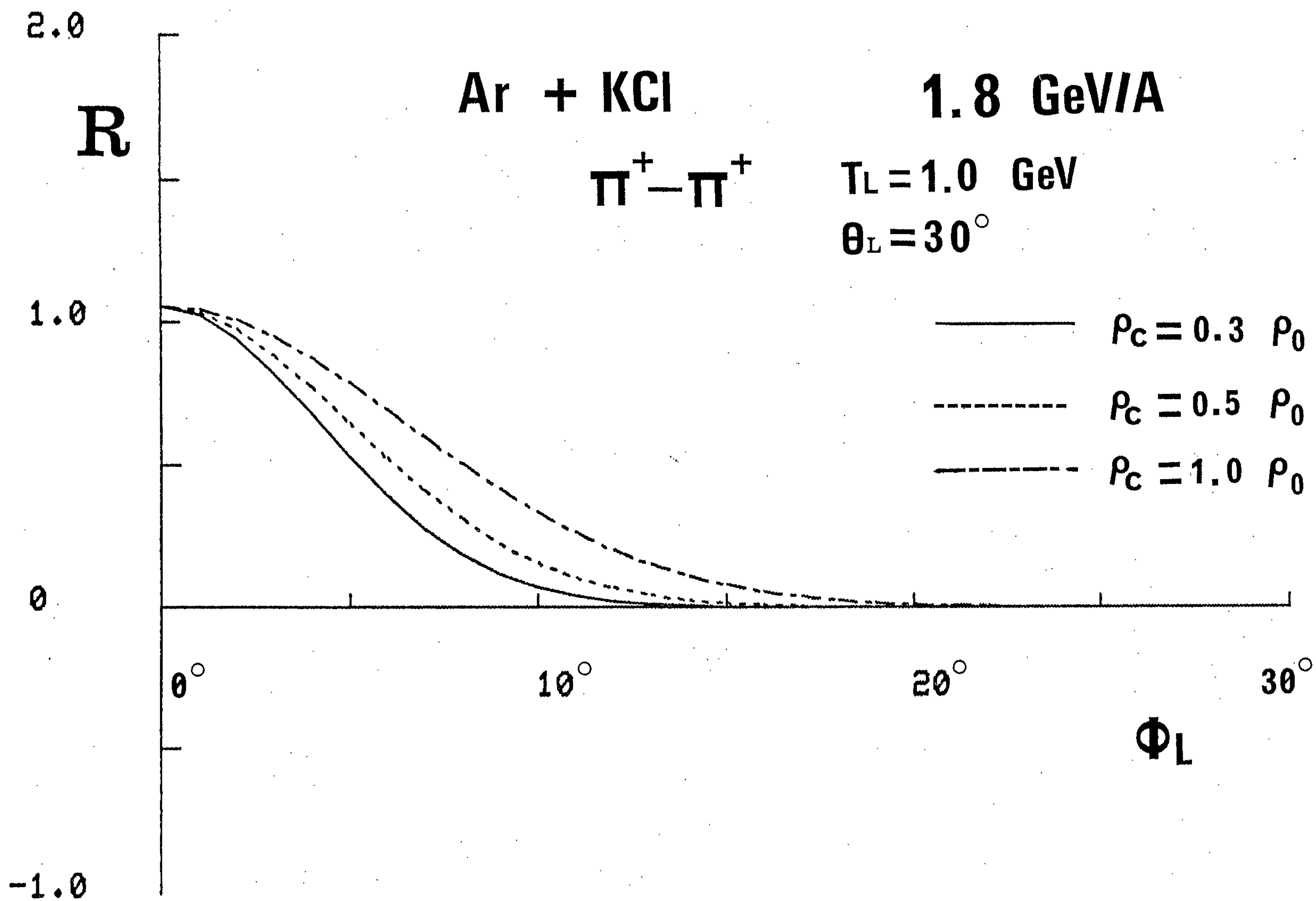
2.0
1.0
0
-1.0
R
Ar + KCl
1.8 GeV/A
π+–π+
TL = 1.0 GeV
θL = 30°
ρc = 0.3 ρ0
ρc = 0.5 ρ0
ρc = 1.0 ρ0
0°
10°
20°
30°
ΦL

Fig. 20

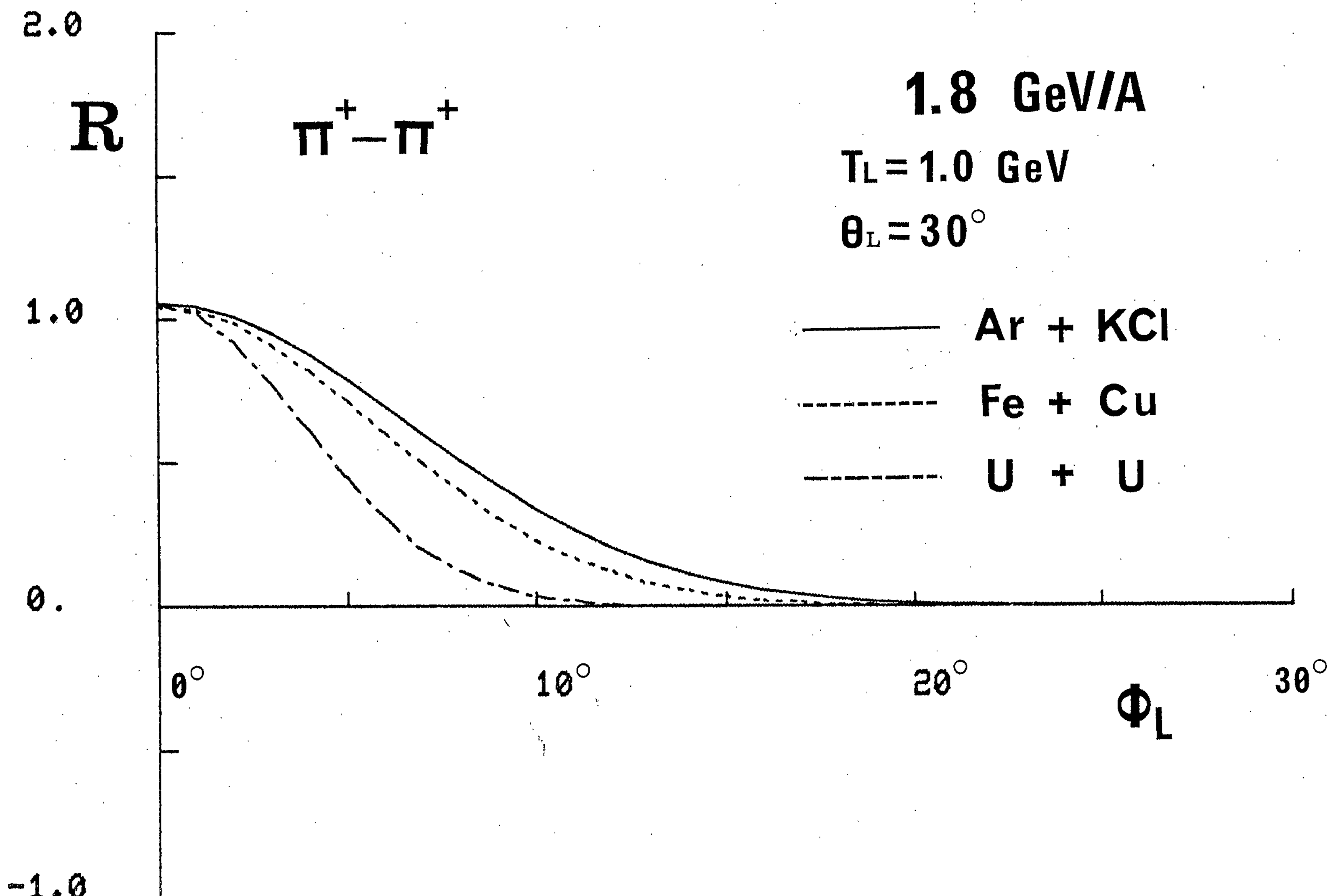

Fig. 21

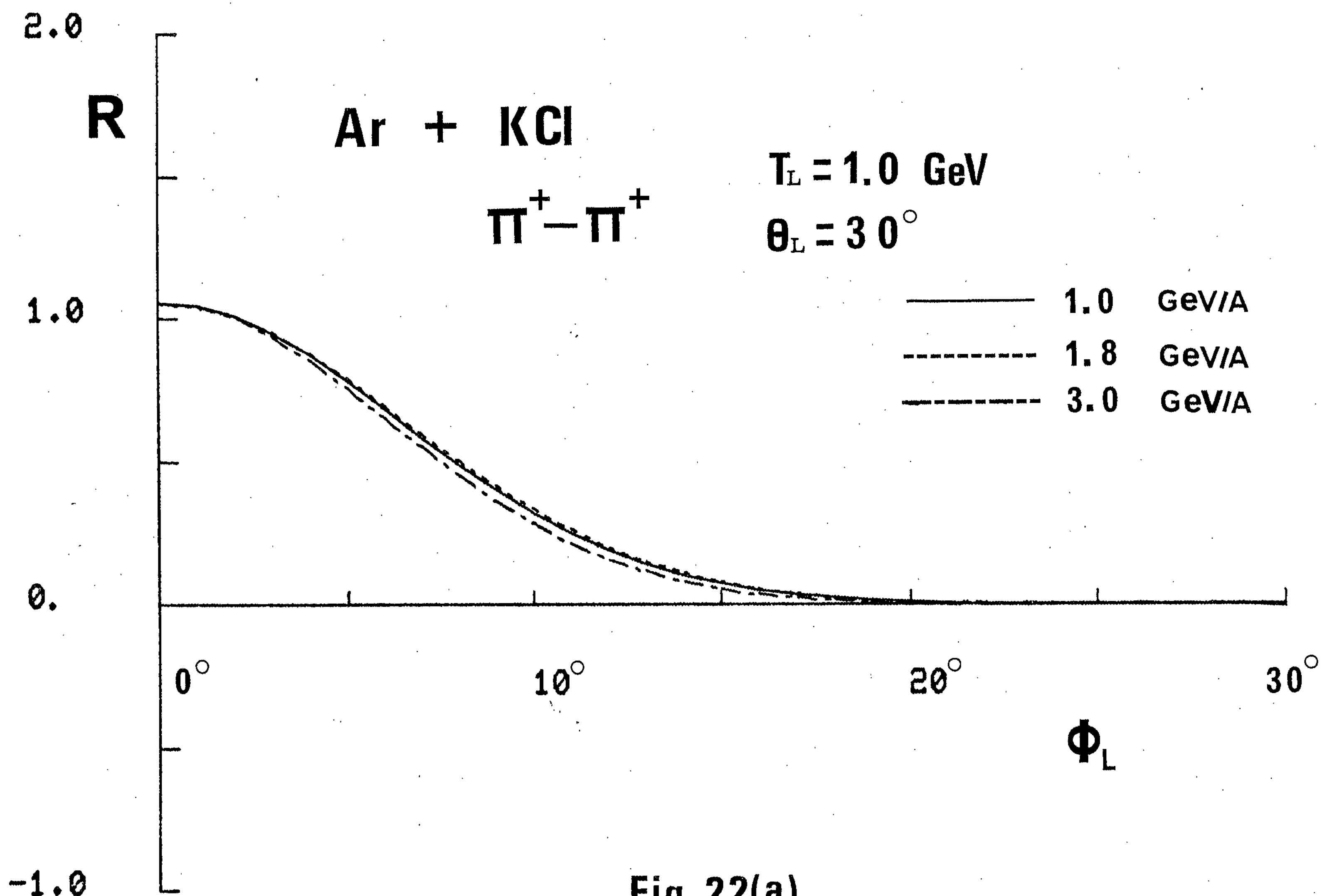

2.0
1.0
0.
-1.0
R
Ar + KCl
π+−π+
TL = 1.0 GeV
θL = 30°
1.0 GeV/A
1.8 GeV/A
3.0 GeV/A
0°
10°
20°
30°
ΦL

Fig. 22(a)

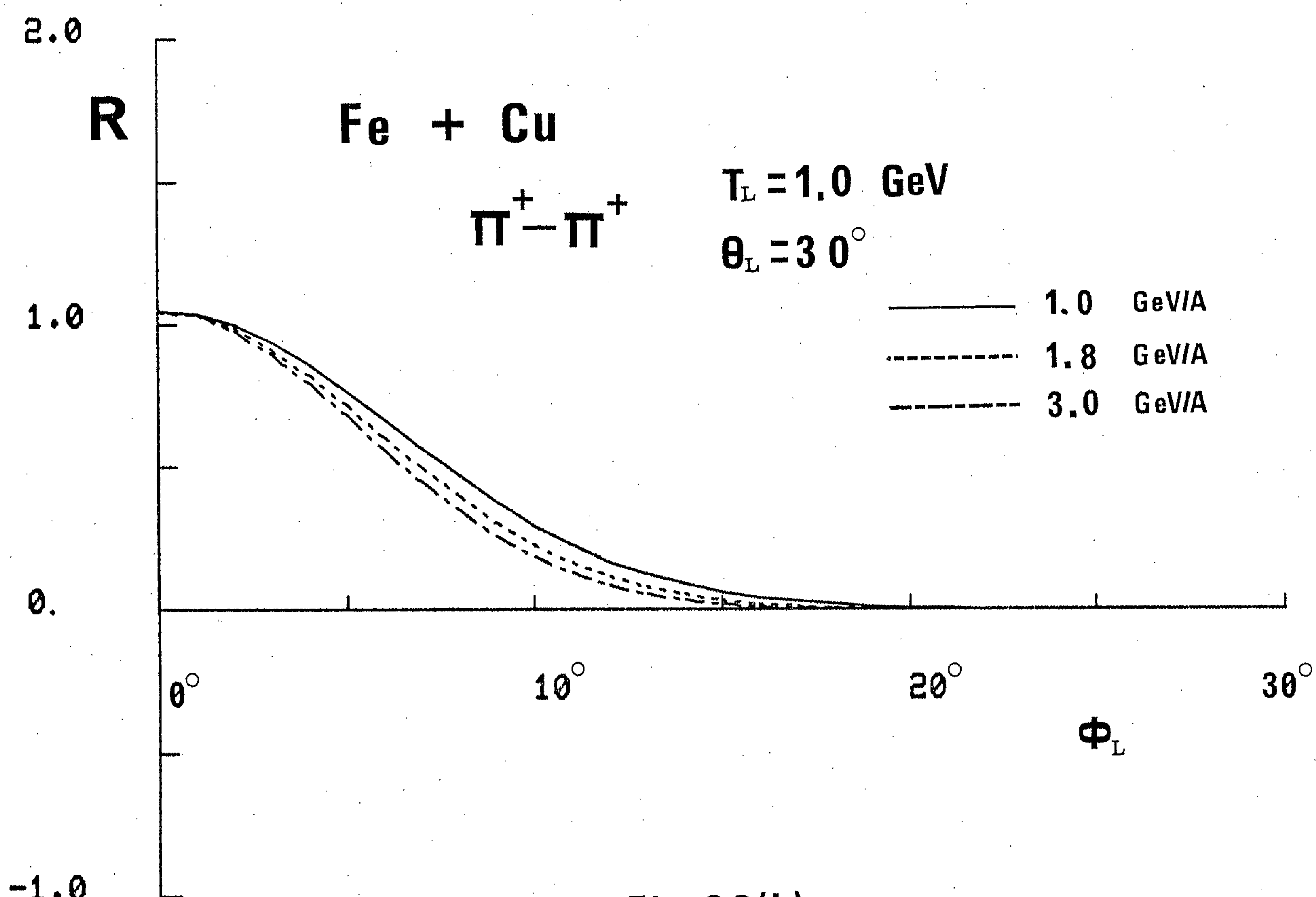
2.0
R
Fe + Cu
$\pi^+ - \pi^+$
T_L = 1.0 GeV
θ_L = 30°
1.0 GeV/A
1.8 GeV/A
3.0 GeV/A
1.0
0.
-1.0
0°
10°
20°
30°
Φ_L

Fig. 22(b)

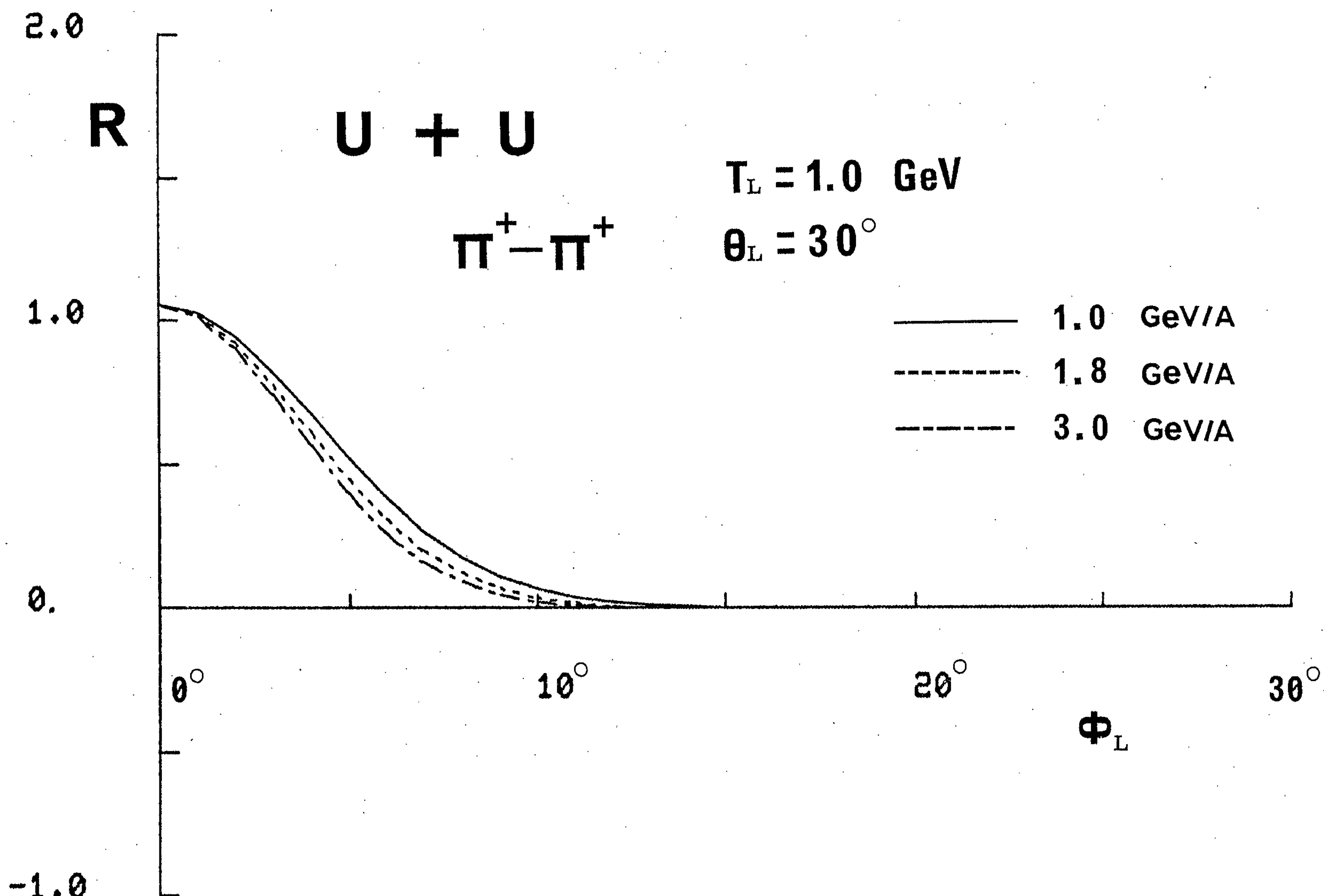

2.0
R
U + U
T_L = 1.0 GeV
$\pi^+ - \pi^+$
θ_L = 30°
1.0
1.0 GeV/A
1.8 GeV/A
3.0 GeV/A
0.
0°
10°
20°
30°
Φ_L
-1.0

Fig. 22(c)

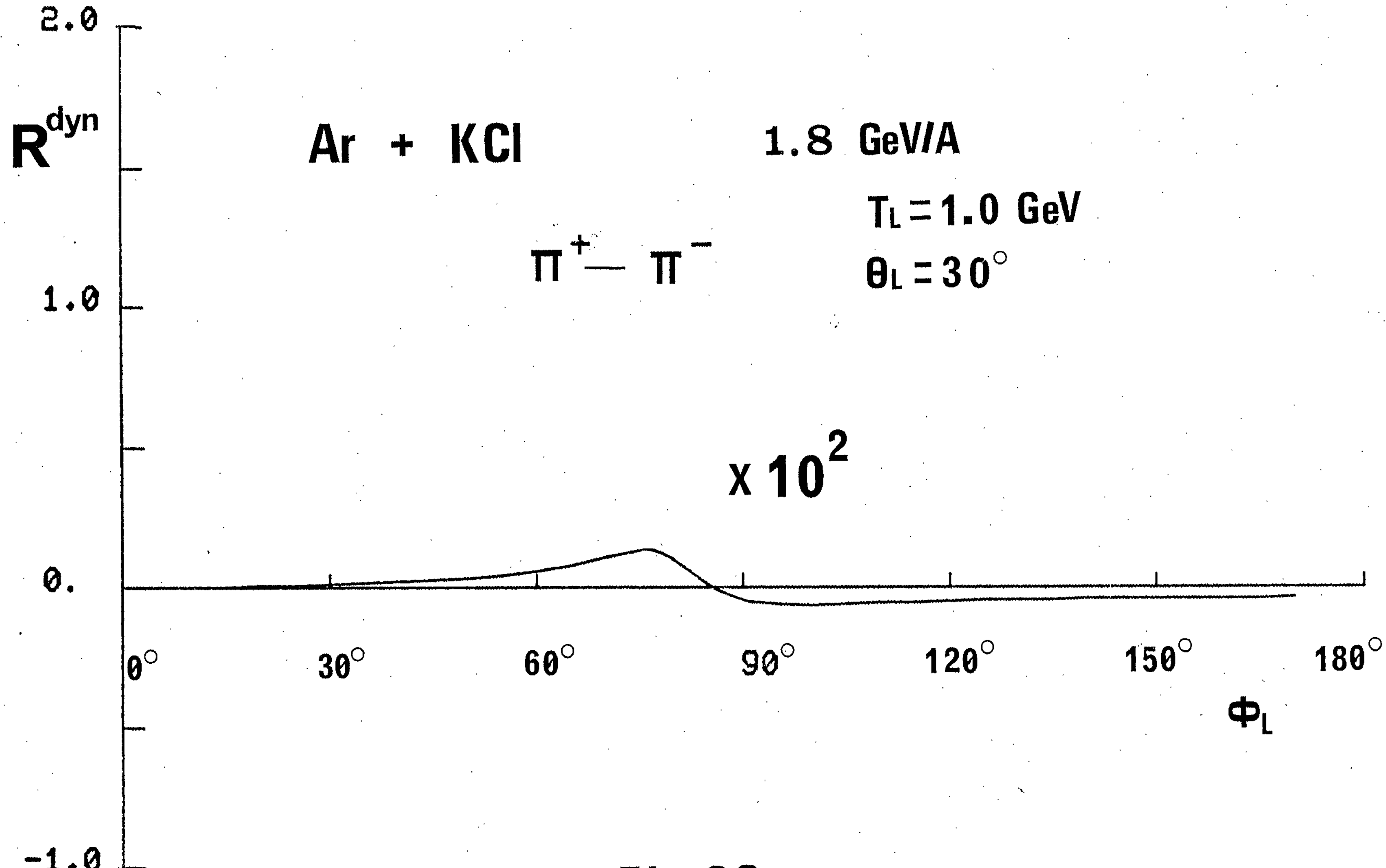
2.0
1.0
0.
-1.0
R^dyn
Ar + KCl
1.8 GeV/A
T_L = 1.0 GeV
θ_L = 30°
π⁺ − π⁻
x 10²
0°
30°
60°
90°
120°
150°
180°
Φ_L

Fig. 23

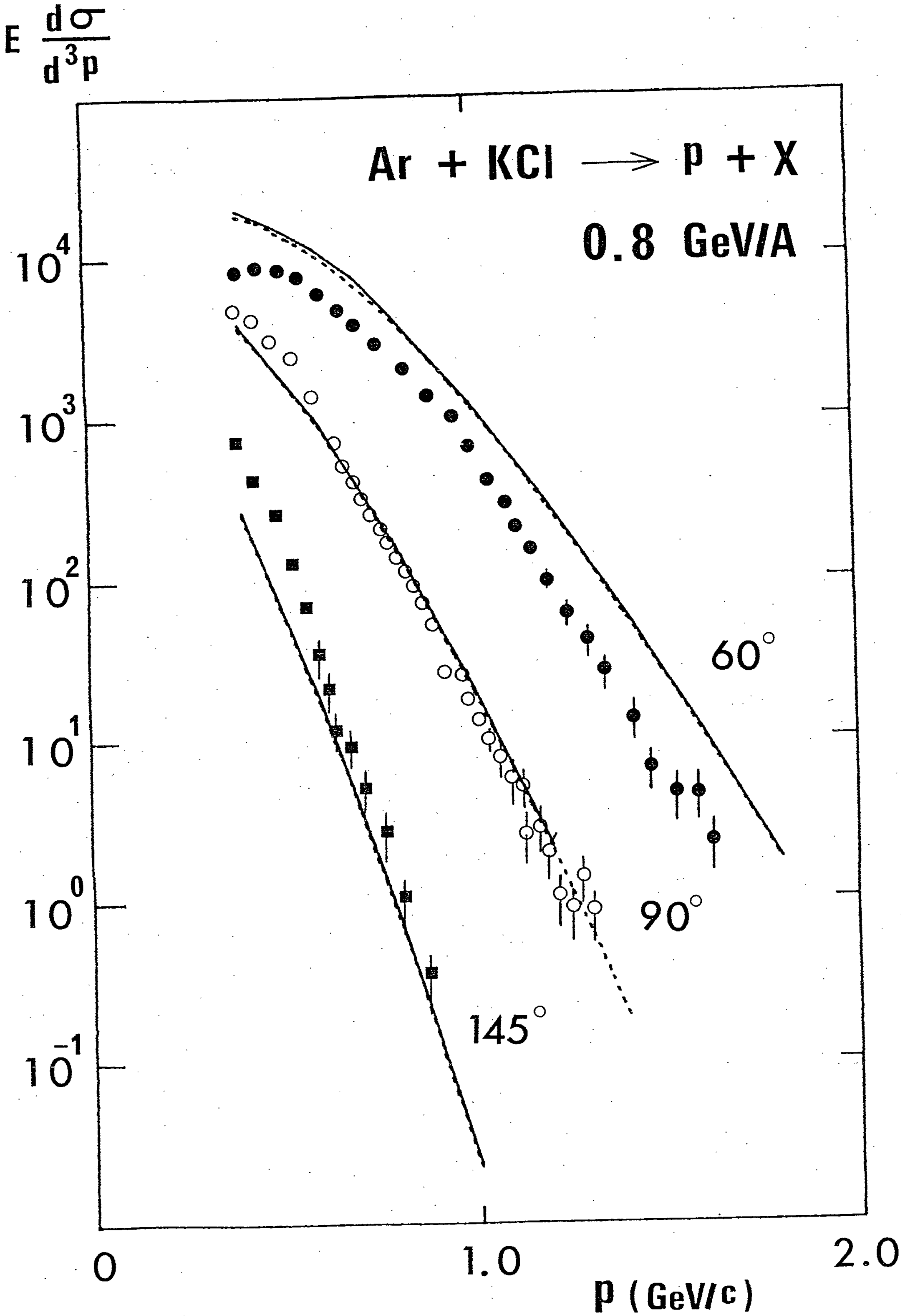

E dσ/d³p
Ar + KCl → p + X
0.8 GeV/A
10⁴
10³
10²
10¹
10⁰
10⁻¹
60°
90°
145°
0
1.0
2.0
p (GeV/c)

Fig. 24

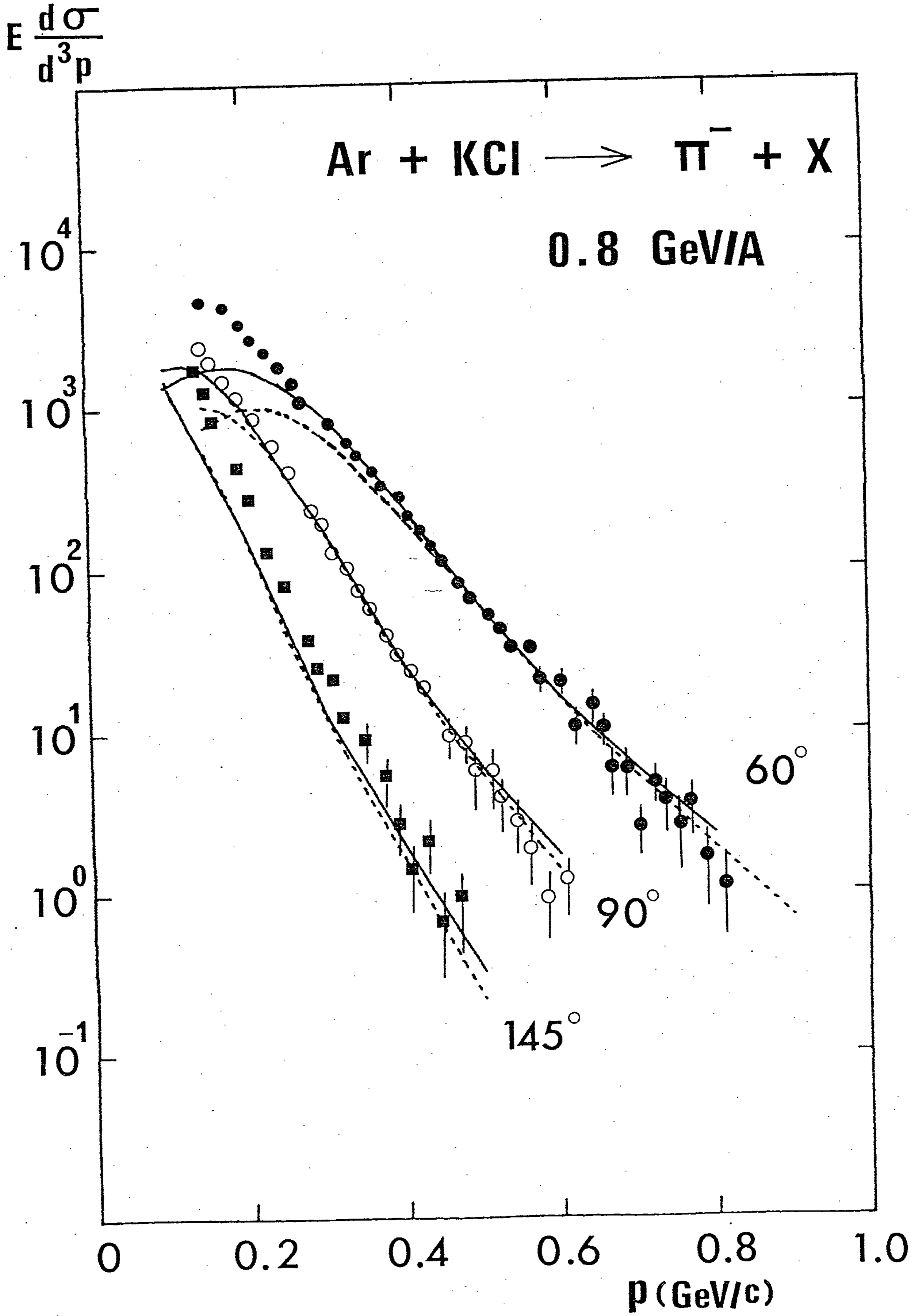

E dσ/d³p
Ar + KCl ⟶ π⁻ + X
0.8 GeV/A
10⁴
10³
10²
10¹
10⁰
10⁻¹
60°
90°
145°
0
0.2
0.4
0.6
0.8
1.0
p (GeV/c)

Fig. 25

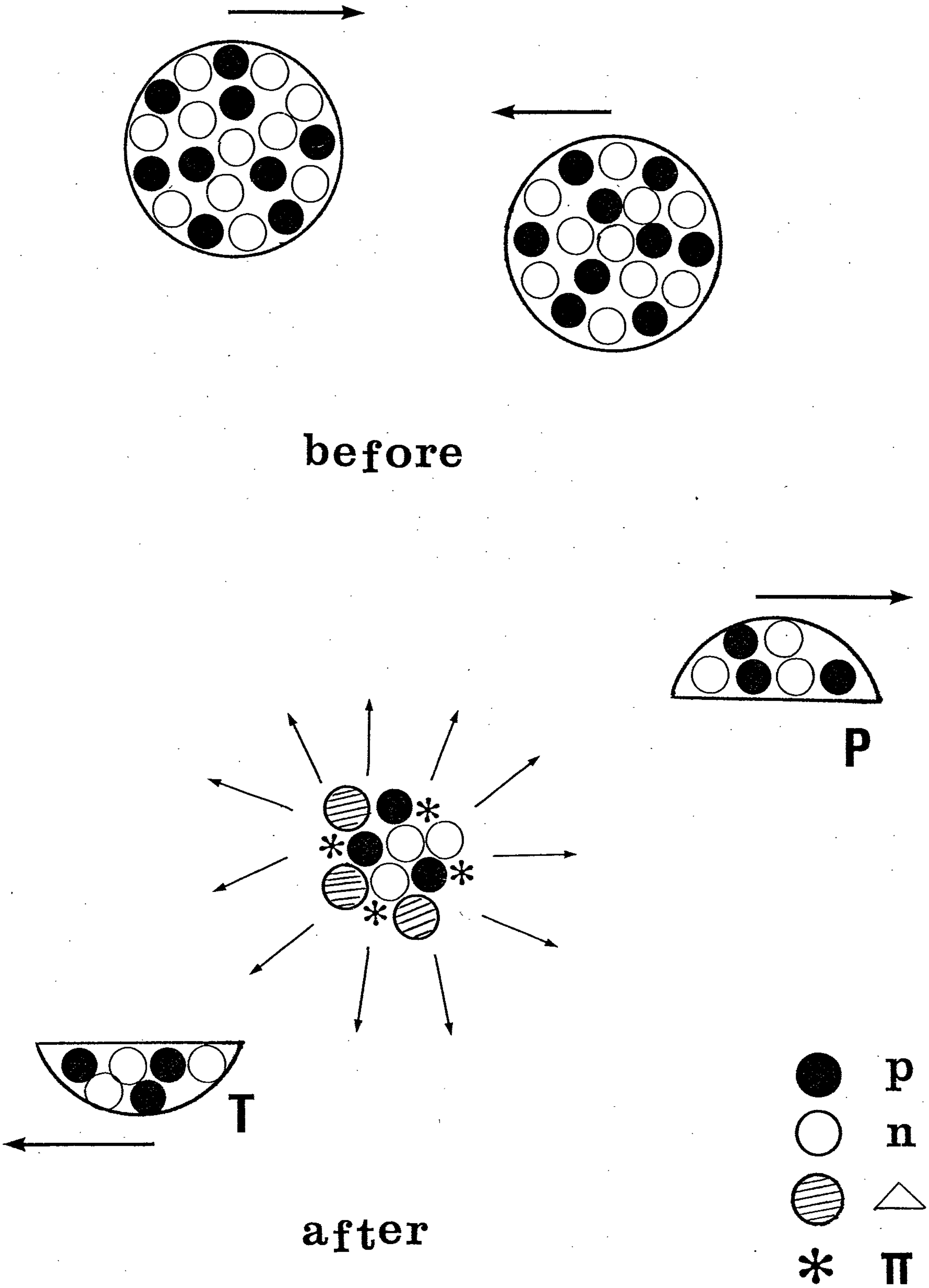

Fig. B-1

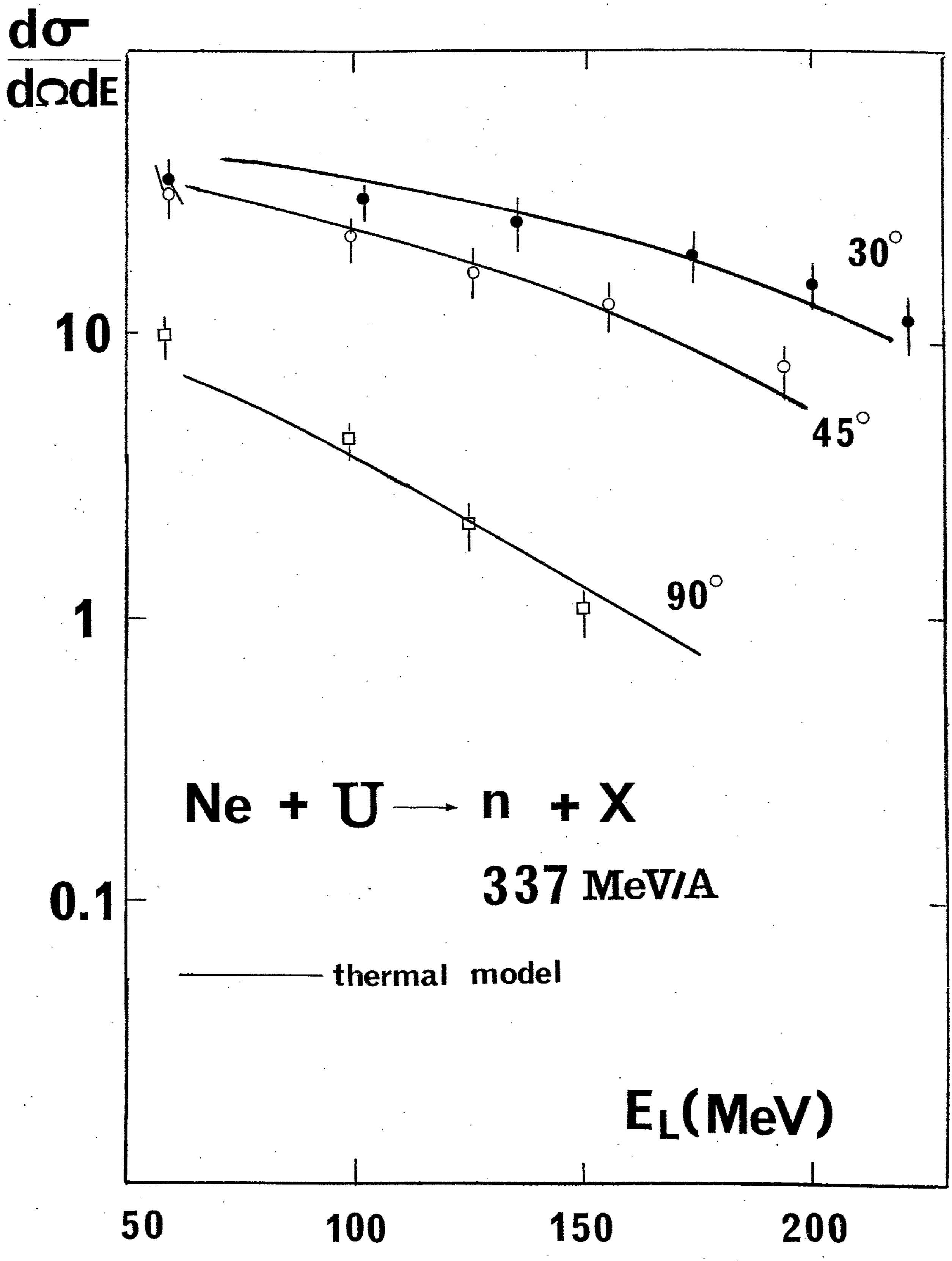
dσ
dΩdE
10
1
0.1
30°
45°
90°
Ne + U → n + X
337 MeV/A
thermal model
E_L(MeV)
50
100
150
200

Fig. B-2

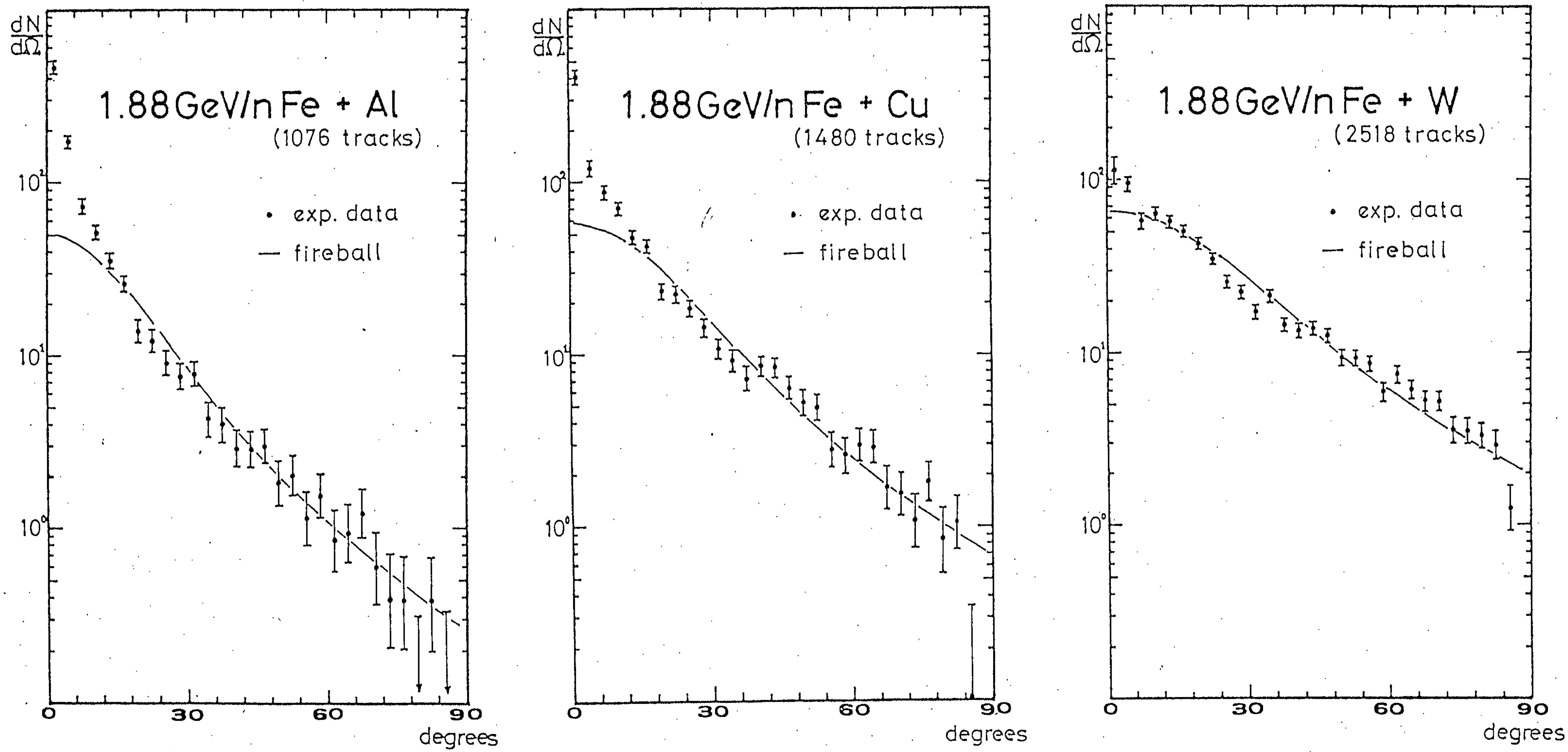
dN/dΩ
1.88 GeV/n Fe + Al
(1076 tracks)
• exp. data
— fireball
1.88 GeV/n Fe + Cu
(1480 tracks)
• exp. data
— fireball
1.88 GeV/n Fe + W
(2518 tracks)
• exp. data
— fireball
0
30
60
90
degrees

Fig. B-3